DISSERTATION

submitted to the

Combined Faculties for the Natural Sciences and for Mathematics

of the Ruperto-Carola University of Heidelberg, Germany

for the degree of

Doctor of Natural Sciences

presented by

Dipl.Bioinf. Christian Eisen

born in: Ansbach

Oral-examination: 30.10.2012

Development and investigation of a novel model system representing all three subtypes of pancreatic ductal adenocarcinoma reveals novel biomarkers and distinct drug sensitivities

Referees: Prof. Dr. Andreas Trumpp

Prof. Dr. Jens Werner

The work presented in this thesis was started in January 2009 and completed June 2012 under the supervision of Prof. Andreas Trumpp in the research group “Stem Cells and Cancer” at the German Cancer Research Center (DKFZ), Heidelberg as well as at the Heidelberg Institute for Stem Cells and Experimental Medicine (HI-STEM), Heidelberg.

Parts of this thesis have been published in:

Eisen et al. *Stratification of pancreatic ductal adenocarcinoma into three subtypes reveals differential overall survival and distinct drug sensitivities,* **Cancer Cell** (2012) (submitted)

Conference presentations:

Eisen et al.
"Subtype-specific models of pancreatic ductal adenocarcinoma reveal signaling pathways that can be exploited therapeutically"
(EACR22 2012, Barcelona, Spain)

Eisen et al.
"An advanced culture system for pancreatic cancer reveals tumor heterogeneity and facilitates stratification of novel targets"
(ISREC Symposium 2011 – Lausanne, Switzerland)

1 Summary

Pancreatic ductal adenocarcinoma (PDAC) is a highly aggressive disease with dismal prognosis. Despite the discovery of several promising drug candidates, recent trials with targeted therapies have shown limited or no benefit. For a number of cancers, subclasses have been uncovered that allow the use of therapies that target specific molecular alterations present in only a subset of patients. Recently three distinct subtypes of PDAC have been identified based on gene expression profiles derived from laser-microdissected human tumor tissue. This raised the possibility that differences between such subclasses could be exploited to stratify patients and develop novel targeted therapies. However, a major bottleneck for subtype-specific drug discovery was the lack of pre-clinical models that faithfully recapitulate the full heterogeneity of human pancreatic cancer.

The aim of this thesis was the development and verification of such models, analysis of subtype-specific differences and the subsequent discovery of novel treatment options for human PDAC. Our newly developed serum-free culture, termed PACO, preserves the molecular features of the corresponding primary tumors, and describes the first models of the exocrine-like subtype. Moreover, orthotopic transplantation of PACO cells re-initiates patient similar tumors that recapitulate these features *in vivo*, including the characteristic histopathology of the primary tumor specimens. The PACO-cells thus provide a consistent platform for subtype specific *in vitro* discovery and subsequent *in vivo* verification.

The power of our system is demonstrated by the identification of a novel set of biomarkers – Keratin-81 and HNF-1 – that can be easily integrated into routine pathology. Application of this marker set on a tissue microarray representing a cohort of >200 patients revealed that the three subtypes significantly differ in frequency (21-44%) and overall survival (16-43 months).

A combined approach of *in silico* predictions coupled with biochemical and immuno-histochemical verification demonstrated that the three subtypes differ in activation of important oncogenic pathways. Moreover we could show that the three PDAC subtypes vastly differ in their response to cytotoxic and targeted therapy.

Summary

An *in vitro* drug screen identified selective sensitivity of classical PDAC to Dasatinib, while growth of the otherwise multi-resistant exocrine-like PDAC was inhibited by the BH3-mimetic ABT-737. The PACO-derived xenograft model confirmed the *in vivo* efficacy of Dasatinib, which, in combination with Gemcitabine, led to tumor-regression only in the classical subtype.

Taken together our data demonstrate the need for stratification of PDAC-patients to individualize and improve treatment. Our study introduces novel patient-specific pre-clinical models for pancreatic cancer. Importantly these models are phenotypically consistent from the *in vitro* to the *in vivo* application, providing major improvements in pre-clinical drug studies. The PACO model thus enables stratification of individual patients and concomitant personalized treatment according the specific subtypes of human PDAC.

2 Zusammenfassung

Das duktale Pankreasadenokarzinom ist ein hochgradig aggressiver Tumor mit äußerst schlechter Prognose. Obwohl in den vergangenen Jahren einige, vielversprechender Wirkstoff-kandidaten entdeckt wurden, konnte keine der zahlreiche Studien die klinische Effektivität dieser Therapien nachweisen. Zahlreiche Krebserkrankungen konnten in der Vergangenheit in Subklassen unterteilt werden. Dadurch ist es möglich auf spezielle molekulare Veränderungen abzielende Therapien anzuwenden, welche nur in spezifischen Subgruppen von Patienten vorliegen. Erst kürzlich wurden für das duktale Pankreasadenokarzinom - auf Basis von Genexpressionsprofile generiert durch Laser mikrodissoziertes, humanes Tumorgewebe - drei unterschiedliche Subtypen beschrieben. Dies eröffnete die Möglichkeit, dass spezifische, molekulare Unterscheide zwischen diesen Subtypen zur Stratifizierung von Patienten sowie zur Entwicklung Subtyp-spezifischer Therapien verwendet werden können. Die Entwicklung solcher Therapien wird jedoch derzeit erschwert durch die Tatsache, dass bisher kein prä-klinisches Modell existiert, welches die Heterogenität des duktalen Pankreas-adenokarzinoms widerspiegelt.

Das Ziel diese Arbeit war die Entwicklung und Evaluation eben solcher Modelle, speziell im Hinblick auf die Erforschung von Subtyp-spezifischen, molekularen Unterschieden sowie die Entwicklung neuer Therapiemöglichkeiten für das humane duktale Pankreaskarzinom. Durch unsere neu entwickelte Serum-freie Kulturmethode, genannt PACO, werden die charakteristischen, molekularen Eigenschaften der entsprechenden Primärtumore erhalten. Zusätzlich beschreiben wir hier das erste Modell für den exokrinen Subtyp des duktalen Pankreaskarzinoms. Weiterhin zeigen wir, dass orthotope Transplantate von PACO Zellen einen Tumor generieren, welcher dem originalen Patiententumor sowohl auf molekularer als auch auf histopathologischer Ebene sehr ähnlich ist. Mit dem PACO Model beschreiben wir eine stabile Plattform mit welcher Subtyp-spezifische *in vitro* Ergebnisse, *in vivo* verifiziert werden können.

Zusammenfassung

Wir präsentieren ein neues Set an Biomarkern – Keratin-81 und HNF-1 – welche problemlos in die pathologische Diagnostik integriert werden können. Mit Hilfe dieser Marker konnten wir in einer Kohorte von über 200 Patienten zeigen, dass sich die drei Subtypen sowohl in der Frequenz (21-44%) also auch im Gesamtüberleben (16-43 Monate) signifikant unterscheiden. Durch die Kombination zahlreicher *in silico* Vorhersagen, welche wir mit Hilfe biochemischer und immunhistologischer Methoden verifizierten, konnten wir zeigen, dass die drei Subtypen unterschiedliche, onkogene Signalwege aktivieren. Unsere Studie zeigte weiterhin, dass die drei Subtypen unterschiedlich auf zahlreiche zytostatische und gezielte Therapien ansprechen. In einem *in vitro* Sensitivitätsscreen zeigten Zellen des klassischen Subtyps exklusive Sensitivität gegenüber Behandlung mit Dasatinib, wohingegen der multi-resistente exokrine Subtyp selektiv auf den BH3-mimetic ABT-737 ansprach. Mit Hilfe unseres PACO Xenograft Models konnten wir die *in vivo* Wirksamkeit von Dasatinib aufzeigen. Die Kombination mit Gemcitabine konnte die Größe von Tumoren des klassischen Subtyps verringern.

Zusammenfassend zeigt unsere Studie die Notwendigkeit Patienten zu stratifizieren mit dem Ziel der Etablierung personalisierter Therapien. Wir präsentieren hier patienten-spezifische, prä-klinische Modelle für alle Subtypen des duktalen Pankreas-adenokarzinoms. Unsere Modelle rekapitulieren sowohl *in vitro* als auch *in vivo* weitestgehend die Situation im primären Karzinom, was einen wesentlichen Fortschritt für prä-klinische Studien darstellt. Durch das PACO Model ist es möglich einzelne Patienten zu stratifizieren um somit spezifische, personalisierte Therapien für jeden Subtyp anzuwenden.

3 Introduction

Pancreatic ductal adenocarcinoma

Pancreatic cancer is one of the most malignant types of solid tumors. Estimates of the American Cancer Society (ACS) predict that in the US, 43,920 people will be diagnosed with pancreatic cancer and an estimated 37,390 people will succumb to this disease in 2012 [1]. Despite having a rather low morbidity of 3% among all cancers diagnosed, its high mortality makes pancreatic cancer the fourth leading cause of cancer related death in the US [1] **(Figure 1)**. Improved treatment and early detection methods led to a significant decrease of cancer-related deaths over the past 30 years in most types of human cancer. However mortality rates for pancreatic cancer patients did not change in the last decade [1]. Diagnosed at localized stages, patients have a 5-year survival rate of 22%, once the tumor has spread to distant sites, such as lymph nodes, liver or lung, the survival rate drops to 2%, making pancreatic cancer the tumor with the worst 5-year survival rate reported by the ACS over many years [1].

Pancreatic cancer incidence is linked to a number of risk factors, but evidence for a causative association has only been reported for cigarette smoking, as it doubles the risk of developing pancreatic cancer [2]. Some studies have shown an increased risk for patients with a history of chronic pancreatitis or diabetes. Data are limited on the role of high-cholesterol and high-fat diets, obesity, alcohol consumption, coffee intake and the use of aspirin as potential contributing factors [3]. Pancreatic cancer incidence can also be associated with genetic predisposition. Individuals with a family history of this disease have an up to 32-fold increased risk of developing the malignancy themselves. A number of susceptibility loci have been identified in such families, with mutations in *BRCA2, PALB2, CDKN2A, STK11*, and *PRSS1* genes being associated with increased risk of developing pancreatic cancer.

However, many aspects of this high penetrance of tumor development in individuals with such a genetic predisposition remains unexplained [3].

Estimated New Cases*

Males			Females		
Prostate	241,740	29%	Breast	226,870	29%
Lung & bronchus	116,470	14%	Lung & bronchus	109,690	14%
Colon & rectum	73,420	9%	Colon & rectum	70,040	9%
Urinary bladder	55,600	7%	Uterine corpus	47,130	6%
Melanoma of the skin	44,250	5%	Thyroid	43,210	5%
Kidney & renal pelvis	40,250	5%	Melanoma of the skin	32,000	4%
Non-Hodgkin lymphoma	38,160	4%	Non-Hodgkin lymphoma	31,970	4%
Oral cavity & pharynx	28,540	3%	Kidney & renal pelvis	24,520	3%
Leukemia	26,830	3%	Ovary	22,280	3%
Pancreas	22,090	3%	Pancreas	21,830	3%
All Sites	**848,170**	**100%**	**All Sites**	**790,740**	**100%**

Estimated Deaths

Males			Females		
Lung & bronchus	87,750	29%	Lung & bronchus	72,590	26%
Prostate	28,170	9%	Breast	39,510	14%
Colon & rectum	26,470	9%	Colon & rectum	25,220	9%
Pancreas	18,850	6%	Pancreas	18,540	7%
Liver & intrahepatic bile duct	13,980	5%	Ovary	15,500	6%
Leukemia	13,500	4%	Leukemia	10,040	4%
Esophagus	12,040	4%	Non-Hodgkin lymphoma	8,620	3%
Urinary bladder	10,510	3%	Uterine Corpus	8,010	3%
Non-Hodgkin lymphoma	10,320	3%	Liver & intrahepatic bile duct	6,570	2%
Kidney & renal pelvis	8,650	3%	Brain & other nervous system	5,980	2%
All Sites	**301,820**	**100%**	**All Sites**	**275,370**	**100%**

Figure 1 – Cancer statistics derived from Siegel et al. [1] depicting estimated new cases (upper table) and estimated cancer deaths (lower table) in the US both in males and females in 2012.

Pathophysiology

Infiltrating pancreatic ductal adenocarcinoma (PDAC) accounts for almost 90% of all malignant pancreatic neoplasms [3]. They present as a highly sclerotic masses with poorly defined edges often blocking the distal common bile and pancreatic ducts. 65% of pancreatic tumors are located in the head of the pancreas, 15% in the body, 10% in the tail and the remaining 10% are multifocal [4].

Microscopically, PDACs are characterized by their intense desmoplastic reaction with neoplastic cells, forming ducts of varying shapes and sizes, being sparsely scattered among a massive stromal compartment. PDACs are extremely infiltrative malignancies with vascular and perineural invasion present at time of clinical detection. Additionally in most cases the tumors already metastasized to distant sites such as lymph nodes, liver and lung [3]. Several variants of PDAC have been described based on differing histopathology. These include adenosquamous carcinoma, medullary carcinoma, colloid carcinoma, undifferentiated carcinoma and undifferentiated carcinoma with osteoclast-like giant cells **(Figure 2A-D)**. The classification of PDAC tumors according to these variants is of great interest as they differ in pathogenesis and prognosis [5].

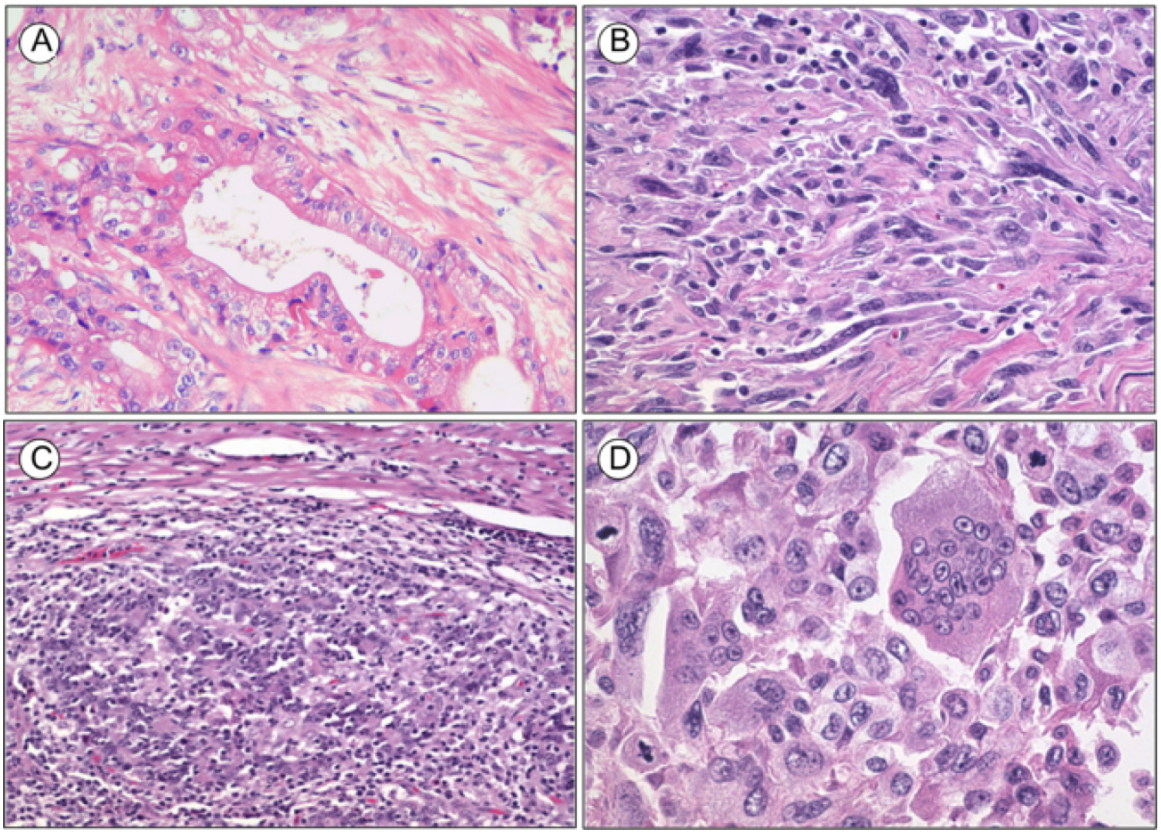

Figure 2 – Histopathological staining of different types of pancreatic ductal adenocarcinoma. (A) The classic adenocarcinoma displays a more differentiated morphology with clear ductal structures whereas the undifferentiated type of PDAC (B) presents with a completely undifferentiated morphology. (C) Medullary carcinoma of the pancreas displays a poor differentiation and syncytial growth pattern (D) Undifferentiated carcinoma with osteoclast-like giant cells is characterized by mitotically active, large pleomorphic cells (B-D adapted from Hruban et al. [5]).

Precursor lesions of PDAC

Pancreatic ductal adenocarcinomas arise through non-invasive, histologically distinct precursor lesions – pancreatic intraepithelial neoplasia (PanIN), intraductal papillary mucinous neoplasm (IPMN) or mucinous cystic neoplasm (MCN) **(Figure 3A)** [3]. Depending on the grade of tissue-specific architectural degeneration, PanINs are sub-classified into PanIN-1, PanIN-2 and PanIN-3. In many patients, such lesions are found adjacent to an invasive pancreatic ductal adenocarcinoma **(Figure 3B)**. Molecular analyses of PanINs, together with recent findings made by exon-sequencing of PDAC, confirmed that these precursor lesions harbor the most frequent genomic alterations found in invasive PDAC [6,7]. Activating mutations in codon 12 of the *KRAS2* gene, shared by more than 90% of all pancreatic cancers, is considered to be the driver mutation of PDAC and typically occurs in early PanIN-1 lesions [3]. Shortening of telomeres is another early event predominantly found in PanIN-1 lesions, which contributes to genetic instability in these pre-neoplastic lesions and hence leads to accumulation of additional chromosomal aberrations [3]. Inactivating mutations of the *p16/CDKN2A* gene occurs in PanIN-2 and inactivating mutations of *TP53*, *SMAD4* and *BRCA2* occur in late lesions (PanIN-3) **(Figure 4)** [4].

Another form of precursor lesion, IPMNs, are characterized as mucin-producing epithelial neoplasms with a mostly papillary architecture. Only a small minority displays inactivation of *SMAD4*, whereas loss of *STK11/LKB1* is more predominant in IPMNs **(Figure 3B)** [6]. MCNs precursor lesions are primarily found in women. They consist of mucin-producing epithelial cells and a distinctive ovarian-type stroma. About one third of them are associated with invasive PDAC **(Figure 3B)** [6]. Even though IPMNs and MCNs can progress to invasive adenocarcinoma over time, both of them can be detected early, as they are significantly larger than corresponding lesions of the PanIN type [6]. This suggests a potential of early detection of such precursors before they develop into invasive PDAC.

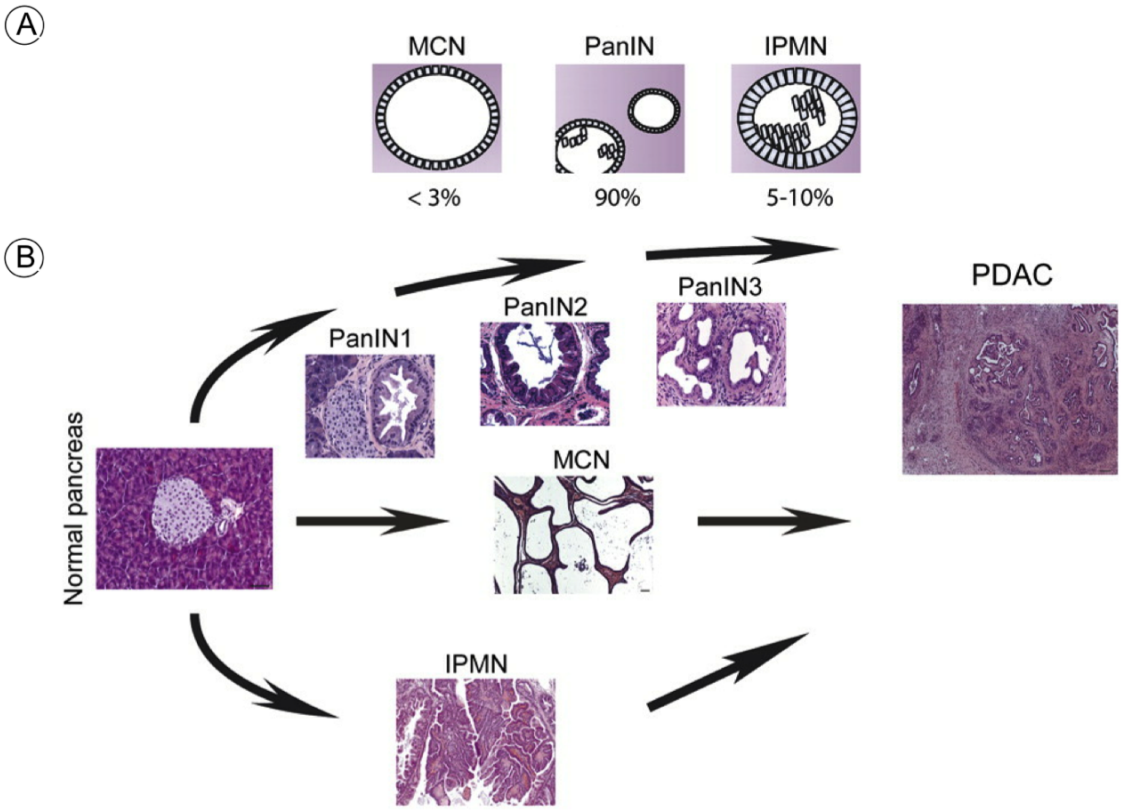

Figure 3 – (A) Different subtypes of PDAC precursor lesions have been identified with PanIN lesions being predominant over MCNs and IPMNs. (B) Progression model of PDAC from normal pancreas via the three described precursor lesions (PanIN1-3, MCN and IPMN). All three can develop into pancreatic cancer with various latency (Figure modified from Mazur et al. [8]).

Molecular Genetics of PDAC

Nearly all patients diagnosed with PDAC carry one or more of four "hallmark" genetic abnormalities **(Figure 4)** [9]. The most common genetic abnormality, shared by more than 90% of patients, is the activating mutation of the *KRAS2* oncogene [10]. Mutant Kras encodes an abnormal protein, which is "locked" in the active form, thereby aberrantly activating its downstream pathways, like RAF-MAPK, PI3K and RalGDS. Constitutive Ras signaling is not only a prerequisite for pancreatic cancer development, but was also shown to be required for the maintenance of established tumors [3].

Concurrently almost 90% of pancreatic tumors harbor a mutation in the *INK4A* locus resulting in an inactivation of the tumor suppressor p16/CDKN2A - a regulator of G1-S transition - which results in a significant increase in cell proliferation [6,11]. Another tumor suppressor gene *TP53* is mutated in more than 50% of the cases of PDAC [12]. The encoded protein p53 acts as a crucial regulator of G1-S cell cycle checkpoint and induces apoptosis upon DNA damage. Its loss enables neoplastic cells to survive and divide despite DNA damage resulting in accumulation of additional genomic aberrations [6]. The tumor suppressor Smad4 also plays a pivotal role in pancreatic carcinogenesis. Its corresponding gene locus *MADH4* undergoes loss of heterozygosity in almost 90% of the cases, while it is completely lost in at least more than half of the tumors [13]. As a member of the TGF-β signaling family, Smad4 plays an important role in initiating TGF-β induced signal transduction [4].

These four genes represent the mutational hot spots of pancreatic carcinogenesis, however the mutational landscape of pancreatic cancer is quite complex [14]. Interestingly the average number of somatic mutations per PDAC tumor (∅ 48 mutations/tumor) is significantly lower than in breast (101) or colorectal (77) tumors. Even though many of the mutations are not shared among pancreatic tumors, pathway analysis of mutated genes revealed that every tumor carries at least one mutation in each of 12 so-called core-signaling pathways of pancreatic cancer. This shows that despite having a heterogeneous mutational profile, the pathways mutated in pancreatic cancer are shared among patients [14].

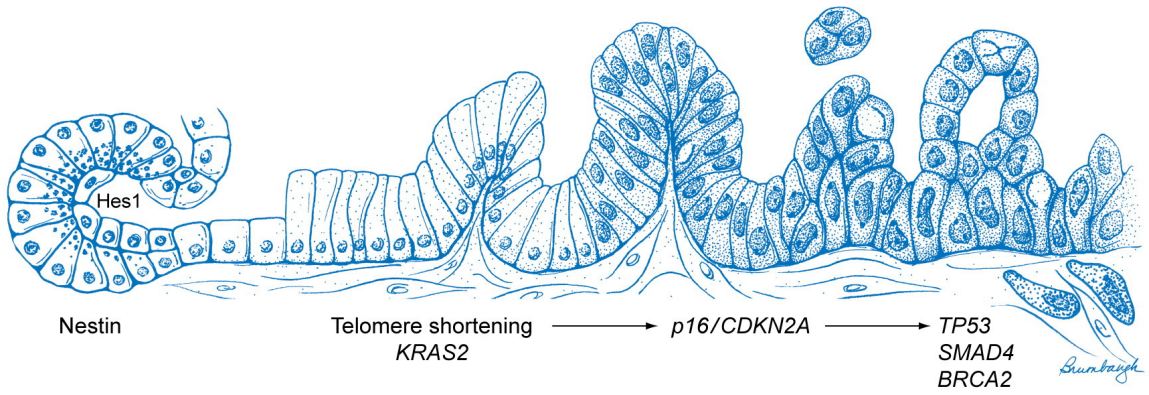

Figure 4 - Genetic progression model of pancreatic ductal adenocarcinoma. The development from histologically normal epithelium via low to high-grade pancreatic intraepithelial neoplasms (PanIN-1-3) to invasive pancreatic ductal adenocarcinoma is displayed. Molecular alterations displayed below can be classified into early (KRAS, telomere shortening), intermediate (p16/CDKN2A) or late (TP53, SMAD4 and BRCA2) (Figure adapted from Vincent et al. [3]).

Diagnosis and staging

Deep sequencing analyses on sections of pancreata of diseased patients showed that pancreatic cancer is a slowly developing tumor, even though being highly malignant once clinically detected. Mathematical modeling of the genetic evolution based upon this data, predicts that it takes around 12 years from the initiation of tumorigenesis, i.e. first hit mutation, until birth of a cell which gives rise to the parental clone. Interestingly the model also predicts a potential "intervention window" of 6.7 years, the time it takes for a metastatic clone to evolve out of the parental clone [7].

However, early stage pancreatic cancer usually does not display any clinical detectable symptoms. Typical presenting symptoms, including abdominal or mid-back pain, obstructive jaundice and weight loss, are rather unspecific and not exclusively associated with pancreatic cancer [3]. The most widely used serum marker for PDAC, the sialyated Lewis blood group antigen CA19-9, has a high sensitivity in patients with advanced disease (roughly 80%). However serum levels of patients with localized or small tumors are often normal thus precluding its use as a diagnostic marker [6]. Novel biomarkers are being evaluated in the clinic, but none of them has so far been shown to improve diagnosis significantly [3,4].

Patients suspected with pancreatic cancer typically undergo a tri-phasic pancreatic-protocol CT as the standard of initial diagnostic tests, providing nearly 80% accuracy for prediction of respectability [9].

Patients diagnosed with PDAC in almost all cases already suffer of advanced disease. In the majority of cases the tumor already disseminated to surrounding or distant tissues and is surgically inoperable. If the tumor can be resected, pathological assessment of the resected pancreatic tumor provides valuable clinical information [3]. It is also important to note the extend of resection (R0 = complete resection; R1 = grossly negative but positive microscopic margins of resection; R2 = grossly and microscopically positive margins of resection) which has great prognostic relevance [15].

Table 1 – Staging of pancreatic cancer based on the description by the AJCC (adapted from Hidalgo [9])

Stage	Tumor grade	Nodal Status	Distant Metastasis	Median survival	Characteristics
IA	*T1*	*N0*	*M0*	24.1	Tumor limited to the pancreas, ≤2 cm in its longest dimension
IB	*T2*	*N0*	*M0*	20.6	Tumor limited to the pancreas, >2 cm in its longest dimension
IIA	*T3*	*N0*	*M0*	15.4	Tumor extends beyond the pancreas but does not involve the celiac axis or superior mesenteric artery
IIB	*T1, T2, T3*	*N1*	*M0*	12.7	Regional lymph-node metastasis
III	*T4*	*N0 or N1*	*M0*	10.6	Tumor involves the celiac axis or the superior mesenteric artery
IV	*all T's*	*N0 or N1*	*M1*	4.5	Distant metastasis

Staging of pancreatic cancer is performed according to the most recent edition of the American Joint Cancer Committee (AJCC) based on TMN (Tumor Node Metastasis) classification [16] **(Table 1)**. T1, T2 and T3 tumors are considered potentially resectable, whereas T4 tumors, many already invaded the mesenteric artery, are unresectable.

Treatment of pancreatic ductal adenocarcinoma

Surgery

For patients with a resectable tumor, surgery still remains the best curative treatment. The goal of surgical treatment is the complete resection of the primary tumor, aiming for an R0 resection: complete removal of macroscopic tumor with clear resection margins [3]. However for the majority of patients, surgery is not an option, as they already present with advanced disease. Only 10-20% are considered as candidates for curative surgical treatment [17].

PDAC patients are best treated by a multidisciplinary team of surgeons and oncologists at expert, high-volume clinical centers. At such, operative mortality is low and ranges at around 3% [15]. The standard operation technique mostly depends on the location of the tumor.

For tumors of the head of the pancreas, the Kausch-Whipple partial pancreatoduodenectomy is the standard of care. Patients with tumors in the pancreatic body or tail will undergo left pancreatectomy with hilar and spleen lymph nodes being removed at the same time [4]. In general a minimum of 12-15 lymph nodes are resected for staging and prognosis. Several clinical studies showed that more extensive resection in order to achieve a clear resection margin, does not result in a significant survival benefit for patients, but in turn increases post-operative mortality [9]. Even at expert clinical centers, post-operative morbidity is high at around 40% [4].

The 5-year overall survival rate for patients with surgically resected pancreatic ductal adenocarcinoma ranges from 20-25%. Poor prognostic factors include positive resection margins (R1 or R2), nodal involvement, presence of distant metastases and a large or poorly differentiated primary tumor [3]. Approximately 20% of patients operated develop local recurrence and more than 70% metastatic recurrence in the peritoneum, liver and lung [4].

Neoadjuvant therapy

The aim of neoadjuvant treatment is to improve the efficacy of primary treatments. Studies on patients with advanced bladder cancer for example showed, that patients which received platinum-based combination chemotherapy prior to radiotherapy or surgical intervention showed a significant benefit in overall survival [18]. The small number of patients eligible for surgical treatment and the devastating overall survival rates led to the exploration of neoadjuvant therapies in PDAC. They aim to identify patients, which might benefit from such treatment options, in particular those with borderline resectable disease [19]. The goal of neoadjuvant therapy is to shrink the primary tumor mass in order to enable surgical intervention [19]. One significant advantage of neoadjuvant therapy is its applicability as soon as the tumor has been diagnosed, whereas post-surgical recovery of patients often delays adjuvant therapy [19]. In PDAC patients either a combination of radiotherapy and chemotherapy (5-fluorouracil, cisplatin, Gemcitabine) or monotherapy of either have been evaluated as neoadjuvant treatment options [20]. Current clinical studies are investigating if patients might benefit from a combination of pre- and intraoperative radiotherapy [21].

Median survival rates reported in these studies argue for a survival benefit of patients treated with neoadjuvant therapy, however to date no randomized trials comparing neoadjuvant vs. adjuvant therapy exist, precluding a final statement [19]. It is still heavily debated, if PDAC patients will benefit from neoadjuvant therapy. Arguments against this form of treatment are the limited response rates and a delay of surgery that allows the primary tumor to progress and ultimately impair curative resection [3]. On the other hand, efficient neoadjuvant therapy might downstage patients in order to receive curative surgery, which otherwise would not be possible. However to date, neoadjuvant therapy for pancreatic cancer has not been added to the standard of care options in treating pancreatic cancer patients.

Adjuvant therapy

Adjuvant therapy is usually administered to patients, who underwent resection of the primary tumor, once they have recovered from surgery. In order to improve outcome of these patients, systemic chemotherapy, radiotherapy or a combination of both are applied in clinical practice. Patients most likely to benefit from adjuvant treatment are those with R0 resections, as patients with R1 resection margins have a decreased median overall survival (8-18 vs. 20-25 months) [3], however, association of therapy response with resection status is still questioned [9].

In the late 1970s the Gastrointestinal Tumor Study Group designed the first randomized trial of adjuvant therapy in pancreatic cancer, testing 5-fluorouracil (5-FU) against surgery alone. This study established 5-FU as the first front-line therapy for treating pancreatic cancer patients, providing a superior median overall survival compared to patients that received surgery only (20 vs. 11 months) [19,22]. For nearly 20 years, 5-FU was considered as the only therapeutic option with efficacy in pancreatic cancer until the development of Gemcitabine. A pivotal Phase III trial in 1997 found that Gemcitabine is more effective in treating pancreatic cancer patients than 5-FU [23]. Despite a modest increase in median overall survival (5.7 vs. 4.4 months) the 5-year survival rate for Gemcitabine-treated patients was significantly higher than for those treated with 5-FU (18% vs. 2%) [23].

Due to its efficiency in monotherapy [24] several clinical trials investigated if a combination of Gemcitabine with several other cytotoxic agents like 5-FU, Cisplatin, Docetaxel, Oxaliplatin and Irinotecan could increase therapy response [9,19]. Many of these studies could not show a significant survival benefit for combination treatment. However different Phase III studies have shown that the combination of Capecitabine and Gemcitabine leads to a significant survival benefit (10.1 vs. 7.4 months) [25,26], indicating a further evaluation of this combination treatment.

Single or combinatorial radiotherapy in an adjuvant setting is still controversial in pancreatic cancer treatment albeit the fact of being a valuable treatment option in other types of cancer, like for example lung and breast cancer [27].

Data on the efficacy of radiotherapy in pancreatic cancer patients is sparse and it is still heavily debated if this type of therapy improves the outcome of patients [28]. Currently it depends in which country a patient is treated whether radiotherapy is given or not. While chemo-radiotherapy followed by chemotherapy is described as standard of care in Northern America, European centers rely on chemotherapy as their current standard adjuvant therapy [19].

Targeted therapy

Targeted therapies are becoming increasingly important in a number of different tumor types. Based on the biology of pancreatic tumors, an increasing number of compounds targeting substantial pathways of pancreatic tumorigenesis are under clinical investigation [3]. These include molecular targets either overexpressed or mutated in PDAC such as the epidermal growth factor receptor (EGFR)/KRAS, human epidermal growth factor receptor type 2 (HER2) and vascular endothelial growth factor (VEGF) [9].

The first targeted compound that has been approved by the US Food and Drug Administration (FDA) for treatment of pancreatic cancer is Erlotinib - a tyrosine kinase inhibitor of the catalytic domain of EGFR [3,9]. The principal Phase III study showed that the combination of Gemcitabine with Erlotinib was modestly superior to Gemcitabine alone and increased overall survival by roughly one month [29].

Even though this difference has been reported to be significant, clinical benefit for pancreatic cancer patients is limited, leaving substantial room for improvement [19]. Many compounds which are currently evaluated in Phase II/III clinical trials target specific pathways, which have been reported to be involved in pancreatic tumorigenesis, metastasis development and relapse [9,30]. They include, but are not limited to, Shh inhibitors such as GDC-0449 (NCT01064622), Src inhibitors such as Dasatinib (NCT01395017), Notch inhibitors such as MK0752 (NCT01098344), or mTOR inhibitiors (NCT01077986). Although many of such compounds are currently investigated in treatment of PDAC patients, several promising drug candidates recently failed in clinical Phase III trials, having shown limited or no benefit for patients [9].

Targeted therapy in pancreatic cancer is for almost all cases still experimental and has not entered, except for Erlotinib, clinical standard of care. Future studies deciphering the major driving pathways in PDAC will help to more specifically tailor targeted therapies for pancreatic cancer, which might ultimately improve patient treatment.

Management of advanced disease

Few trials exist evaluating second-line therapeutic options for patients who have failed first-line chemotherapy with Gemcitabine. Many patients with advanced disease progress rapidly and many of them are already in a bad medical condition impairing additional treatment. For selected groups of patients with minimal symptomatic disease that initially responded to Gemcitabine treatment, second-line therapy based on Oxaliplatin/Fluoropyrimidine combinations may provide a valuable treatment opportunity [19]. Patients receiving combinations of Oxaliplatin and Capecitabine [31] as well as of Oxaliplatin, 5-FU and Folinic acid [32] showed a significantly better overall survival and prognosis.

Management of unresectable disease

Only 20% of patients diagnosed with pancreatic cancer qualify for surgical treatment. For the remaining part, mostly patients with PDAC in the body and tail of the pancreas, surgery is not an option. Unresectable tumors in many cases already infiltrated into surrounding vascular structures, impairing vascular reconstruction after surgery.

Studies have shown that in such patients, partial resections of the tumor with no curative intend, did not result in a significant improved survival in these patients [33,34]. In order to alleviate the symptoms in patients with unresectable disease, chemotherapy (Gemcitabine, 5-FU) and/or radiotherapy is administered to slow down growth of the tumor and release the pressure on the surrounding tissues. The goal of palliative care is to improve the patient's quality of life and to extend the overall survival compared to no treatment [3].

Pancreatic cancer models

Conventional cell lines

Cancer cell lines cultured in fetal calf serum (FCS) have long been the historical standard in tumor biology. Both *in vitro* and *in vivo* usage of such cell lines are a standard tool for studying the biology of cancer and serve as a pre-clinical platform for screening of novel therapeutic regimen [35]. The American Type Culture Collection (ATCC) currently holds 17 human pancreatic ductal adenocarcinoma cell lines (June 2012), with many of them being routinely used in labs throughout the world [36]. The advantages of such cell lines are that they can be easily maintained in culture in simple media formulations, they can be manipulated *ex vivo* and have an excellent engraftment efficiency both in initial and serial transplantation settings. Despite these advantages, it is becoming increasingly clear that many of these models lack the capability to accurately mirror the human disease. Long-term *in vitro* culture based on FCS leads to a multitude of genomic aberrations and phenotypic alterations, which bear little resemblance with the corresponding primary tumors **(Figure 6A)** [35]. Selective pressure during culture may lead to overgrowth and selection of certain sub-clones, impairing the analysis of the heterogeneous nature of cancer [36]. Furthermore, *in vivo* generated tumors from these cell lines often fail to represent the morphological features of patient PDAC tumors, as they form a rather undifferentiated mass of tumor cells. Moreover, absence of the characteristic stromal compartment of PDAC, precludes any analysis of intra-tumor bioavailability of compounds in a clinically relevant setting.

Altogether it is noteworthy to mention that studies on such "conventional" cancer cell lines expanded our knowledge of the biology of pancreatic cancer and allowed to dissect several crucial signaling pathways involved in tumor maintenance and metastasis development. However such models inconsistently predict the efficacy of novel therapeutic strategies in a pre-clinical setting due to the lack of resemblance to primary PDAC tumors [37]. Hence, this is one of the reasons why most of the clinical trials for PDAC failed in Phase II/III over the last decade [38].

Genetically engineered mouse models

Genetically engineered mouse models (GEM) represent an invaluable tool in the compendium of pancreatic cancer models as they accurately mimic the pathophysiological and molecular features of human pancreatic tumors. They have lead to a greater understanding in pancreatic tumorigenesis, tumor-host cell interaction and in the elucidation of the role of the immune system in pancreatic tumor maintenance and development. Genetically engineered mice usually express an oncogene or dominant-negative tumor suppressor genes in a non-physiological manner [8]. A tissue-specific promoter drives a Cre-recombinase, which in turn activates / inactivates the transgene specifically in sites of *Cre* expression. In PDAC models the two primary promoters used are the *Pdx1* homeobox transcription factor and *Ptf1a* helix-loop-helix transcription factor, both of which are active in the pancreatic progenitor compartment **(Figure 5A)** [39]. However both are also expressed in other tissues (*Pdx1* in the developing foregut and *Ptf1a* in the brain), making the system "leaky" to possibly generate extra-pancreatic phenotypes [8].

Pancreatic tumorigenesis is predominantly initiated by an activating mutation in codon 12 of the *KRAS2* oncogene, altering the codon from glycine to aspartic acid. The first mouse model described for PDAC was the $KRAS^{G12D}$ mouse, using *Pdx1* to drive Cre expression, specifically targeting mutant Ras expression to the pancreas [40]. Even though tumors of these mice faithfully recapitulate the initial steps of pancreatic carcinogenesis, developing multiple stages of PanIN lesions, only few of them progress into invasive and metastatic PDAC. This led to the design of improved mouse models based on the $KRAS^{G12D}$ mouse **(Figure 5B)**.

All of these "2nd generation mouse models" share the *KRAS*^{G12D} transgene but carry additional loss-of-function or dominant-negative alleles of specific tumor suppressor genes. Whereas both models carrying either *CDKN2* [41] haplo-insufficiency or loss of / dominant-negative mutations of the *TP53* gene [42] develop PDAC along the PanIN-to-ductal adenocarcinoma sequence, mice deficient for *SMAD4* develop mucinous cystic neoplasms, which develop into pancreatic ductal adenocarcinoma [43]. These mouse models are the most widely used GEMs for studying PDAC and have led to several major advances in PDAC research [44,45]. Even though genetically engineered mouse models recapitulate the human disease to a large extend and are still a closer fit than conventional cell lines, they also have several disadvantages inherent to the models and irrespective of the genetic alterations they are based upon. Due to the complexity of the model, where at least three different transgenic strains have to be interbred, high-throughput analysis to unravel novel therapeutic compounds are as far as impossible. Additionally many of the findings about drug potencies being made in a murine setting fail to perform equally well in a human setting [37].

In sum GEM are a valuable tool to study the genesis of pancreatic tumors and interactions with the immune system and microenvironment, however every finding being made in GEMs has to be ultimately validated in a human setting.

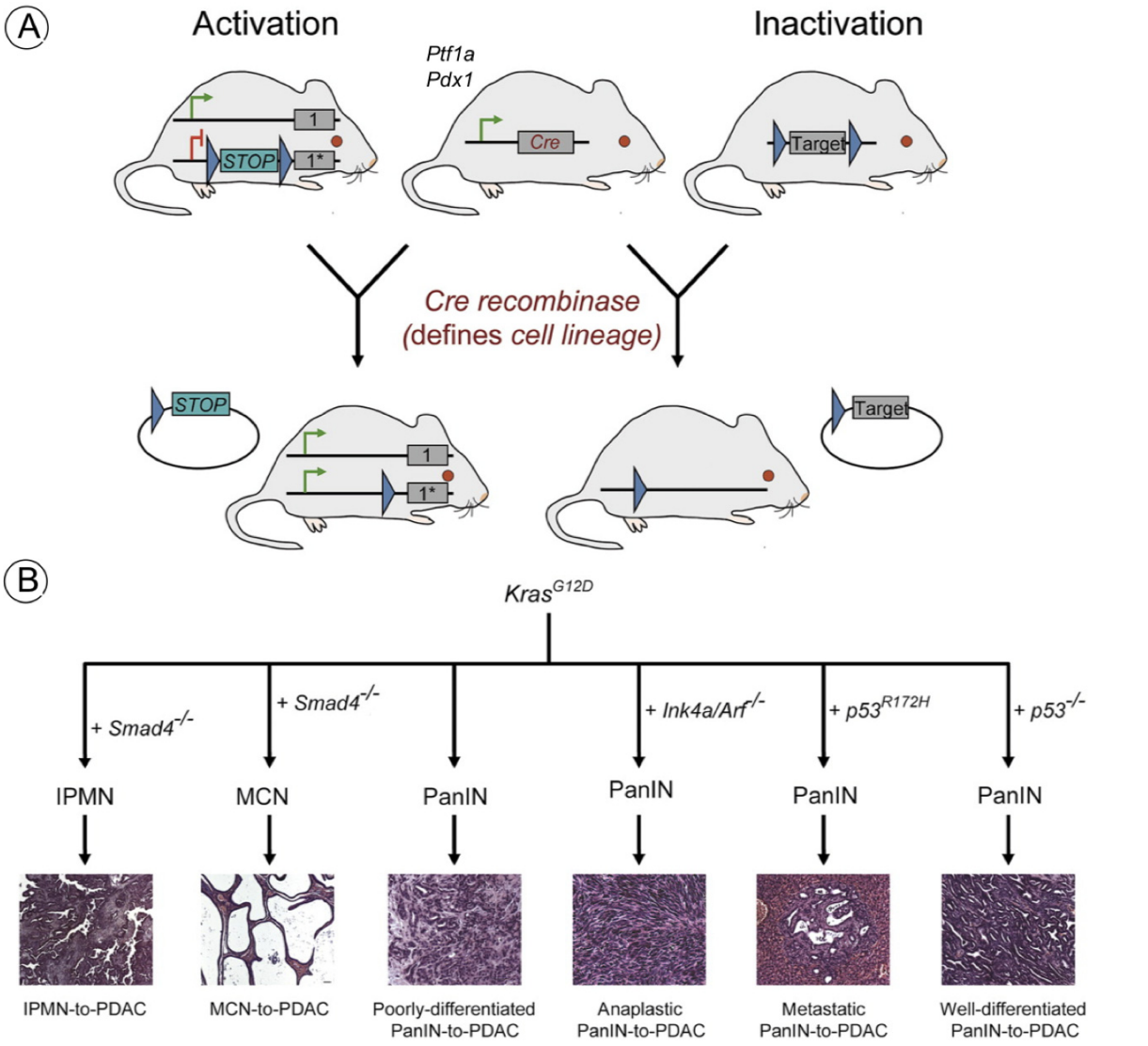

Figure 5 – (A) Cre-mediated conditional activation or deletion of oncogenes respectively tumor suppressors genes in the pancreas by using tissue-specific promoters. (B) Interbreeding KRAS^{G12D} mice with conditional knockout mice for distinct tumor suppressors, leads to development of morphologically different tumors, which resemble the human malignancy (Figure modified from Mazur et al.[8]).

Primary xenograft models

Another strategy for generating tumor-specific models is the direct implantation of primary patient tumor tissue at heterotopic or orthotopic sites of recipient immunodeficient mice. In this perspective many different types of mice have been used for xenograft establishment.

Early studies used athymic nude mice for xenografting as they facilitated monitoring of tumor development through the absence of fur [46]. However, since these mice are only T-cell deficient and otherwise still retain a more or less intact immune system, xenograft efficiency is generally low [47]. Besides that tumors grown in nude mice may be selected for certain subpopulations thus limiting analyses of the whole spectrum of tumor heterogeneity [47]. The model was improved by introduction of nonobese diabetic mice with severe combined immunodeficiency (NOD/SCID), lacking functional T and B cells [48], which improved engraftment efficiency and reduced host immune interference. A variant of these mice lacking functional NK cells by a mutation in the interleukin 2γ receptor (NOD/SCID Il2rg$^{-/-}$), allowed to further increase transplantation efficiency, ultimately permitting engraftment of single human tumor cells [49].

The advantages of utilizing primary human xenografts are the retention of tumor heterogeneity in the xenografts, recapitulation of many aspects of tumor/micro-environment interactions, maintenance of important genetic features and most importantly, faithful recapitulation of disease progression **(Figure 6B)** [47]. Human xenograft models are applied for drug-efficiency studies in pre-clinical settings [50], and have been shown to improve prediction of clinical efficacy of tested compounds [37,51,52]. Primary xenografts are a better match to the patient situation as conventional cell line derived tumors, as they recapitulate the crucial stromal compartment of PDAC, but also are genetically representing the original primary patient carcinomas.

However large-screen compound analyses are as far as impossible, as generation of a large xenograft cohort for screening libraries of ~10000 compounds is impaired by the laborious procedure. Furthermore variations are also observed in tumors generated from different implantation sites. Tumors transplanted at orthotopic sites recapitulate the characteristic histology of primary human PDAC, including vascularization and desmoplastic reaction. In contrast, tumors grown at subcutaneous sites barely develop any vascularization and are composed of huge necrotic areas (personal observation). Besides that the site of tumor sampling also plays a huge role in successful generation of primary xenografts and largely determines the course of a xenograft study.

Primary tumors are heterogeneous; therefore studies using xenograft cohorts have to ascertain that each tumor generated faithfully recapitulates the heterogeneous nature of its original tumor. In sum primary tumor xenografts accurately recapitulate the human disease, however the site of implantation and sampling site in the primary tumor has to be scrutinized carefully as they influence success of the experiment. Furthermore, as more and more immunodeficient mice are used for xenograft studies, the influence of the immune system on tumor progression is omitted in primary xenograft models.

Primary cell culture

Cancer cells derived from primary tumors have long been cultured using FCS-based techniques, however the issues of this methodology have been elucidated above. Improved methods omitting FCS for the culture of primary cells have initially been developed in neuronal stem cell research. It was shown that serum-based culture of neural stem cells (NSC) leads to an irreversible differentiation *in vitro* [53,54]. A major advance was thus the development of a culture model for NSCs based on serum-free media formulations that keeps a population of undifferentiated, multipotent neural cells growing in suspension as so called neurospheres [53,54]. Such spheres are characterized as aggregates of several ten to hundred cells that re-establish mutual contacts allowing them to form specific microenvironments. Later studies showed that this methodology can also be applied to culture normal stem cells from different organs, like mammary progenitor/stem cells [55], but also malignant "stem-like" cells from glioblastoma [56], colon [57] and pancreatic cancers [58]. Many studies comparing both spheroid and FCS-based culture concluded that the major advantage of spheroid culture lies in the preservation of the original tumor's gene expression profiles and morphology upon xenotransplantation **(Figure 6C)** [35,57,59]. However, spheroid culture has several limitations. Sphere aggregation impedes clonal analysis and treatment; large-scale miniature screens for novel drug targets are almost impossible [60]. The fact of growing epithelial cells in suspension, which in the *in vivo* setting need adhesion to avoid anoikis, is also a valid counterargument against spheroid culture.

Most problematic in the sphere environment is the spontaneous differentiation and cell death of cultured cells [60]. Newer approaches have improved the culture of primary cells by growing them in a more physiological setting on adherent substrates [60,61]. As described for spheroid culture, adherent culture of primary cells maintains stability of the genotype and morphology of the original tumors [60]. Additionally adherent culture offers several advantages over sphere culture: it provides uniform access to growth factors for all cells thereby limiting spontaneous differentiation and death of cells and can it be easily miniaturized for large high-throughput analyses. In sum, culture of primary tumor cells in the absence of FCS offers provides a closer match to the clinical situation. Hence it is thought that findings made by using such models are more easily translated to the clinic than those derived from studies on FCS-based lines.

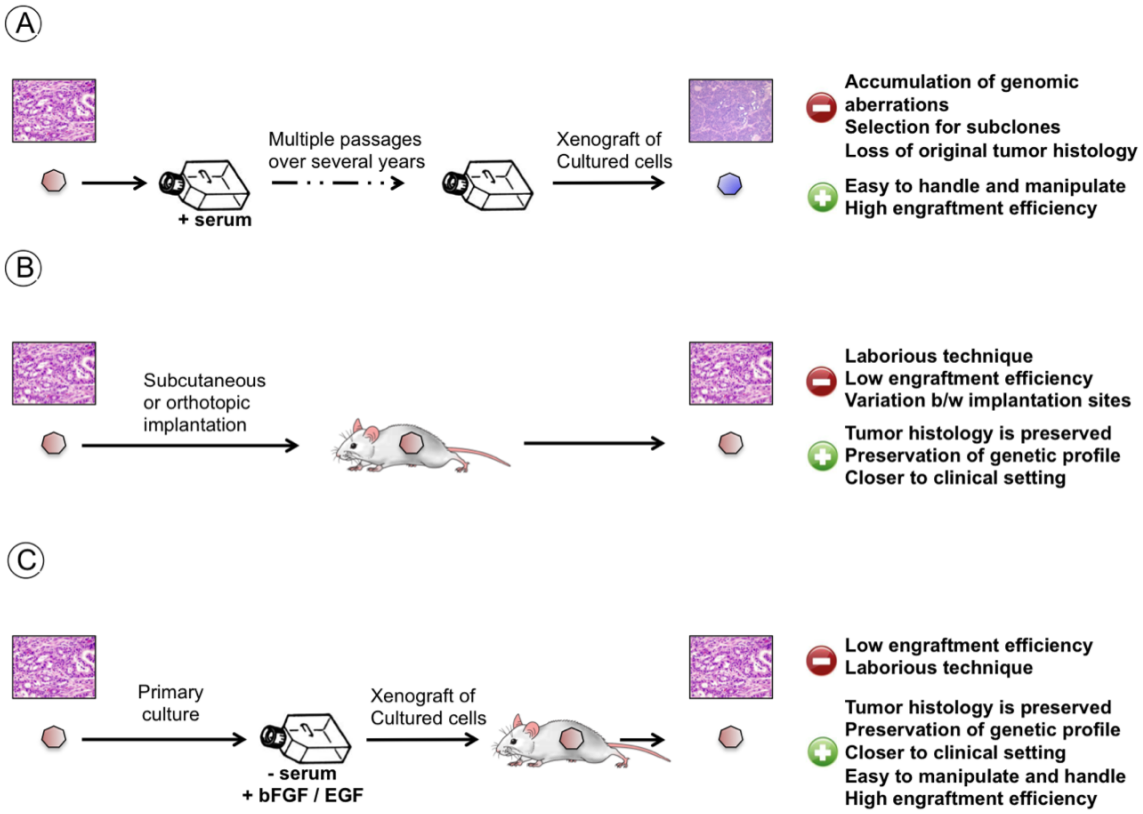

Figure 6 – Overview of different pancreatic cancer models. (A) Conventional cell culture based on fetal calf serum leads to accumulation of genomic aberrations and xenografts of these cells do not resemble the original tumor's histopathology. (B) Primary tumor xenografts retain tumor morphology and genetic profile of the original tumor but are a laborious technique and impair large-scale analyses. (C) Primary cell culture, either spheroid or adherent is complicated to set up but offers the advantage of preserving primary tumor's histology and genetic profile as well as representing the clinical setting.

Tumor subtypes

The cell of origin and cancer subtypes

Cancer was historically perceived as one disease with marked differences in histopathology, proliferative indices, genetic precursor lesions and response to therapeutics. This variability is not only observed between tumors of different tissues, but also occurs in tumors arising in the same organ (intertumoral heterogeneity) [62]. Two models have been proposed to explain such intertumoral heterogeneity: different tumor subtypes either result from genetic / epigenetic alterations occurring in the same cell **(Figure 7A)** or they arise from distinct cells within the tissue that serve as potential cell of origin **(Figure 7B)** [62]. Additionally, extrinsic factors like interaction of malignant cells with the microenvironment might also play a substantial role determining tumor heterogeneity [63]. Tumor heterogeneity might also stem from clonal heterogeneity within individual tumors. The traditional, linear model of tumor progression **(Figure 7C)** became obsolete with the large-scale sequencing of many types of cancers. Although all tumor cells originate from one single initiated cell, tumors do not consist only of one clone at a given time but rather of multiple clones **(Figure 7D)**, co-existing and co-evolving within the same tumor [64]. The existence of such clonal heterogeneity has been documented for various types of malignancies [64] including pancreatic cancer [7]. However, none of these factors are mutually exclusive, but rather act together in determining tumor behavior and diversity [62].

The first clinically applied tumor subtyping was established for breast cancer. From the beginning of the early 1970's breast tumors were subdivided according to the expression of the estrogen receptor (ER), which determined clinical therapy decision. In subsequent years additional markers such as the progesterone receptor (PR), epidermal growth factor receptor 2 (HER2/ERBB2) status as well as the proliferative index assessed by Ki67, resulted in the establishment of five distinct breast cancer subtypes [65]. Based on these subtypes, treatment decisions are made according to rather subjective clinicopathological observations of marker expression and anatomical features like tumor size, nodal status and differentiation grade. All of them are not an accurate predictor of patient response [66,67].

Even though the establishment of such therapy guidelines were a first step towards individualized therapy for breast cancer patients, resulting in a reduction in mortality since the late 1970s, they are still not sufficient for implementing personalized therapy into clinical practice.

Molecular profiling of tumors provided a deeper understanding of their mutational profile and identified distinct subtypes that might benefit from targeted therapy. This led to the development of tailored treatments like EGFR inhibition in patients with EGFR mutations in lung cancer, treatment with EGFR antibodies in KRAS-non-mutated cancers like colon and pancreas [68] or targeting of oncogenic BRAF in a subset of melanoma patients [68]. Gene expression analyses also helps to guide therapy as it identifies subgroups of patients with a significantly worst prognosis, which might need more aggressive treatment, and such with good prognosis that can be treated mildly [68]. Concurrently, these observations showed that cancer consists of a collection of different diseases that may not always be characterized by anatomical prognostic factors and histopathological features. Rather genetic characteristics of tumors should be evaluated in order to subgroup tumors and guide therapy accordingly [66]. Through the combined efforts of the Cancer Genome Atlas, the International Cancer Genome Consortium, and many individual academic projects more and more cancer genomes are getting sequenced over the next years [66]. These studies already led to the identification of novel, molecularly defined cancer subtypes in many different tumor entities [69-71]. The results obtained from these studies will help to further subgroup patients according to identical mutations and pathway activity. Furthermore they will lead to a deeper understanding of therapeutic responses to targeted agents, which will ultimately result in the development of more individualized and specific therapies.

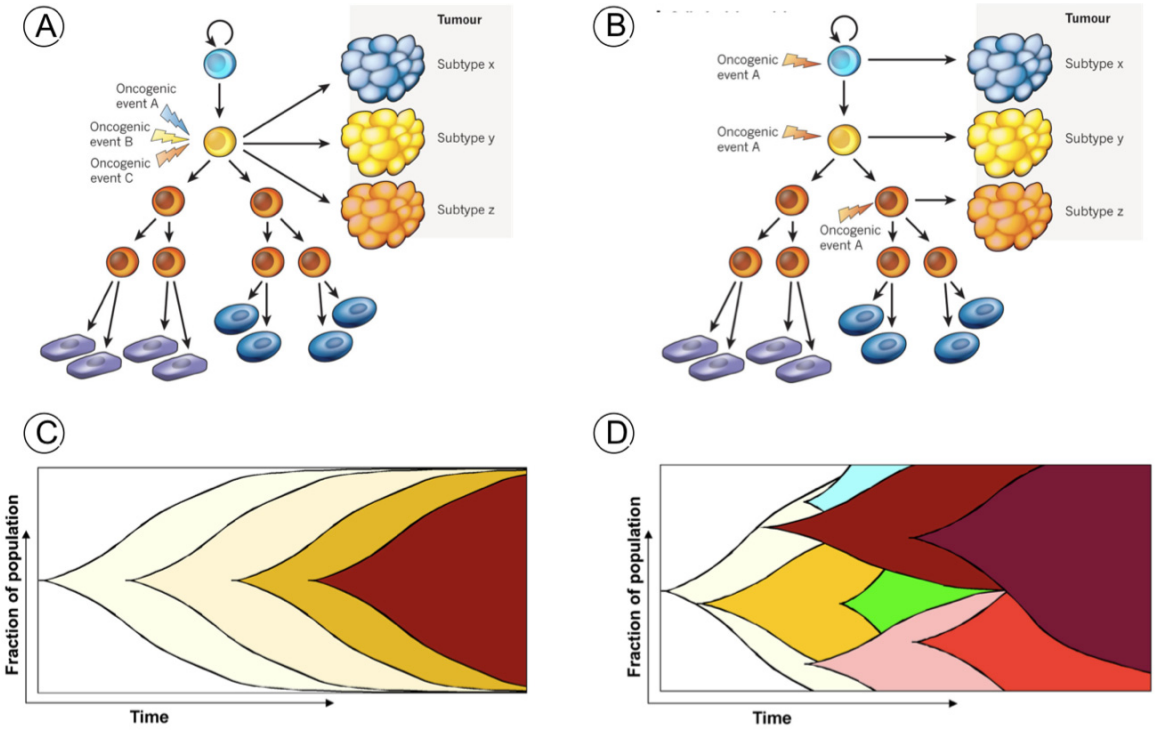

Figure 7 – Two possible models of tumor subtype development have been proposed. (A) Subtypes arise from the same cells acquiring different mutations and thus evolving differently, or alternatively (B) different subtypes evolve from distinct cells within the same tissue. (C) Tumor evolution was long perceived as linear model of clonal succession with progressive mutations in oncogenes / tumor suppressors that drive multiple rounds of clonal selection. (D) Nowadays tumor evolution is rather defined as multi-clonal model of tumor progression, with genetically divergent clones existing at the same time. As the tumor progresses, one clone might become dominant in advanced stages of tumor evolution. Increasing color intensity correlates with tumor progression, different colors represent different clones. (A,B adapted from Visvader[62] ; C,D adapted from Marusyk and Polyak[64])

The cell of origin of PDAC

For many solid malignancies, including pancreatic cancer, the cell of origin still remains unknown. One emerging hypothesis being explored in many types of cancer is that precancerous lesions arise from normal stem cells. This model has been validated for some forms of leukemia [72] and also for brain tumors [73], whereas compelling evidence has recently been presented for tumors of the lung and prostate [74].

To date, the identity of a "pancreatic stem cell" with multilineage differentiation potential remains elusive [6]. Although the histologic appearance of PDAC suggests a ductal origin, hypotheses of other cellular origins have been developed over the past years [75]. Premalignant acinar-to ductal metaplasia has been frequently observed both in humans and mice [75] suggesting an acinar origin of PDAC.

Indeed, lineage-tracing studies have shown that in the damaged pancreas, a trans-differentiation of acinar cells occurs, accounting for many newly developed ducts [76]. Other studies even proposed an endocrine origin of PDAC; expression of endocrine lineage markers and endocrine enzymes in PDAC cells hints at a developmental plasticity in pancreatic tumorigenesis [75]. In the context of a stem cell model, it still remains to be determined if PDAC may arise from a rare precursor population in the pancreas [75]. The recent identification of pancreatic cancer stem cells [58,77] might now provide an opportunity to study the identity of the cell of origin of PDAC on the premise that such a cell may serve as precursor for pancreatic cancer stem cells [6]. One potential candidate, serving as pancreatic cancer cell of origin are the centroacinar cells (CAC), located at the junction of the acinar and ductal system. The fact that the CACs are the only cell type retaining Notch pathway activity, which in the developing pancreas represses differentiation, suggests the persistence of a precursor-like transcriptional program in such cells [6].

Much has been learned from studies on mouse models, targeting oncogenic mutations to different compartments of the pancreas, thereby dissecting out the contributions of different cellular lineages to pancreatic tumorigenesis [74]. Targeting activated $KRAS^{G12D}$ to the entire pancreas using the *Pdx1* promoter, exclusively results in the development of pancreatic ductal adenocarcinomas, while islet and acinar tumors are not observed [75]. On the contrary, targeting $KRAS^{G12D}$ to the mature ductal compartment, using the cytokeratin-19 promoter, failed to produce PanIN lesions or PDACs [75], while targeting activated KRAS to the acinar compartment using *elastase* or *Mist1* promoters, yielded a spectrum of neoplasms including isolated ductal lesions with resemblance to PanIN [75]. Taken together, this suggests that the neoplastic phenotype resulting from activated KRAS expression is determined by multiple factors, including cell of origin and cellular differentiation status. From the insights gained by these models, it is tempting to speculate that transformation of a uniquely susceptible cell compartment, not located in the more differentiated compartments of the pancreas, results in pancreatic tumorigenesis [75].

Pancreatic cancer subtypes

Despite the fact that different pancreatic cancer subtypes have been described based on differing histopathological features and prognosis (**Figure 2**), the overall acceptance of these subtypes in terms of different treatment approaches is low. The first approaches of defining molecular-based subtypes of pancreatic cancer were based on its mutational spectra. Since almost 90% of PDAC tumors carry a mutation in the *KRAS2* gene [10], this led to the assessment of KRAS inhibition in pancreatic cancer. A Phase III trial including 668 patients evaluated the potency of a farnesyltransferase inhibitor tipifarnib, which inhibits posttranslational modification of the Ras kinase, in combination with Gemcitabine. The study concluded that there were no significant differences in overall survival or progression-free survival between combination and Gemcitabine mono-therapy [78]. A second study employed a different farnesyltransferase inhibitor, salirasib, in combination with Gemcitabine in a Phase I trial. This study consistently concluded that patients did not significantly benefit from KRAS inhibition treatment [79]. Both trials however did not stratify patients based on their KRAS mutational status, which might have resulted in a more favorable outcome.

KRAS mutational status has already been shown to predict effectiveness of EGFR signaling inhibition by Erlotinib in colorectal cancer [38]. The correlation of KRAS mutational status and overall survival of PDAC patients was determined in a Phase III trial evaluating the efficacy of Erlotinib treatment in PDAC patients [80]. Hazard ratio for Erlotinib in patients with mutated KRAS (78%) was 1.07, while for patients with wild-type KRAS (21%) it was 0.66. These data did not reach statistical significance due to the low number of KRAS wild-type patients, warranting further investigation in larger patient cohorts in order to evaluate if KRAS might serve as a predictive marker for Erlotinib sensitivity [38]. Another loss of function mutation which has been recently evaluated for potential clinical applicability, is the loss of *SMAD4*, which is inactivated in ~55% of pancreatic tumors [13].

A large-scale compound screen identified a single agent, UA62001, with selective efficacy in *SMAD4*-deficient cell lines [81]. This compound still awaits further investigation in pancreatic cancer.

The *TP53* gene is inactivated in as much as 50-75% of pancreatic tumors, which results in compromised G1 checkpoint activity [6,12]. One study evaluated the potency of a combination of G2/M inhibition by MK-1775 together with Gemcitabine, especially in p53-deficient tumors [51]. This study showed a selective potency of this combination in tumors with loss of p53 function, thus concluding that patients with deficient p53 might benefit from a combination of G2/M inhibition with DNA damaging agents. All of these studies assigned PDAC patients to two different subtypes based on the mutational status of a single locus, however, molecular subtypes as discussed for other tumors, are more complex. The identification of molecularly defined subtypes of pancreatic cancer has long been complicated mainly by difficulties and biases in tumor sampling. As pancreatic tumors consist of a remarkable amount of infiltrating stroma, gene expression profiles of such are often transformed by the noise generated by the cells of its microenvironment. In order to obtain profiles exclusively from pancreatic cancer cells, laborious techniques such as laser micro dissection (LMD) are necessary [82].

In a landmark study Collison et al. in 2011 generated gene expression profiles by LMD of 27 tumors and merged those with previously published datasets in order to identify three molecularly-defined distinct pancreatic subtypes – classical, QM-PDA and exocrine-like – based on a 62-gene classifier [82]. In their limited cohort of 27 patients with available clinical data, they found a significant difference in overall survival between patients of the different subtypes, with the QM-PDA subtype having the worst overall survival. Furthermore they showed a clear difference in drug sensitivity between two subtypes analyzed on available human and *de novo* generated murine cell lines. While the EGFR inhibitor Erlotinib was shown to be more potent in cells of the classical subtype, Gemcitabine was found to be more effective in inhibiting growth of cells of the QM-PDA subtype [82]. Despite screening a large collection of publicly available and *de novo* generated cell lines, none of them matched to the exocrine-like subtype.

This raised the possibility that the exocrine-like signature found in patient tumors might have been caused by contaminating cells of normal exocrine pancreas. However since the gene profiles of 27 tumors were generated by LMD this argues that only minimal contamination of non-malignant cells occurred. Therefore it can be safely assumed that the exocrine-like subtype represents a *bonafide* PDAC subtype [82].

Taken together various studies already exploited the genetic differences present in pancreatic tumors, by tailoring treatments according to distinct genetic alterations. However none of these have so far been evaluated in clinical trials or failed to significantly improve outcome of patients [9]. As for other cancer entities, molecular differences between pancreatic tumors might be more complex and the subgrouping of patients has to be based on more parameters than a single mutant locus. Collison et al. defined the first gene-expression-based PDAC subtypes and showed that a 62-gene identifier enables stratification of PDAC patients accordingly. This opens up the possibility of preclinical evaluation subtype-specific therapies and potential improvements in pancreatic cancer treatment.

Therapy resistance

Therapy resistance in cancer

Resistance of tumors and concomitant treatment failure can result from mainly two different factors: specific molecular alterations inherent to the cancer cells or host-specific factors, including low tolerance of specific drugs and inability to target drugs to sites of the tumor [83]. The genetic background of each cancer cell is vastly different in patients. Even though clonally derived, different clones can co-exist within the same tumor, as indicated above. The acquisition of mutations in distinct oncogenes and tumor suppressors, establishes expression of a multitude of different drug tolerance genes, resulting in a broad heterogeneity in resistance to anticancer drugs [84,85]. Even if not intrinsically resistant to specific drugs, the high genetic instability provides a fruitful soil for selection of drug-resistant clones during treatment. This results in outgrowth of drug-tolerant clones and thus accounts for acquisition of drug resistance observed in many types of tumors [83].

Mechanisms of resistance have been unraveled over the past few years indicating a need for targeting multiple cellular ends to eradicate cancerous cells. However, such cells all too often exhibit resistance to multiple, functionally- and structurally unrelated drugs, which makes them hard to treat. The so-called multi-drug resistance can result from changes in many molecular mechanisms within the cancer cell and include: alterations that limit intracellular accumulation of drugs thereby enhancing efflux of such, blockage of apoptosis, re-activation of DNA-repair mechanisms and alterations in cell-cycle regulators [83] **(Figure 8A)**. Another recently developed hypothesis of tumor resistance is that such resistance is inherent to a specific subpopulation of tumor cells, the cancer stem cells. For several tumor entities including pancreatic cancer, it has been shown that the tumor-initiating subpopulation of cancer cells exhibits a higher tolerance towards chemo- and radiotherapy [86,87]. Such cells not only exhibit higher expression of multi-drug efflux transporters, anti-apoptotic proteins and pro-survival pathways but also have a lower proliferative index than the bulk of the tumor cells.

One emerging hypothesis suggests that such cancer stem cells are responsible for therapy resistance and tumor relapse as they exhibit a higher tolerance towards cytotoxic drugs **(Figure 8B)**. This hypothesis has already been exemplified in hematological malignancies such as CML [88]. Treatment of CML with imatinib results in complete molecular remission in many patients, albeit its discontinuation results in high relapse rates probably owing to outgrowth of CML-stem cells [89]. Hence one promising strategy could be a combined eradication of CML-stem cells and their highly proliferative progeny in order to cure the patient [88] **(Figure 8B)**. Taken together, therapy resistance in cancer is a multifocal phenomenon, which cannot be generalized. In the future, large-scale sequencing of individual tumors will help to identify molecular targets in order to tailor individualized therapies for each patient, thereby maximizing therapy response and limiting resistance and relapse.

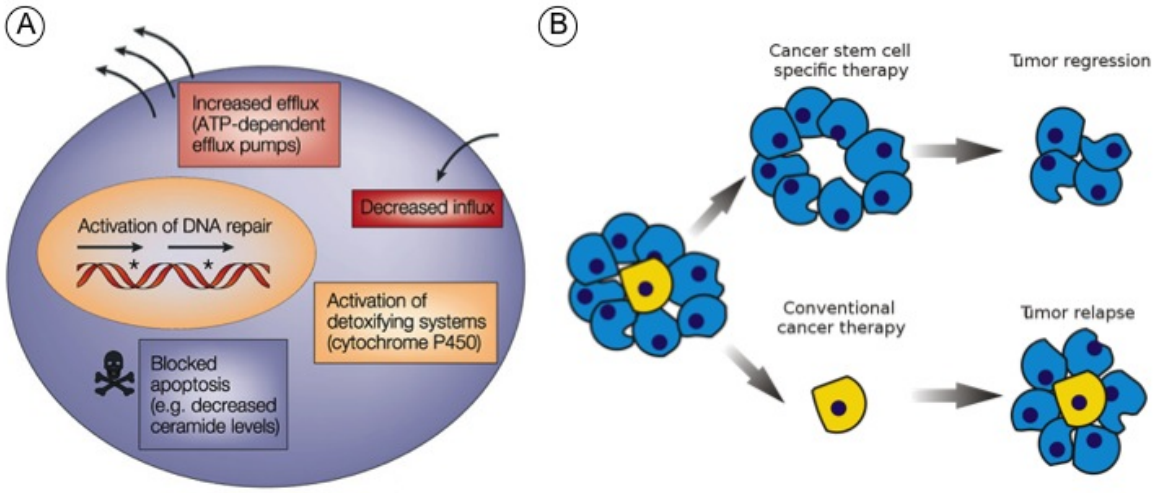

Figure 8 – (A) Cancer cells posses several mechanisms of acquired or intrinsic drug resistance like enhanced or decreased drug efflux, blocked apoptosis, hyper activated DNA repair machinery, activation of detoxifying enzymes and alike (B) Schematic illustration of cancer stem cell resistance to therapy and potential impact of specific eradication of such cells. Conventional therapy spares the cancer stem cells, which re-constitute the tumor after end of therapy. Cancer stem cell-specific drugs deprive the tumor of its regenerative pool of cells thereby leading to tumor regression (Figure (A) adapted from Gottesman [90] and (B) from Wikipedia)

Therapy resistance in pancreatic cancer

One major limitation in either conventional or targeted therapy of pancreatic cancer is the marked resistance of pancreatic cancer cells to any kind of treatment. Even though most tumors initially respond to treatment with Gemcitabine, progression free survival is less than 6 months in most cases [38]. Pancreatic cancer is not only an intrinsically highly chemoresistant tumor, the initial response to cytotoxic drugs leads to development of acquired chemoresistance against selected compounds [4]. Many possible explanations exist for these observations. One of them is that an altered balance of pro- and anti-apoptotic proteins protects the tumor cells from anti-cancer drugs by reducing the potential of such compounds [91]. Another concept of therapy resistance emerged within the last couple of years, with the discovery of so-called tumor-initiating cells not only in pancreatic tumors [77]. It is believed that these cells have a lower proliferative index than normal cancer cells and an increase in ABC drug transporter activity [92]. Upon challenge with cytotoxic regimen, tumor-initiating cells have a higher potential to survive treatment, while their highly proliferative progeny does not. After withdrawal of treatment, the tumor relapses from these tumor-initiating cells and acquires selective chemoresistance [77]. The recent sequencing of pancreatic cancers already uncovered crucial insights into the biology of PDAC und will result in the development of therapies targeting specific resistance pathways in the future.

Aim of the study

Pancreatic cancer remains the tumor with the worst overall survival worldwide with little progress in terms of novel treatments being introduced into clinical practice. A multitude of models are available for studying pancreatic cancer, however many of the therapies tested in such models fail to equally perform in a clinical setting. This can be partly explained by the failure to correctly model the disease (conventional FCS-based cell lines) or by the complexity of the model systems (direct xenografts and GEMs). Novel *in vitro* models are needed to study pancreatic cancer in a clinically relevant setting that can be easily manipulated and used for large-scale screening approaches. Recently, spheroid culture of primary tumor cells has been introduced in pancreatic cancer culture. While overcoming many of the problems of conventional cell culture, spheroid culture still precludes high-throughput screening approaches due to its complexity.

The aim of our study was the development of a monolayer, *in vitro* pancreatic cancer model that preserves the tumor heterogeneity in terms of histopathology and molecular profiles. We demonstrate that our novel system preserves the histopathological distinct features of the primary tumor as well as the tumor-specific molecular profile after xenografting. Furthermore, we showed that all three previously described PDAC subtypes are stably maintained by our model. Therefore our study provides an improved model system, based on monolayer culture that can be used for studying the biology of pancreatic cancer in a clinical relevant setting and can be applied to high-throughput analyses for identifying novel therapeutic targets in PDAC.

4 Materials and Methods

Materials

Mouse strains

NOD.Cg-*Prkdc*^{scid} *Il2rg*^{tm1Wjl} (NSG) mice were obtained from Jackson Laboratory (Bar Harbor, USA) and bred in the DKFZ animal facility. All mice were housed under specific pathogen-free conditions and used for experiments at 10-15 weeks of age. All animal care and procedures followed German legal regulations and were previously approved by the governmental review board of the state of Baden-Wuerttemberg, Germany.

Cell lines

Name	Origin	Media
BxPC3	ATCC (CRL-1687)	IMDM + 10% FCS
PANC-1	ATCC (CRL-1469)	IMDM + 10% FCS

Cell culture products

Product	Company	Catalog No.
15 ml canonical falcon tubes	TPP	Z707724
40 µM cell strainer	BD	352340
5 ml round-bottom polypropylene tubes	BD	352008
5 ml round-bottom polypropylene tubes	Sarstedt	55.526
50 ml canonical falcon tubes	Greiner	T2318

50ml reagent reservoir, sterile	Corning	4870
70 µM cell strainer	BD	352350
ART XLP 1000, 200, 10 µl Reach filter tips	VWR	732-2215, 732-2233, 732-2221
Cryotube, 1.8 ml sterile	Nunc	375418
Nalgene Freezing Container Mr.Frosty	Bunc	5100-0001
Primaria Cell Culture Flask, 25 cm²	BD	353808
Primaria Cell Culture Flask, 75 cm²	BD	353810
Primaria Cell Culture Plate, 24-well	BD	353847
Primaria Cell Culture Plate, 6-well	BD	353846
Primaria Cell Culture Plate, 96-well	BD	353872
Safe lock tubes: 0.5, 1.5, 2.0 ml	Eppendorf	13625, 12682, 12776
Serological Pipettes: 2, 5, 10, 25 and 50 ml sterile	BD	3565-07/-29/-30/-35/-50

Cell culture media

Product	Company	Catalog No.
Advanced DMEM medium	Life Technologies	12491015
Basic-FGF	Peprotech	100-18B
Bovine Serum Albumine	PAA	K35-011
CO2-independent medium	Life Technologies	18045088
Collagen	Life Technologies	A1048301
Cryostor CS10	Sigma	C2874
D-PBS	Sigma	P5368
EGF	Peprotech	100-15
FCS Gold	PAA	A11-151
Fetal Calf Serum, Origin: EU approved	Life Technologies	10270

Fungizone (Amphotericin B)	Life Technologies	15290-018
Gentamycine (50mg/ml)	Life Technologies	15750-060
Glucose 45% solution, sterile	Sigma	D8769
Growth factor reduced Matrigel	BD	354230
Heparine	Sigma	H-3149-10KU
HEPES	Life Technologies	15630106
IGF-R3	Sigma	I1271
IMDM	Life Technologies	12440061
Jagged1 recombinant	StemRD	JAG-1-pep-100
L-Glutamine 200mM (100x)	Life Technologies	25030
L-Glutathione	Sigma	G6013
Lipid-Mixture	Sigma	L0288-100ML
N-2 supplement	Life Technologies	17502048
Penicillin/Streptomycin	Sigma	P4333
Sonic Hedgehog recombinant	Peprotech	100-45
Trace Elements A, B, C	VWR	99-182-Cl, 99-175-Cl, 99-176-Cl
Water for Injection (WFI) for Cell Culture	Life Technologies	A12873-01
Y-27632	Selleck	S1049
β-Mercaptoethanol	Life Technologies	31350010

Kits

Product	Company	Catalog No.
BCA Protein Assay Kit	Pierce	23227
miRNeasy Mini kit	Qiagen	217004

Antibodies

FACS

Antigen	Clone	Company	Catalog No.
CD133 – PE	AC133	Miltenyi	130-080-801
CD44 – PE-Cy7	IM7	Biolegend	103030
CD24 – PB	ML5	Biolegend	311121
EpCAM – FITC	EBA-1	BD	347197
H2-kD – AlexaFluor647	SF1-1.1	Biolegend	116612

Isotype controls	Clone	Company	Catalog No.
AlexaFluor647 Mouse IgG2a	MOPC-173	Biolegend	400234
FITC Mouse IgG1	MOPC-21	Biolegend	400108
PB Mouse IgG2a	MOPC-173	Biolegend	400260
PE Mouse IgG1	MOPC-21	Biolegend	400114
PE-Cy7 Rat IgG2b	RTK4530	Biolegend	400618

Western Blot

Antigen	Company	Catalog No.
Actin	Sigma	A2066
Akt	Cell Signaling	4685
Akt Ser473	Cell Signaling	4060
Akt Thr308	Cell Signaling	2965
Bad	BD	610391
Bcl-2	Cell Signaling	2870
Bcl-Xl	Cell Signaling	2764

c-Src	Millipore	14-117
Donkey Anti-Rabbit IgG-HRP	Southern Biotech	6445-02
eIF4B Ser422	Cell Signaling	3591
ERK	Cell Signaling	4695
ERK1/2 Tyr202/204	Cell Signaling	4730
Goat Anti-Mouse IgG(H+L), Human ads-HRP	Southern Biotech	1031-05
Mcl-1	Cell Signaling	5453
mTOR	Cell Signaling	2983
mTOR Ser2448	Cell Signaling	5536
p110α	Cell Signaling	4249
p110β	Cell Signaling	3011
p110γ	Cell Signaling	5405
p70S6K	Cell Signaling	2708
p70S6K Thr389	Cell Signaling	9234
p85	Cell Signaling	4257
p85 Tyr458	Cell Signaling	4228
PI3K Class III	Cell Signaling	3358
Raptor	Cell Signaling	2280
Rictor	Cell Signaling	2114
S6 RP Ser235/236	Cell Signaling	4858
S6 RP Ser240/244	Cell Signaling	5364
Src Tyr419	Cell Signaling	2101
Src Tyr527	Cell Signaling	2105
Vinculin	Cell Signaling	4650

c-Src	Millipore	14-117
Donkey Anti-Rabbit IgG-HRP	Southern Biotech	6445-02
eIF4B Ser422	Cell Signaling	3591
ERK	Cell Signaling	4695
ERK1/2 Tyr202/204	Cell Signaling	4730
Goat Anti-Mouse IgG(H+L), Human ads-HRP	Southern Biotech	1031-05
Mcl-1	Cell Signaling	5453
mTOR	Cell Signaling	2983
mTOR Ser2448	Cell Signaling	5536
p110α	Cell Signaling	4249
p110β	Cell Signaling	3011
p110γ	Cell Signaling	5405
p70S6K	Cell Signaling	2708
p70S6K Thr389	Cell Signaling	9234
p85	Cell Signaling	4257
p85 Tyr458	Cell Signaling	4228
PI3K Class III	Cell Signaling	3358
Raptor	Cell Signaling	2280
Rictor	Cell Signaling	2114
S6 RP Ser235/236	Cell Signaling	4858
S6 RP Ser240/244	Cell Signaling	5364
Src Tyr419	Cell Signaling	2101
Src Tyr527	Cell Signaling	2105
Vinculin	Cell Signaling	4650

Immunohistology

Antigen	Company	Catalog No.
AIM2	Sigma	HPA031365
CEACAM3	Sigma	HPA011041
CEACAM6	Dako	A0115
CEL3A	Abcam	ab56564
CFTR	Abcam	ab2784
HNF1	Santa Cruz	sc-8986
REG1A	R&D Systems	431202
S100A1	Assay Biotech	C0318
S100P	Dako	Z0311
SLC2A3	Sigma	HPA006539
SLC4A4	Millipore	AB3212
SMAD4	Sigma	HPA019154
SPINK1	Sigma	HPA027498
TFF3	SDIX	2994.00.02
VIM	Dako	M7020

Chemical and biological reagents

Product	Company	Catalog No.
ABT-737	Selleck	S1002
Accutase	Life Technologies	A11105
ACK Lysis Buffer	Lonza	10-548E
CellTiterBlue	Promega	G8081
Dasatinib	LC Labs	D-3307
Erlotinib	LC Labs	E-4007
Ethylenediaminetetraacetic acid (EDTA)	Sigma	E9884
FiColl Paque Plus	GE	17-1440-02
Gemcitabine	LC Labs	G-4177
Halt™ Protease/Phosphatase Inhibitor Cocktail	Pierce	78440
Isofluran B	Braun	6724123.00.00
LY-294002	LC Labs	L-7962
Matrigel	BD	356234
NuPAGE® Antioxidant	Life Technologies	NP0005
NuPAGE® LDS Sample Buffer	Life Technologies	NP0007
NuPAGE® MOPS SDS Running Buffer	Life Technologies	NP0001
NuPAGE® Sample Reducing Agent	Life Technologies	NP0004
Phenylmethanesulfonyl fluoride (PMSF)	Sigma	P7626
Propidium Iodide	Biolegend	421301
Rapamycin	LC Labs	R-5000
Saracatinib	LC Labs	S-8906
Torin-1	Tocris	4247
Western Blot Stripping Buffer	Pierce	21059
DNase	Sigma	D4263

Collagenase IV	Sigma	C5138
RIPA Buffer (10x)	Cell Signaling	9806
MagicMark™ XP Western Protein Standard	Life Technologies	LC5602
Novex® Sharp Pre-stained Protein Standard	Life Technologies	LC5800
Tween 20	Sigma	P5927
Ponceau S solution	Sigma	P7170
Kinase inhibitor library	Enzo	BML-2832
Staurosporine	LC Labs	S-9300

Solutions and media formulation

Cancer Stem Cell Medium
500 ml Advanced DMEM/F12
5 ml N2 Supplement
2 mM Glutamine
1.7 ml Glucose (45%)
500 µg GSH (250 ul Stock)
500 µl each Trace Elements B, C
250 µl Trace Elements A
25 ml Sterile H_2O Cell Culture Grade
5mM HEPES for cell culture
2 µg/ml, Heparine
1ml Sigma Lipid Mixture-1
50 ng/ml hBasic-FGF
20 ng/ml hEGF
10 ng/ml IGFR3
100 µM β-Mercaptoethanol

PEB Buffer
1x PBS
1% BSA
2 mM EDTA

CBP Buffer
500 ml CO_2-independent medium
1% BSA
2 mM Glutamine

10x TBS Buffer (1L)
24.2 g Tris base
80 g NaCl
adjust pH to 7.6

20x Transfer Buffer (100ml)
10.2 g Bicine
13.1 g Bis-Tris

Laboratory equipment

Equipment	Name	Company
Analytical scale	AE163	Mettler Toledo
Caliper	Digital Caliper	Langirele
Centrifuge	5810R	Eppendorf
Flow Cytometer	BD FACS LSR Fortessa	BD
Flow hood	1300 Series A2 Class II	Thermo
Freezer -20°C	G1221	Liebherr
Freezer -80°C	Forma 904	Thermo
Fridge	Premium, Profi Line	Liebherr
Ice Machine	SCE170	Hoshizaki
Incubator	HERAcell 150i / 240i	Thermo
Microplate reader	SpectraMax	Molecular Devices
Microscope	OPMI PENTERO® 900	Zeiss
Multiwell pipet (8-well / 12-well)	Multipette Plus	Eppendorf
pH meter	S20 SevenEasy	Mettler Toledo
Pump	Vacusafe	Integra
Rotator	MACSmix™ Tube Rotator	Miltenyi
Thermomixer	Thermomixer comfort	Eppendorf
Tissue homogenizer	gentleMACS™ Dissociator	Miltenyi
Vortexer	Vortex Genie	VWR
Surgical clamps	Surgical clamp	Fine Science Tools
Suture	Safil	B.Braun

Bioinformatic tools

Tool	Version	URL
Bioconductor	2.1	www.bioconductor.org
DAVID	6.7	www.david.abcc.ncifcrf.gov
Gene Set Enrichment Analysis	3.7	www.broadinstitute.org/gsea
GraphPad Prism	5	www.graphpad.com
R	2.15	www.**r**-project.org
TMeV Experiment Viewer	4.8	www.tm4.org/mev

Methods

Xenograft methods

Human Tissue Specimen

All human tissue samples were obtained from the Department of Surgery, University Clinic Heidelberg, with written informed consent under protocols approved by the review board of the Medical Faculty of the University of Heidelberg. Pancreatic cancer tissue was collected from patients undergoing routine therapeutic surgery and was confirmed as pancreatic ductal adenocarcinomas.

Xenografts of Primary Tumor Specimens and PACO Cell Lines

To establish primary xenografts, tumors were cut into pieces of 1-2mm^3 and implanted onto the pancreatic body of NOD.Cg-*Prkdc*^{scid} *Il2rg*^{tm1Wjl} (NSG) mice, bred in the animal facility of the German Cancer Center. For the generation of xenografts from the PACO-cell lines, a suspension of 10^5-10^6 cultured cells diluted in 2 mg/ml Matrigel was prepared and injected into the body of the pancreas of NSG mice. For both transplantation of cells and tumor pieces, the mice were anesthetized by injection of Ketamine/Xylazine anesthesia solution. After a small incision on the left flank, the spleen was located and explanted with the attached pancreas. Following transplantation of the cells/tumor piece, the spleen and the pancreas were relocated into the abdomen and the incision site was closed with suture and surgical clamps.

Successful engraftment of tumors and subsequent growth was monitored by regular palpation of the implantation site. All animal care and procedures followed German legal regulations and were previously approved by the governmental review board of the state of Baden-Wuerttemberg, Germany.

Dissociation of tumor material

First passage xenografts were resected after attaining a volume of approximately 1 cm^3. Tumors were first finely cut using sterile scalpels into small pieces <0.1 mm^3 and dissociated into single cells by incubation with 1 µg/ml Collagenase IV for 2h at 37°C fixed on the

MACSMix rotator with occasional periods of vortexing. The resulting suspension was filtered through a 40 µm mesh following which cell debris and dead cells were removed by density centrifugation. Remaining erythrocytes were removed using ACK Buffer.

Cryopreservation of single cells derived from xenograft tumors

Single cell suspensions derived from xenograft tumors were cryopreserved as described for the PACO cultures.

Serial transplantation assay

Xenografts derived from PACO cells were processed into single cell suspensions as described. For analysis of serial transplantation efficacy, $5x10^5$ xenograft-derived cells were transplanted using 2 mg/ml Matrigel into secondary respectively tertiary recipient NSG mice.

Determination of *in vivo* repopulation frequency

PACO cells were processed into a single cell suspension and cell number was determined as described below. A group of five or six female NSG mice were injected with 10^4, 10^3 or 10^2 PACO cells using 2 mg/ml Matrigel at orthotopic sites. After 100 days follow-up, mice were euthanized by cervical dislocation and evaluated for tumor growth at the injection site. Tumors were fixed in 10% PFA/PBS for subsequent histological analyses. Resulting repopulation frequencies were determined using the ELDA webtool (http://bioinf.wehi.edu.au/software/elda).

Cell culture methods

Coating of tissue culture flasks

For coating of tissue culture flasks, Collagen at 50µg/ml, Matrigel at 50 µg/ml and FCS at 2% were added for to tissue-culture treated flasks for 4h at 37°C. After a wash with PBS, flasks were either directly used or store until further use at 4°C.

Generation of PACO cultures

For establishing PACO culture, single cells ($1\text{-}2x10^6$) derived from xenograft explants were seeded in T75 Primaria flasks in CSC medium supplemented with 50 µg/ml Gentamycin, 0.5

µg/ml Fungizone and 10 µM Y-27632. Adherent monolayer cultures were maintained and incubated at 37°C and 5% CO_2. After outgrowth of tumor cells, contaminating fibroblasts were removed by trypsinization with Accutase and cells were subsequently propagated in antibiotic/ROCK-inhibitor-free CSC medium. Growth factors other than in the basic CSC medium were used at 1 µg/ml for both Jagged-1 and Shh.

Splitting of PACO cultures

Medium was removed from culture flasks and 6 ml Accutase per T75 flask was added to remove the cells from the substrate. After 10-15 minutes, cells dislodged from the surface and the single cell suspension was transferred into a falcon tube as a 2:1 dilution in CBP medium. After centrifugation (1200 rpm, 5 min, 4°C), the supernatant was removed and the pellet re-suspended in 1-5 ml of CBP buffer depending on the application. Splitting ratio for classical subtype cells is 1:5 – 1:10, for QM-PDA 1:3 – 1:5 and for exocrine-like cells 1:2 – 1:5, depending on the application.

Freezing of PACO cultures

For cryopreservation of PACO cells, single cell suspensions were pelleted as described above and the resulting pellet was dissolved in Crystor CS10 and subsequently aliqouted into cryovials. The vials were placed on ice for 10 minutes after which they were transferred, placed in a pre-cooled Mr.Frosty, to the -80°C freezer. Approximately 5 hours later, the cells were placed in the liquid nitrogen tank for long-term storage.

Determination of cell number

An aliquot of cell suspension was diluted 1:10 – 1:50, depending on the expected number of cells, with trypan blue solution (0.05% w/v) to quantify the amount of viable cells. Cells were counted with a Neubauer chamber, whereas the number of viable cells was calculated according the formula:

Average cell number/chamber square x dilution factor x 10^4

Proliferation assay

PACO cells were seeded into 96-well plates at 1000 cells/well on Day 0. Cell number was determined as a measure of cell viability using the CellTiterBlue assay as described in the manual. In order to establish a baseline, the first row was evaluated 4h post cell plating, setting the derived emission values in relation to the plated cell number. Each day, subsequent rows were evaluated accordingly, thereby normalizing the derived emission values to the baseline derived from Day 0. Therefore, cell growth was expressed as a function with respect to the initial number of cells.

Determination of *in vitro* repopulation frequency

PACO cells were plated in 96-well plates in a limiting dilution assay, starting from 8000 cells per well in Row 1, diluted 2-fold in the subsequent rows. Plates were wrapped in saran wrap and incubated for 72h in a humified environment. After this incubation period, each well was evaluated for clonal outgrowth. A well was scored positive if it contained a substantial cell clone, mostly comprised of more than 10 cells. If no or only small clusters of cells (<10 cells/clone) were present, the well was scored negative. Resulting repopulation frequencies were determined using the ELDA webtool (http://bioinf.wehi.edu.au/software/elda).

Flow cytometric analysis of PACO cells and xenograft-derived cells

For staining of cell surface antigens, $1x10^6$ single cells were placed in PEB Buffer. In case of primary tumor cells and xenograft-derived tumor cells, Fc receptors were blocked by incubation at 4°C for 15 min with 50 µg/ml Intratect human IgG fraction.

For surface staining, antibodies were added in appropriate dilutions and incubated in the fridge for at least 20 minutes. Following this incubation, cells were washed with PEB buffer and filtered through a mesh prior to FACS analysis. Staining of equal amounts of cells were prepared with corresponding isotypes for each antibody. Just prior to analysis, 1 µg/ml Propidium Iodide was added for death cell exclusion.

Samples were acquired on a FACS LSR Fortessa cytometer and data was analyzed with FlowJo analysis software.

Gene expression analyses

RNA isolation

Total RNA was isolated from different PACO lines at early passage and late passage (80% confluent) or tumor tissue (30 mg) using the miRNeasy kit according the provided manual. PACO cells were directly lysed in the supplemented QIAZol Buffer, tumor tissue was submerged in the same buffer, using the GentleMACS Dissociator according the manufacturer's instruction. RNA quantity was determined using the NanoDrop, quality and integrity of the RNA samples were assessed on the Agilent Bioanalyzer, using a NanoChip. Only samples with a RNA Intergrity Number (RIN) greater than 8 were subjected to expression analysis.

Microarray analysis and data processing

Hybridization and data normalization was performed by the Genomics core facility of the German Cancer Research Center

Gene expression analysis was performed using the Illumina BeadChip Technology (HumanHT-12v4). cDNA and cRNA synthesis , hybridization and scanning was performed according to the manufacturer's instruction. Signal-to-noise ratio was very high across all chips analyzed with minimal background interference in all experiments. Raw data from the microarray analysis was background subtracted and median-normalized using the Illumina BeadStudio software workbench.

Data and gene-set-enrichment analysis

For analysis of differential gene expression and clustering we employed the TM4 Microarray Software Suite. Significant Analysis of Microarray (SAM) was used to identify differentially regulated genes between subtypes selected at a FDR < 0.05 and with a fold change of > 2. Correlation plots and respective Pearson coefficients (R^2) between samples were generated using 'R'. Gene set enrichment analysis on normalized data was conducted as described previously [93] using the complete MSig database on the Broad Institute server. Gene sets were considered significantly enriched with an FDR < 0.2.

Drug screening

Small-scale drug screen

Paco cells were seeded at 8000 cells/well 24h prior treatment. Compounds were pre-diluted in a 96-well plate in complete CSC-M with 0.1% DMSO/well at maximum with 10 µM tested for each compound. Negative (DMSO only) and positive control (20 µM Staurosporine) wells were alternated in Columns 1 and 12 of each plate. After 72h of incubation, the screen was evaluated using CellTiter Blue as described. Absolute values for percent growth inhibition/promotion were calculated using Z-values in relation to the negative/positive values on each individual plate. Data were visualized and clustered using TMeV Experiment Viewer.

Determination of individual IC_{50} values

All compounds used were dissolved in water-free DMSO according to the manufacturer's instruction at stock concentrations of 100 mM (50 mM for Rapamycin). Gemcitabine was dissolved at 1 mM in sterile buffered saline.

For calculation of the IC_{50} serial dilutions of the compounds were screened in quadruplicates, starting at 100 µM as the highest concentration. 8000 cells/well of each PACO line were seeded 24h prior to addition of individual compounds in 96-well plates. Solvent-only wells served as negative control, wells incubated with 20 µM Staurosporine as positive control. After incubation for 72h, cell viability was assessed using CellTiterBlue as described. Raw data was normalized to positive and negative controls present on each individual plate. IC_{50} values were calculated using GraphPad Prism (Graph Pad Software, La Jolla).

***In vivo* treatment**

Tumors from three model lines of each subtype were established by injecting 5 x 10^5 PACO cells subcutaneously into a cohort of 40 NSG mice. After the tumor reached a size of approximately 200 mm^3, mice were randomized into four groups of each 10 mice – Control, Dasatinib, Gemcitabine and Combination. Dasatinib was prepared in citrate/citric acid buffer (pH 3) and administered daily via oral gavage at 25 mg/kg, Gemcitabine was prepared in sterile buffered saline and administered twice weekly via intraperitoneal injection at 125 mg/kg. Control mice received vehicle only. Tumor volume was determined twice weekly via caliper measurements and calculated according the formula (length x height x width) x (π/6). Relative tumor growth was calculated for each individual tumor in relation to the volume calculated as of the start of the experiment. Significance was calculated with a 2-way ANOVA comparing the individual treatment groups, a p-Value of <0.05 was considered significant.

Immunohistology methods

Immunohistology and initial evaluation of staining and tissue morphology were performed by the department of Pathology, University Clinic Heidelberg

Immunohistology

Tumor specimens were fixed in 10% PFA overnight and embedded in paraffin. For immunohistochemistry, slides were de-paraffinized and rehydrated. Antigens were retrieved by boiling in in a steam pot at pH 6 (Dako target retrieval solution, Dako, Glostrup) for 15 min, allowed to cool for 30 min and washed in distilled water. Nonspecific binding was blocked using the Linaris Avidin/Biotin blocking Kit (Vector Labs, Burlingame) according to the manufacturers instructions. Slides were incubated with primary antibodies for 30 min, rinsed in PBS-T (PBS with 0.5% Tween-20), incubated for 20 min with the appropriate secondary antibody using the Dako REAL Detection System and rinsed in PBS-T. After blocking of endogenous peroxidase and incubation with Streptavidin HRP (20 min at RT), slides were developed with AEC and counterstained with Hematoxylin.

Primary antibodies were used at the following dilutions EMA 1:20, HNF1 1:50, Keratin81 1:100, S6 RP Ser235/236, S6 RP Ser240/244, Src Tyr419 and p70S6K Thr389 (all at 1:100) All antibodies were diluted in Dako antibody diluent and two pathologists scored all sections independently.

Tissue Microarray

The tissue microarray was constructed from patients that received partial pancreatoduodenectomy for PDAC between 1991 and 2006 at the Charité University Hospital Berlin. The use of this tumor cohort for biomarker analysis has been approved by the Charité University ethics committee (EA1/06/2004). Patient characteristics are summarized in **Appendix Table 2**.

Formalin-fixed and paraffin-embedded tissue samples were used to generate tissue microarrays as described previously [94]. Briefly, three morphologically representative regions of the paraffin 'donor' blocks were chosen. Three tissue cylinders of 0.6 mm diameter representing these areas were punched from each sample and precisely arrayed into a new 'recipient' paraffin block using a customer built instrument.

Western Blot methods

Cell lysis

PACO cells were seeded into T75 flasks and grown till 80-90% confluence. After three washing steps with ice-cold PBS, remaining PBS was drained and 400 µl of 1x RIPA Buffer supplemented with 1x HALT Proteinase/Phosphatase Cocktail, 1mM EDTA and 1mM PMSF was evenly dispersed onto the cells. Flasks were incubated for 5 minutes on ice with occasional rocking of the flask. After the incubation, the cells were scraped with sterile spatulas and the resulting homogenate was transferred into a pre-cooled Eppendorf tube. The lysate was vortexed at full speed for one minute and transferred into a pre-cooled centrifuge (15 min, 20.000 rpm). The resulting supernatant was transferred into a new Eppendorf tube and separated in 20 µl aliquots. Protein content was determined with a BCA Protein Assay as described in the manufacturer's protocol.

Immunoblotting

Samples were prepared for western blotting prior to loading the gel. 20 µg per sample were mixed with 1x SDS Buffer and 1x reducing agent and heated to 70°C for 10 minutes. After that, the sample was loaded onto a NuPage 4-12% Bis/Tris Gel. A mixture of 2 µl MagicMarkXP and 10 µl Per-Stained Marker was loaded in the first well of each gel and served as marker for determining molecular weight of the detected proteins. Gels were run in 1x MOPS Buffer as described by the manufacturer for 1 h at 120 V/250 mA. Blotting of proteins to nitrocellulose membranes was performed as depicted in the NuPage manual as a wet-blot setup for 2 h at 25V/300mA using transfer buffer as described above. A brief Ponceau S staining prior to blocking of the membrane verified successful transfer of proteins to the membrane.

Membranes were blocked by incubating for 2h at room temperature on an orbital shaker with TBS + 0.1% Tween (TBS/T) + 5% milk. After that the blot was washed 5-times 5 minutes with TBS/T. Primary antibodies were diluted as indicated in the datasheet in TBS/T + 5% milk, in case of phospho-antibodies, 5% BSA was used instead, and incubated at 4°C over night. After another wash (5-times 5 minutes with TBS/T), isotype-matched secondary antibodies were incubated at 1:10000 dilution in TBS/T + 5% milk for 1h at room temperature. After a final wash (5-times 5 minutes with TBS/T), blots were developed using ECL development reagent. An initial 10-second exposure was used to determine the proper exposure time.

Re-probing of blots

Blots were stripped using 10 ml of Stripping Buffer as indicated in the manual. After a brief wash with TBS/T, the membrane was blocked with TBS/T with 5 % milk and re-probed with the desired primary antibody as described above. Blots were generally re-probed only three times until they were discarded.

5 Results

A model system that preserves the heterogeneity of human PDAC

Establishing a primary xenograft model for pancreatic cancer

We set out to establish an improved *in vitro* culture model for pancreatic cancer that better recapitulates the original patient's disease compared to conventional cell lines. At first we investigated the efficiency of growing cells directly isolated from individual tumor tissue specimens. However, none of these cultures resulted in outgrowth of tumor cells (data not shown). Hence, we decided to first establish a murine xenograft model, by transplanting small tissue pieces onto the pancreatic body of immune-deficient NOD.Cg-*Prkdc*^{scid} *Il2rg*^{tm1Wjl} (NSG) mice **(Figure 9A)**. This allowed us to assess the quality of the obtained clinical specimen and verify the histopathology of each successfully grafted tumor. Moreover this step also enabled us to expand the primary tumor mass, as clinical specimens were small. During the period from May 2009 until March 2012 we obtained a total of 39 primary pancreatic tumor samples from the Department of Surgery, University Clinic of Heidelberg. Of those 27 (69%) were histologically verified as pancreatic ductal adenocarcinomas, the remaining 12 tissue samples were autoimmune pancreatitis type 4 (1), mucinous adenocarcinoma of the pancreas (2), adenosquamous carcinoma of the pancreas (2), undifferentiated pancreatic carcinoma (1), neuroendocrine pancreatic cancer (1), acinus cell carcinoma (2), IPMN (1), cystadeoma (1) and cholangiocarcinoma (1) **(Appendix Table 1)**. From each of these 39 tumors, at least six mice were transplanted with 1-2 mm^3 pieces of tissue, within 4 hours after surgery **(Figure 9B)**. Of all the tumors transplanted, we were able to successfully develop xenografts from 17 individual tumors (44%) of which 16 were classified as pancreatic adenocarcinoma (94%), the remaining one was adenosquamous carcinoma of the pancreas (PT10) **(Appendix Table 1)**.

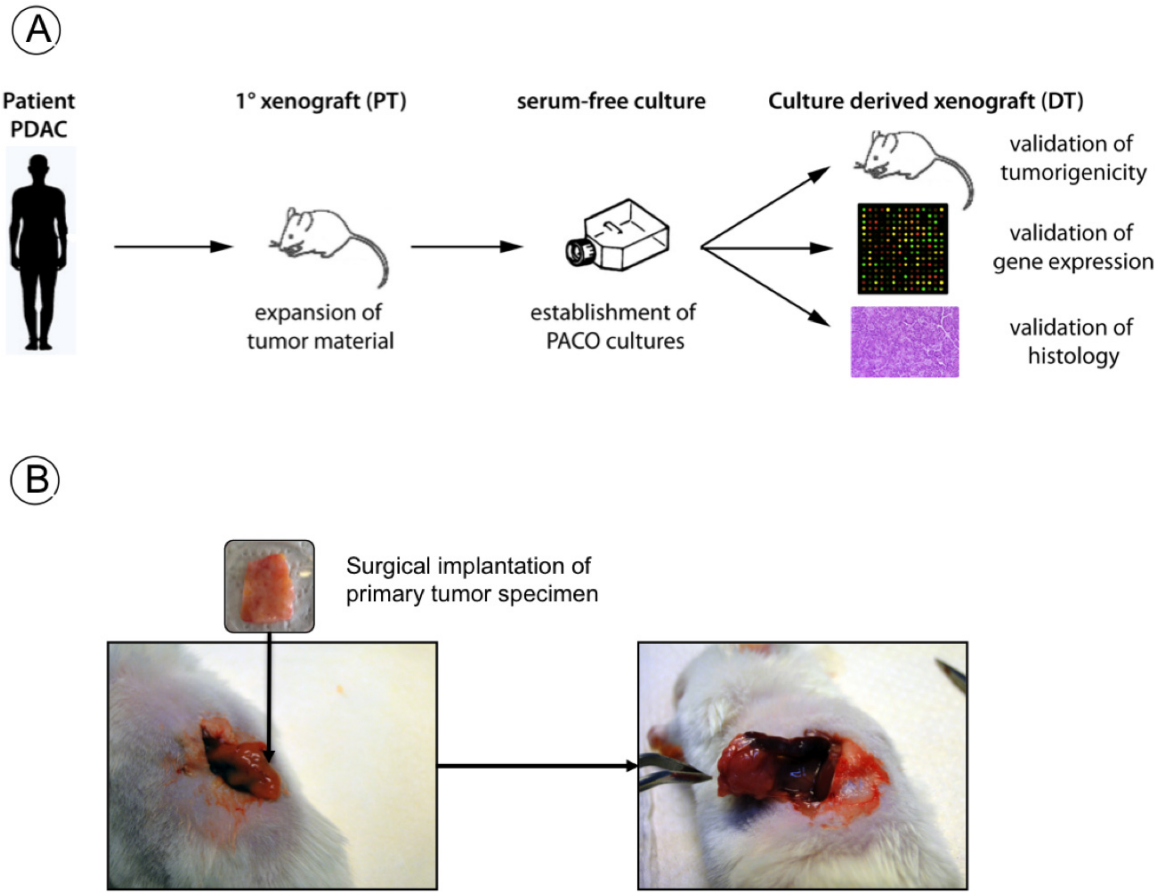

Figure 9 – (A) Schematic overview of the experimental workflow for generating xenografts and PACO cell lines. (B) Schematic representation of the orthotopic transplantation procedure of primary human specimen onto the pancreas of NSG mice

The median latency of xenograft development was 139 (+/- 51) days until a palpable mass could be detected. At the time of excision, the volume of primary xenograft tumors ranged from 0.3 – 1.5 cm^3. We observed that all of the xenografts infiltrated into the murine pancreatic tissue and were localized to the implantation site **(Figure 10)**.

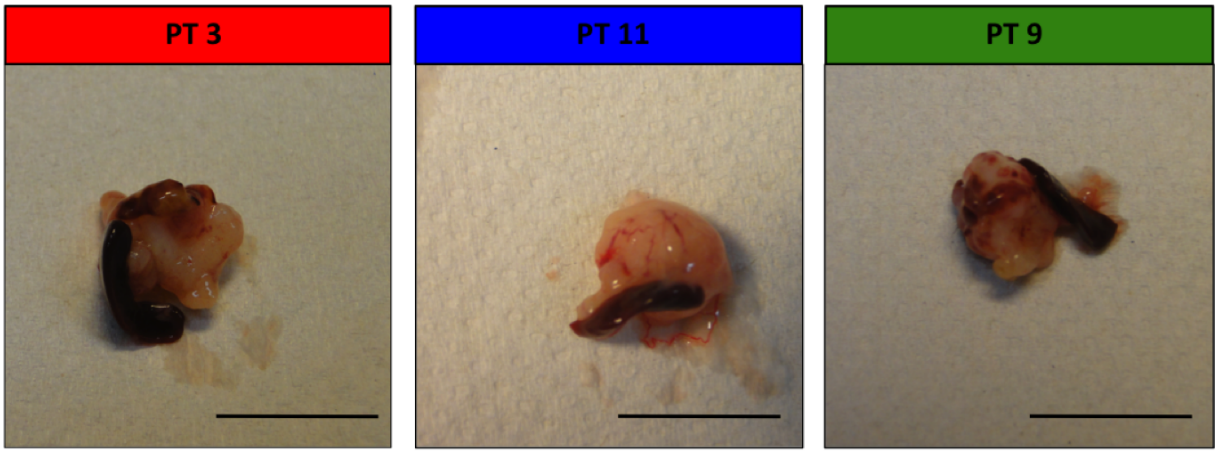

Figure 10 - Representative images of three primary xenograft tumors (PT3, PT11 and PT9) generated by orthotopic transplantation of primary tumor specimen (highlighted in Figure 8B) in NSG recipient mice (scale bar 1 cm)

Comparison of the original patient tumors with the corresponding xenografts of primary recipient mice (PT) revealed that typical histopathological features of PDAC were well conserved in the xenograft tumors **(Figure 11).** Strikingly, we noted differences in the histopathology between individual patient tumors. Some tumors (PT3, 7, 13, and 39) were poorly differentiated, containing cells with large cytoplasm, anisomorphic to pleomorphic nuclei and abundant mitoses with abnormal spindle formation [95]. Another group of tumors (PT8, 9, 11, 12, 19, 21, 24, 25, 30, 32, 36 and 38) showed a more differentiated growth pattern of medium-sized neoplastic duct-like structures with only moderate variation in nuclear size and chromatin structure [95]. Even though the characteristic stromal compartment present in the primary carcinomas was also present in the xenograft tumors, the amount of cancer cells, as assessed by histology, was shown to be higher in the xenograft tumors compared to the patient tumors.

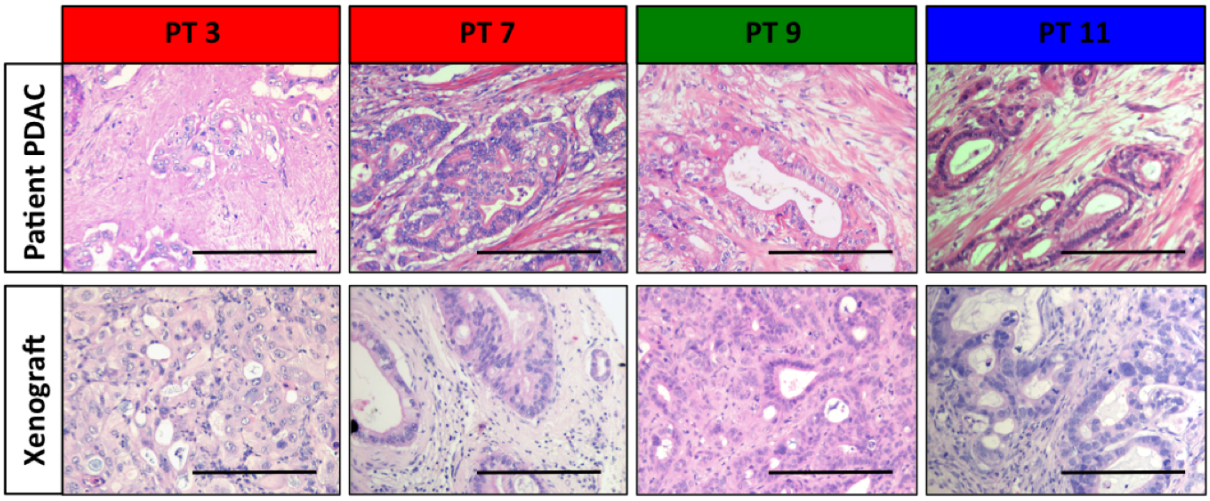

Figure 11 - H&E staining of four primary human PDAC tumors (first row) and corresponding first passage xenograft tumors (second row). Note that all xenograft tumors retained the characteristic, morphological features of the corresponding primary tumor (scale bars 100 µm).

Establishing a primary *in vitro* culture system for pancreatic cancer

Having established primary xenografts of PDAC specimen, we sought to use low passage primary xenografts for the development of a primary cell culture model as they contained a substantial higher amount of cancer cells as depicted above. Once the xenograft tumor had grown to a volume of around 1 cm^3 it was resected and enzymatically disaggregated to obtain a single cell suspension. Dead cells and debris were removed via density centrifugation; viability of the obtained single cell suspension was generally ranging between 80 – 90% as determined by Trypan-blue staining. Single cells were subsequently plated at a concentration of 1 – 2 x 10^6 cells per 75 cm^2 flask in a serum-free media formulation [59] **(Figure 9A)**.

Initially we tested several substrates and growth factors additionally to the basic stem cell medium (SCM) in order to determine the best condition for the culture and expansion of a pure population of human PDAC cells **(Table 2)**.

Table 2 – Summary and results of the different combinations of substrates and growth factors tested to establish a primary culture of pancreatic cancer cells

Substrate	Basic SCM	+ Jagged1	+Shh	+Jagged1/Shh
Primaria	+++	+++	+++	+++
2% FCS	++ F	++ F	++ F	++ F
10 µg/ml Collagen	+ F	+ F	+ F	+ F
25 µg/ml Matrigel	+	+	+	+
Ultra-low attachment	- F	- F	- F	- F

+++ High amount of epithelial tumor cells growing
++ Medium amount of epithelial tumor cells growing
+ Outgrowth of a small number of epithelial tumor cells
- No significant outgrowth of epithelial tumor cells
F Significant outgrowth of fibroblast-like cells

The results of this initial test are summarized in **Table 2**. In general we detected outgrowth of epithelial-like clusters with interspersed growth of fibroblast-like cells within a mean 14-21 days. We observed that the PDAC cells attached on every substrate tested, however with differing frequency. While more cells attached on both Primaria and FCS-coated flasks **(Figure 12AI,IV)**, Matrigel- and Collagen-coated flasks promoted attachment of a significantly lower amount of PDAC cells **(Figure 12AII,III)**. Additionally we observed that a larger fraction of fibroblast-like cells was growing on plates coated with these substrates, suggesting that they not only promote tumor cell attachment but cell attachment in general. We also tested conditions that have been used previously to culture and expand primary human PDAC cells [58]. However we found that spheroid culture on ultra-low attachment flaks promoted significant outgrowth of fibroblast-like cells, as assessed by FACS **(Figure 12AVI** and data not shown).

Importantly spheroid culture impairs the morphological distinction between fibroblast-like cells and epithelial cells, as both types of spheres appear identical.

When we compared both superior substrates, Primaria and FCS, we noted that in FCS-coated flasks, a higher proportion of fibroblast-like cells attached to the substrate **(Figure 12AV)**. Unlike Primaria flasks, where these cells could be sequentially removed by trypzinization, these cells persisted in the FCS-coated flasks.

We also tested several growth factors additionally to the factors bFGF, EGF and IGFR3, which are included in the basic SCM. Here we focused on factors that activate important signaling pathways in PDAC [6] – Jagged1 for NOTCH signaling and Shh for Sonic Hedgehog signaling. However we found neither a significant difference in the number of outgrowing cells in any combination we tested, or in the morphology or growth behavior of these cells **(Figure 12B)**.

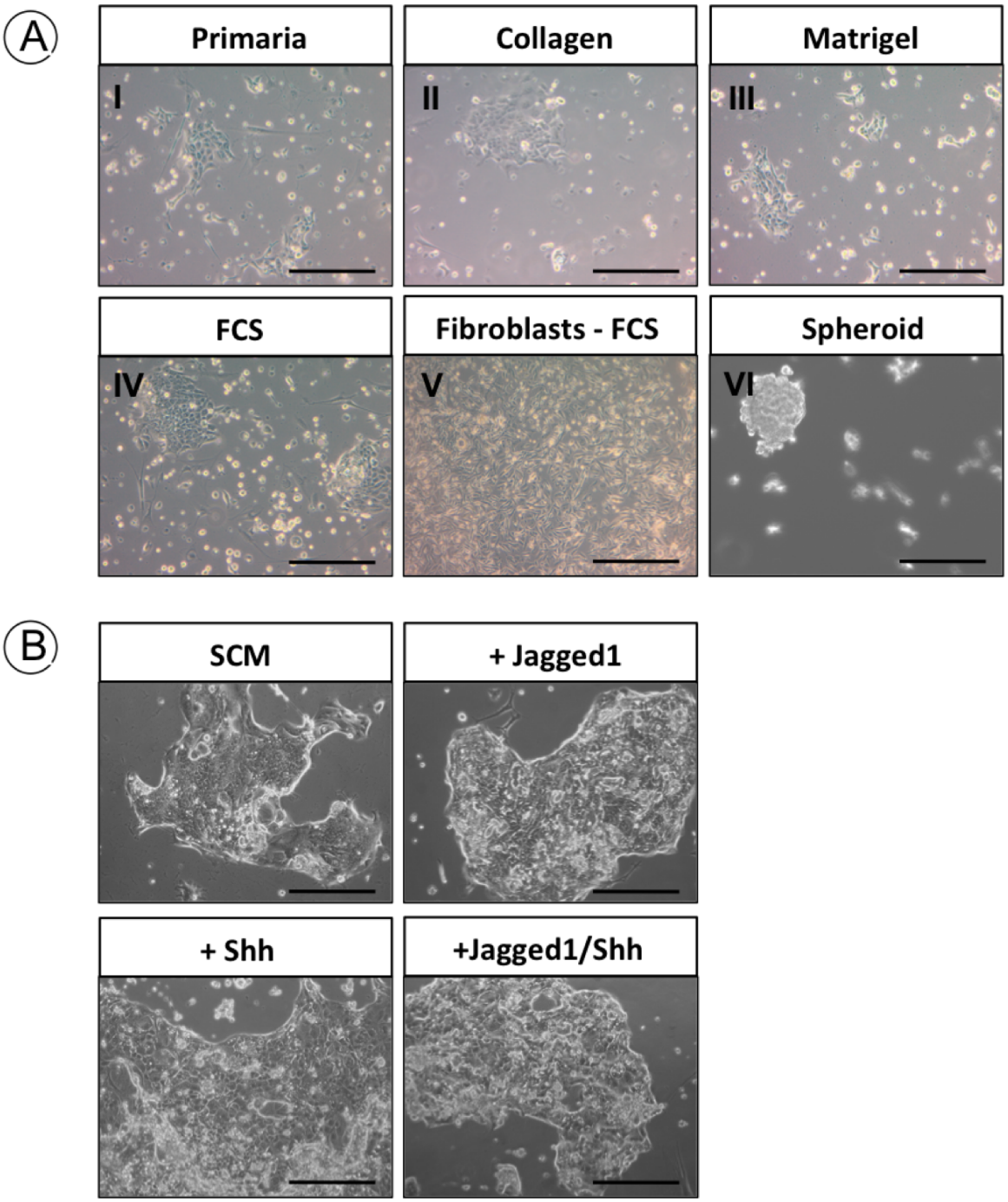

Figure 12 - (A) Exemplary images of cultured cells derived from a primary PDAC xenograft (PT24) on differently coated flasks. (B) Exemplary images of cultured cells derived from a primary PDAC xenograft (PT11) with the addition of several growth factors to the basic stem cell medium (scale bars 100 µm).

Hence we used the basic SCM together with the Primaria coated flasks for establishing a primary human PDAC culture in all our subsequent studies.

By using these conditions, we were able to establish stable lines from twelve out of 16 primary PDAC xenografts, which were termed PACO (**P**ancreatic **A**deno**C**arcin**O**ma). Successive rounds of trypsinization removed contaminating fibroblast-like cells, which were shown to be of murine origin by a positive staining for the pan-MHC marker H2-kd (data not shown). This resulted in a pure population of epithelial, human cells, exemplified by a positive staining for the human epithelial marker EpCAM **(Figure 13)**.

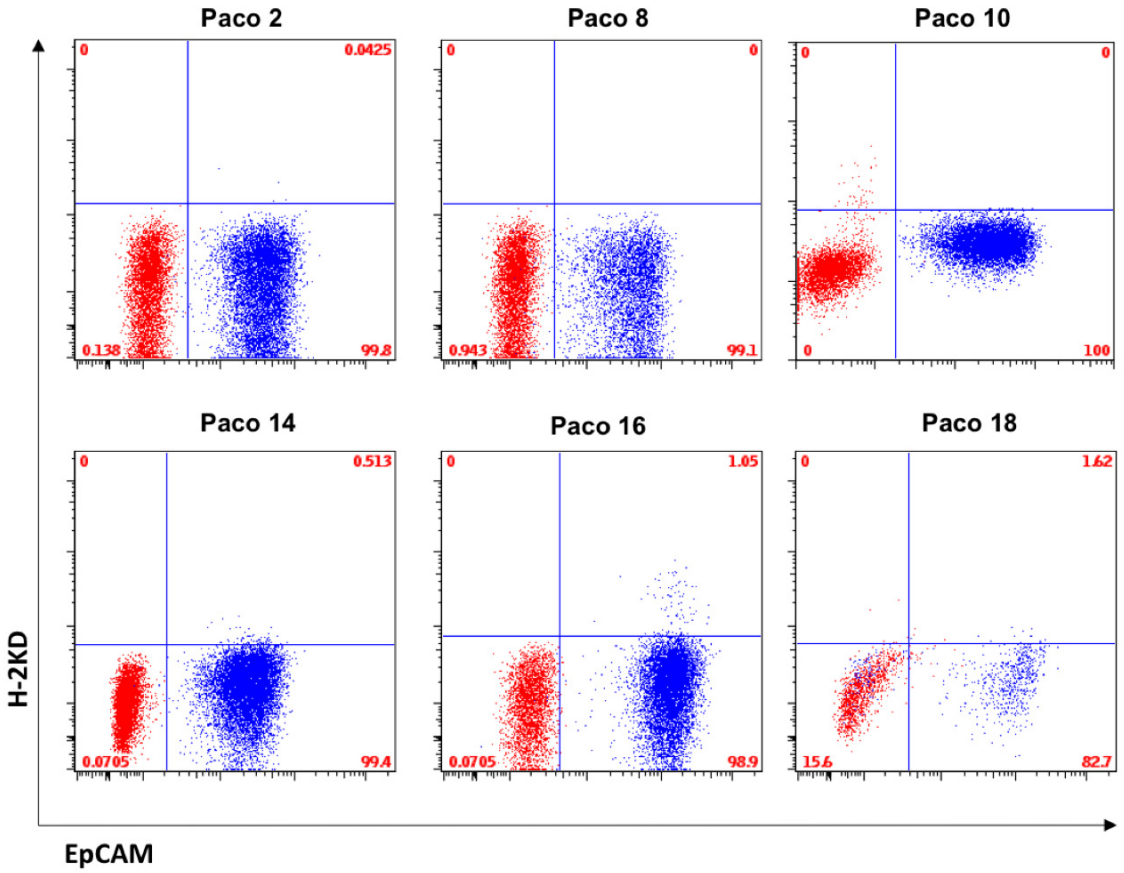

Figure 13 - FACS analysis of PACO cell lines (PACO 2, PACO 8, PACO 10, PACO 14, PACO 16 and PACO 18) revealed that PACO cultures exclusively consist of human, epithelial cells. (Displayed are representative FACS plots for all the PACO lines in our study; blue denotes specific staining, red corresponding isotype)

Surprisingly, the differences we discovered in cellular morphology of our xenografts were also reflected in the different PACO cultures. We observed marked discrepancies in the morphology and growth behavior of the individual PACO lines. One group of PACO cells (PACO 2, 3, 10, 14, 16, 17, 18 and 19) derived from tumors with a well-differentiated histology, grew in small clusters displaying a strict epithelial like growth pattern **(Figure 14)**.

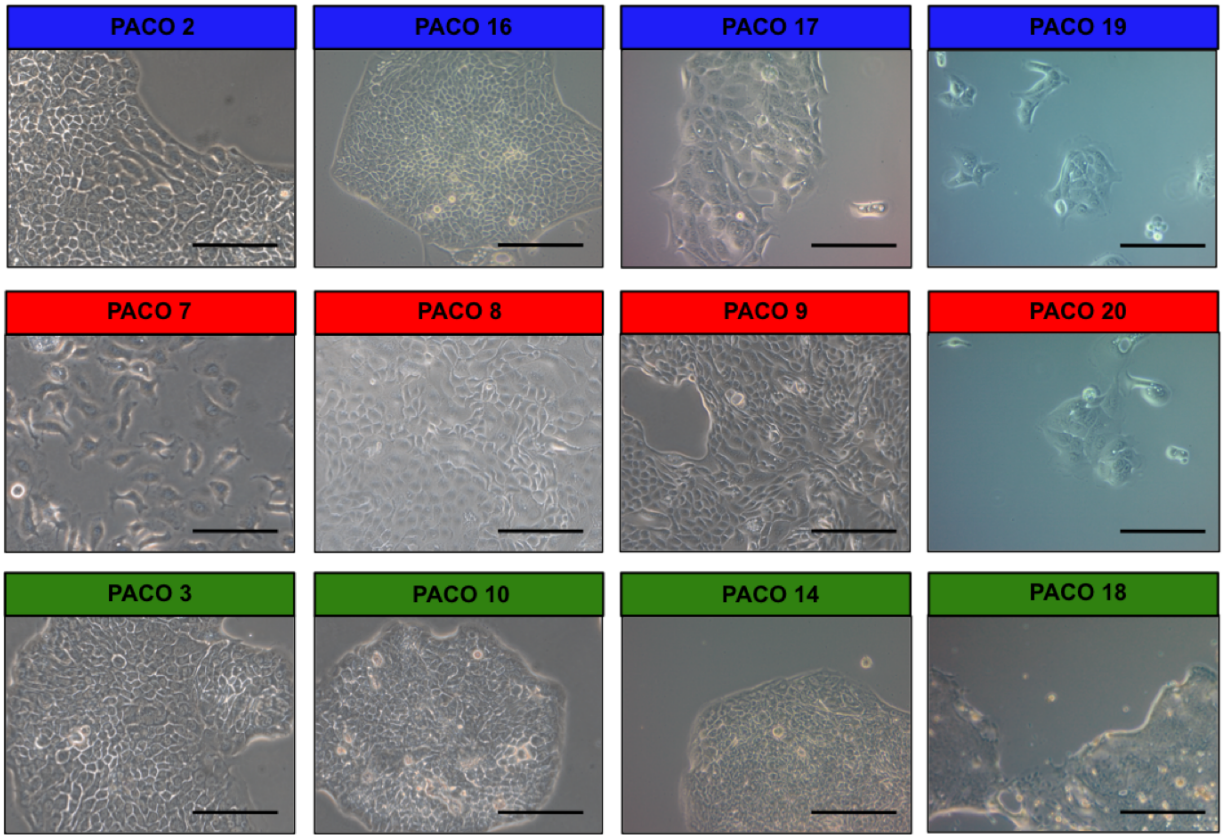

Figure 14 – Representative images of the different cell lines established in this study (scale bar 100 µm).

These clusters consisted of cells with a high nucleus to cytoplasm ratio, very much reminiscent of iPS / eSC cultured cells. The remaining group of cells (PACO 7, 8, 9 and 20) closely mirrored the undifferentiated histology of their primary tumors, as they displayed a loss of epithelial traits, resembling spindle-shaped cells with a low nucleus to cytoplasm ratio **(Figure 14)**.

Interestingly, when we analyzed the growth pattern of these individual PACO cultures, we observed a significant difference in proliferative indices between the lines that displayed an epithelial-like growth pattern.

While one group of lines (PACO 2, 16, 17, 19) was highly proliferative, the remaining four PACO lines (PACO 3, 10, 14, 18) displayed only a growth rate half of that. PACO cells displaying a "de-differentiated" morphology had a rather intermediate growth pattern compared to both other groups **(Figure 15A)**.

Thus we were interested if this difference in proliferation was reflected by differences in the capacity of clonal outgrowth. Therefore we analyzed the *in vitro* clonogenicity of the individual PACO cell lines **(Figure 15B)**. Intriguingly, PACO cells that showed a lower growth rate conversely showed a higher repopulation frequency than cells with a higher proliferative index. Cells with the de-differentiated morphology consistently had the lowest clonogenic potential *in vitro*. We also analyzed the cell cycle status of different model PACO lines. Even though we did not detect significant differences between the individual lines, we consistently observed that the majority of PACO cells remain in G0/G1. We also confirmed our findings that the PACO lines with epithelial growth behavior could be separated into a high-proliferating and low-proliferating group. PACO cells for which we observed a significantly slower growth rate (PACO 3 and PACO 10) also had less cells in active cell cycle (G2/M and S phase) compared to faster growing cells (PACO 2 and PACO 16) **(Figure 15C,D)**.

Given the molecular discrepancies between the individual PACO lines, we asked whether this could be explained by differences in the expression of tumor-initiating cell (TIC) markers. For pancreatic TICs both CD133 and CD44/CD24 positivity has been associated with tumor-initiating capacity [58,77]. We analyzed all lines for the expression of CD133 and CD44/CD24 by FACS and found no significant correlation of clonogenicity and marker positivity. All lines assayed expressed the published TIC markers at comparable levels (CD133 range 90.2-99.4%; CD44/CD24 80.4-95.7%) (**Table 3, Figure 18**). Of note, both PACO 2 and PACO 8 did not express CD133.

Taken together we established a novel pancreatic cancer culture system (PACO) using primary human tumor cells derived from low-passage PDAC xenografts. Our data showed that the individual PACO lines largely differ in morphology, proliferation and clonogenicity but in contrast have a uniform expression of reported TIC markers.

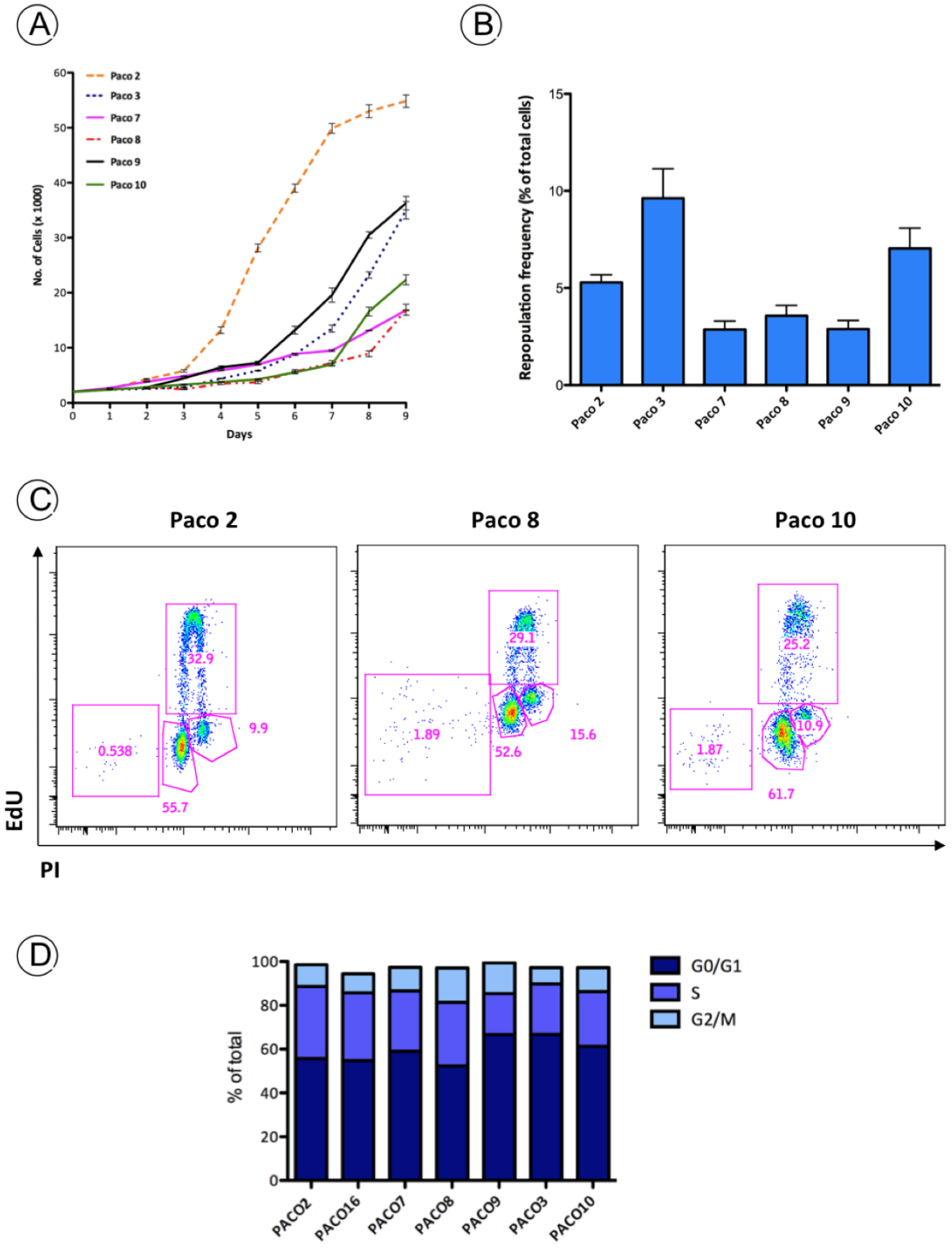

Figure 15 - (A) Analysis of the growth pattern of different model PACO lines showed that they differ in their proliferation index and their (B) *in vitro* repopulation frequency. (C-D) Cell cycle analysis of different model PACO lines confirms the differences in growth behavior as observed in (A)

Table 3 – CD133 and CD44/24 frequency of individual PACO lines as determined by FACS

Cell Line ID	CD133 (+)	CD44 / CD24 (+)
PACO 2	0%	90%
PACO 3	86%	98%
PACO 7	88%	91%
PACO 8	0%	94%
PACO 9	93%	93%
PACO 10	91%	91%
PACO 14	99%	98%
PACO 16	96%	99%

PACO cells preserve the primary tumor heterogeneity upon xeno-transplantation

Having established a primary culture model from low passage, primary pancreatic tumor xenografts, we analyzed whether the PACO cells were able to form tumors in secondary recipient mice. Here we were especially interested if, given that the cells retain the capacity to form tumors, the PACO derived xenografts, closely recapitulate the original primary xenograft's histopathology and gene expression profile **(Figure 9A)**. We therefore injected cell suspensions ranging from 1 – 2 x 10^6 cells diluted in 2 mg/ml Matrigel, into the pancreatic body of NSG mice. We could show that all of the twelve PACO lines we generated retained the capacity to form xenograft tumors. Interestingly, the morphological heterogeneity already observed in the primary tumor xenografts was very well conserved in the PACO derived xenografts (PACO-DT) **(Figure 16A)**. As described for the primary xenografts, we were able to separate the tumors into two morphologically distinct groups – one group of well-differentiated tumors and one group of de-differentiated tumors.

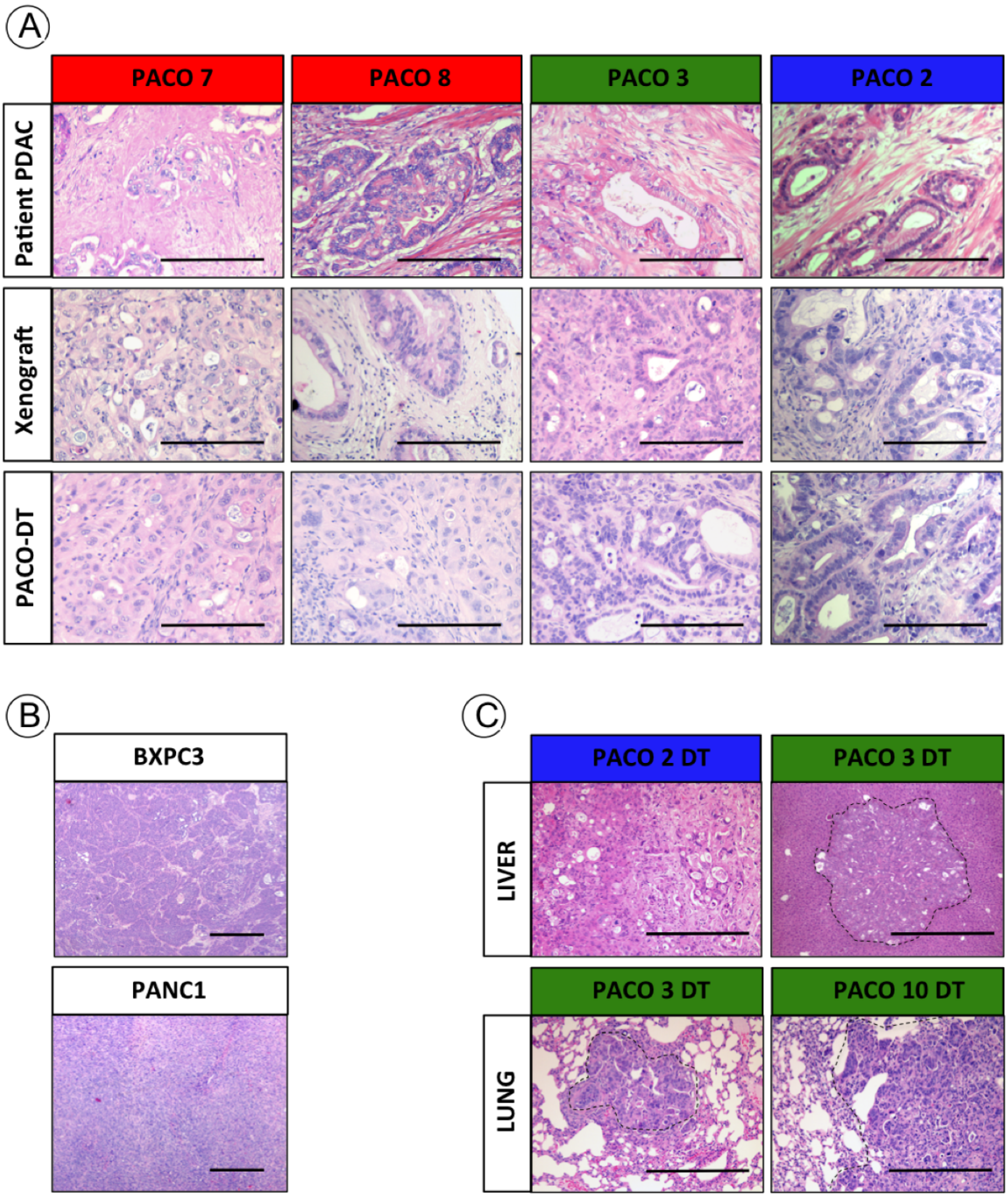

Figure 16 - (A) Characteristic morphological features present in the primary human PDAC (top) and corresponding primary xenografts (middle row) are very well retained in tumors generated from the PACO lines (bottom row). Note that morphological features like e.g. ductal structures present in PACO 3 and PACO 2 corresponding primary PDACs are retained in the PACO derived tumors (B) Xenografts from conventional cell lines do not display a morphology reminiscent of human PDAC (C) Spontaneous metastases to the liver (top) and lung (bottom) of individual PACO derived tumors (scale bars 100 µm)

Likewise, comparison of the original patient tumors with the corresponding primary xenografts PACO-DT xenografts revealed that typical histopathological features of PDAC were well conserved in the model system **(Figure 16A)**. Noteworthy, even though the PACO culture maintains a 100% human epithelial culture, as depicted above, PACO-DT xenografts however develop the characteristic stromal compartment of PDAC. These morphological hallmarks, especially the stromal component, are barely present in xenografts derived from conventional cell lines **(Figure 16B)**.

As for the PACO cultures, we observed a significant difference in growth behavior of PACO-DT xenografts. While the median latency of tumors grafted from cells of the "faster-proliferating" group (PACO 2, 16, 17, 19) was 70 days, cells of the "slower-proliferating" group (PACO 3, 10, 14, 18) grafted with a median latency of 139 days **(Table 4)**.

The PACO-DT tumors also displayed differences in their metastatic potential. We were able to detect spontaneous metastasis formation in 4 out of the 12 different PACO lines once orthotopically grafted in NSG mice. While PACO 3 and 10 both developed liver and lung metastases, both PACO 7 and PACO 16 exclusively developed liver metastases **(Table 4, Figure 16C)**. We could not find a significant correlation of metastatic capacity with either proliferation rate or differentiation status of the corresponding primary tumors. We next were interested whether the PACO-DT xenografts retain their tumorigenic potential *in vivo* and thus prepared secondary (2°) and tertiary (3°) transplantations of single cells derived from respective PACO-DT tumors. We found that all the PACO-DT xenografts retain their *in vivo* tumorigenic potential for at least three passages, while maintaining the individual tumor's histopathology **(Figure 17A)**. Apart from this we were also interested if a single cell was able to regenerate the morphologic heterogeneity observed in the primary xenografts. Therefore we prepared single-cell sorted, clonal lines of both PACO 2 and 3 and transplanted those into NSG mice. When we compared the histology of the resulting tumors with the corresponding primary and bulk-PACO-derived xenografts we found that the clonally derived cell lines again stably maintained the original tumor's morphology **(Figure 17B)**.

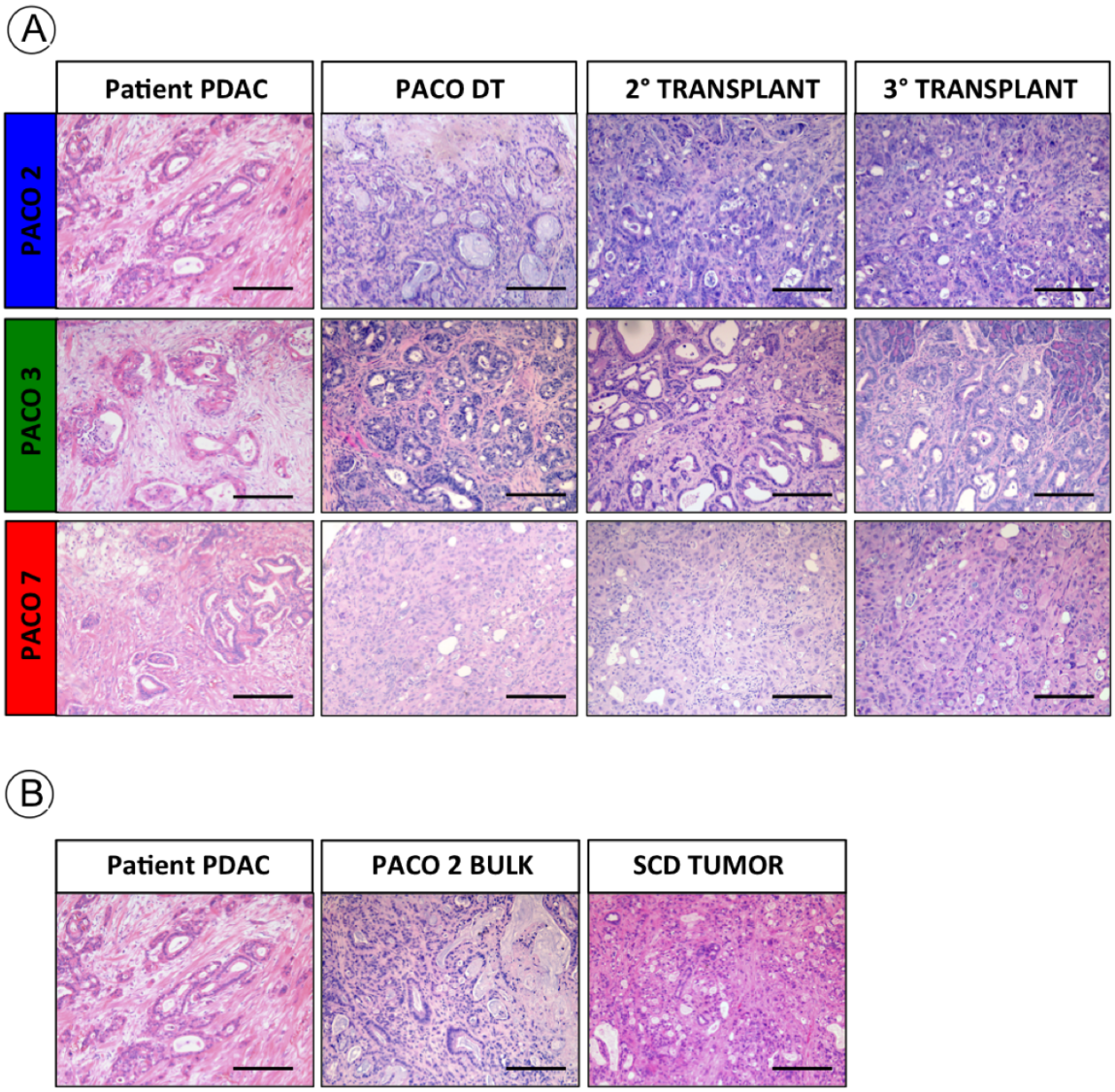

Figure 17 - (A) PACO derived tumors retain *in vivo* tumorigenicity for at least three passages as depicted for three model PACO lines. Note that the characteristic features of the corresponding primary tumors (first column) are maintained throughout all serial passages (2nd to 4th column) (B) Xenograft tumor generated from a single-cell derived (SCD) clone closely resembles the corresponding patient PDAC and retains all of its morphological features (scale bars 100 µm).

As we found a significant difference in clonogenicity between the different PACO lines, we were interested if this also holds true in an *in vivo* setting. Therefore we performed a limiting dilution assay, injecting serial dilutions of 10^4, 10^3 and 10^2 PACO cells into 5-6 NSG mice for each line. After 100 days, the mice were evaluated for tumor growth at the implantation site. We found a high compliance of both the *in vivo* clonogenic potential and *in vitro* clonogenicity of each individual PACO line.

Again cells displaying a well-differentiated morphology with a low proliferation index, displayed the highest clonogenic potential (mean repopulation frequency 1 in 579 cells), while the faster growing PACO cells had a 2-fold lower clonogenic potential (mean repopulation frequency 1 in 1262 cells) **(Table 4)**. Interestingly, cells of the de-differentiated group again had the worst clonogenicity with a mean repopulation frequency of 1 in 14009. However one of these PACO lines (PACO 8) displayed a 10-fold higher clonogenicity than both the other lines belonging to the same group (PACO 7 and 9).

Table 4 – *In vivo* characteristics of the PACO lines, (shown are representative data from different lines; ND – not determined)

Cell Line ID	Tumor latency (days)	Metastases	Repopulation frequency
PACO 2	68	-	**1 / 1262**
PACO 3	167	**Liver, Lung**	**1 / 670**
PACO 7	131	-	**1 / 12270**
PACO 8	77	**Liver**	**1 / 1752**
PACO 9	188	-	**1 / 28004**
PACO 10	174	**Liver, Lung**	**1 / 488**
PACO 14	132	-	**ND**
PACO 16	69	**Liver**	**ND**

Given the observed differences we found in the *in vivo* clonogenicity we were interested if distinct levels of the TIC markers CD133 and CD44/24 might explain these phenomena.

As shown for the PACO lines *in vitro*, their corresponding PACO-DT xenografts did not differ significantly in their TIC marker profile (CD133 range 5.8-22.7%; CD44/CD24 range 4.2-10.2%) **(Table 5)**, indicating that other factors might contribute to the differences observed both *in vitro* and *in vivo*. However, we found that the specific marker profile of the primary tumors was stably maintained in the PACO xenografts (**Table 5, Figure 18**).

Comparison of both CD133 and CD44/CD24 content of initial xenografts and PACO-DT xenografts showed that there was no significant difference in marker expression. Interestingly, even though PACO 2 and 8 both did not express CD133 *in vitro*, both their PACO-DT xenografts did **(Figure 18)**.

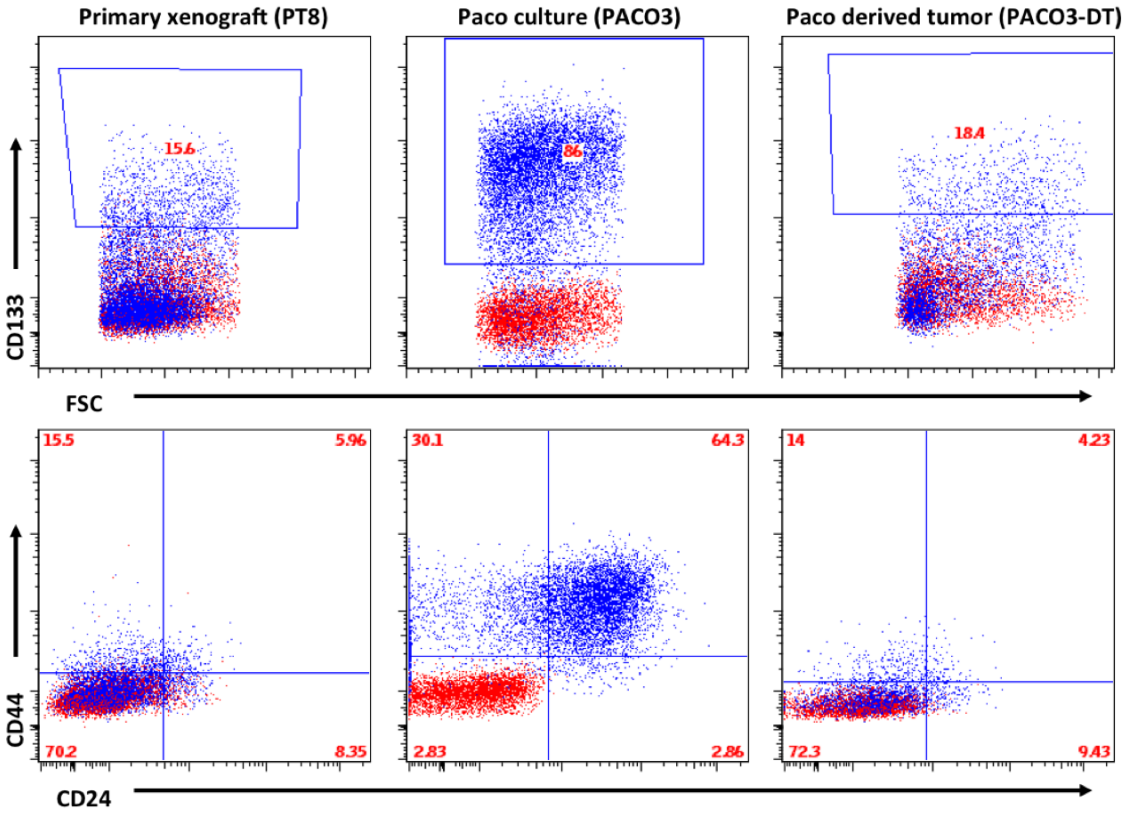

Figure 18 - FACS analysis of primary xenograft PDAC (first column), corresponding PACO culture (second column) and PACO derived xenograft (last column) for the reported TIC markers CD133 (top row) and CD44/CD24 (bottom row). Note that the PACO culture enriches for cells expressing TIC markers, whereas xenografts generated from these PACO cells, express these markers at levels, comparable to the primary xenograft

In summary, our PACO cultures preserve the morphology of the tumor of origin upon orthotopic xenografting and retain a hallmark of the human disease: the abundant stromal compartment. The data further show that pancreatic ductal adenocarcinoma displays a heterogeneous morphology between patients and that this heterogeneity remains preserved by the PACO culture model.

Table 5 – TIC frequencies in selected primary xenografts and PACO derived tumors analyzed by FACS

Cell line ID	CD133 (+)		CD44/24(+)	
	Primary xenograft	PACO-DT	Primary xenograft	PACO-DT
Paco 2	11.7%	22.7%	7.9%	5.9%
Paco 3	15.6%	18.4%	5.9%	4.2%
Paco 7	12.6%	5.8%	2.8%	5.7%
Paco 8	6.9%	16.1%	1.6%	6.5%
Paco 9	7.7%	11.3%	9.7%	10.2%
Paco 10	16.1%	14.7%	4.5%	4.3%

Gene expression analyses on the PACO model

The tumor specific gene-expression profile is stably maintained throughout the PACO system with a high stability across several in vitro passages

Given the observed differences in tumor histology and cell morphology across different PACO lines, we hypothesized that more complex molecular differences might underlie these discrepancies. To uncover such differences, we generated mRNA expression profiles using the Illumina Human HT12 v4 bead chip technology at the Genomics Proteomics Core Facility of the German Cancer Research Center. In our analysis we included PACO lines at early and late passage, PACO-DT xenograft tumors and the corresponding primary PDAC xenografts in the analysis. This allowed the evaluation of the stability of the gene-expression patterns in order to eliminate the possibility of any selective bias inherent to our model.

At first we were interested if the gene-expression profile of the initial xenografts was retained by the xenografts derived from corresponding PACO lines. Using a paired correlation analysis on the data of primary xenografts and respective PACO-derived tumors, we showed that the individual expression profiles were strongly consistent ($R^2 > 0.88$) for all samples tested **(Figure 19A)**. The same analysis of the PACO cultures at early and late time points confirmed that our culture system maintains specific expression profiles over at least 15 passages, indicated by a Pearson coefficient of $R^2 > 0.96$ for all PACO lines **(Figure 19B)**. Together, these data show that the PACO model preserves tumor-specific gene-expression profiles and maintains a population of cells with stable gene expression profiles over at least 15 passages.

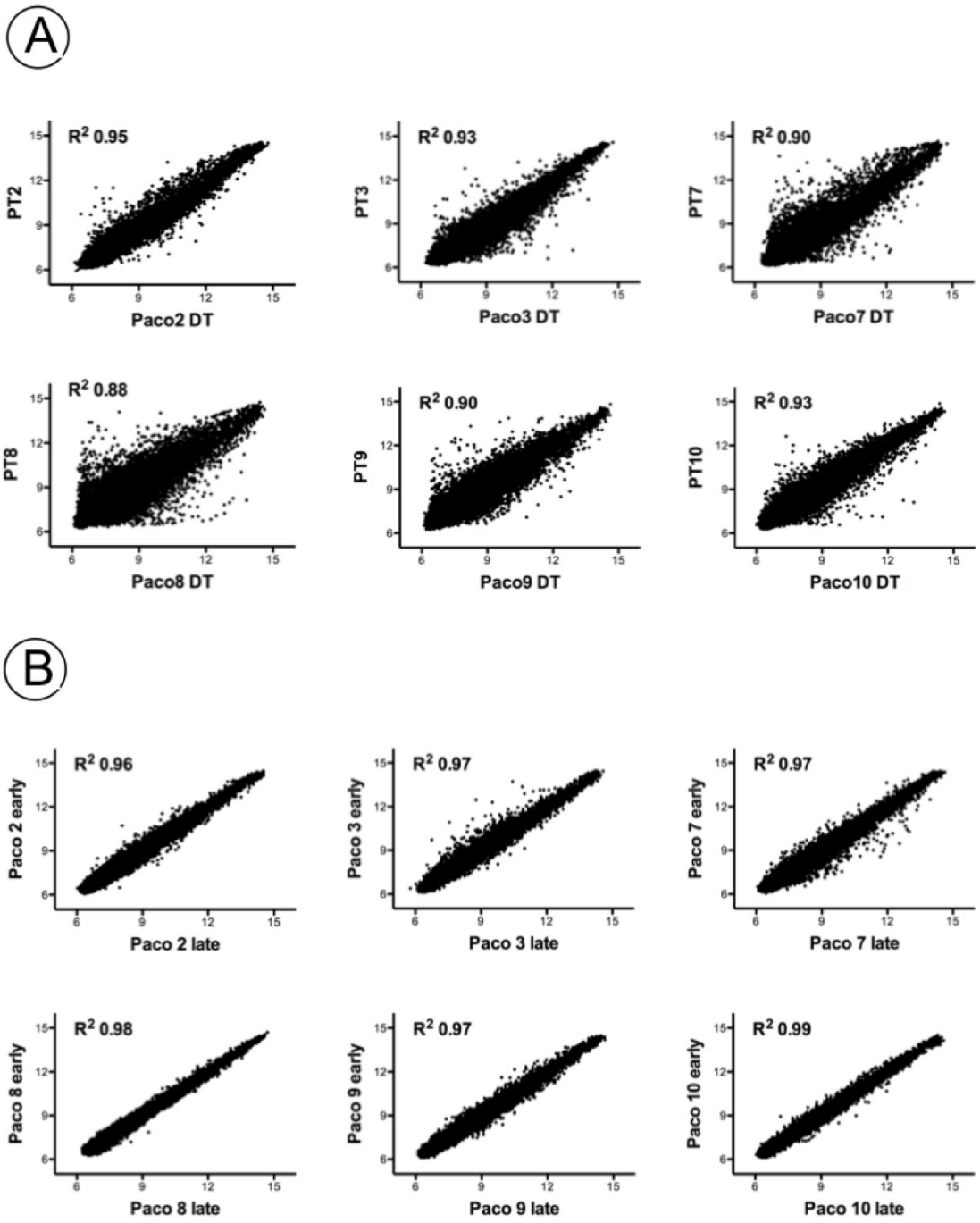

Figure 19 - Scatterplots of log2 expression values for (A) first passage xenograft tumors and their respective PACO-derived tumors and (B) for the early and late passages of the PACO lines. (R^2 – Pearson correlation coefficient)

The PACO model preserves and propagates three distinct molecular subtypes of PDAC

A recent study defined three molecular subtypes of PDAC by analyzing combined gene-expression datasets of human micro-dissected tumor tissue. From those subtypes, termed quasi-mesenchymal (QM), exocrine-like and classical, a 62-gene panel, termed PDAssigner was devised. This gene classifier enables the allocation of individual tumor samples into one of the three subtypes.

Hence we were interested if these three subtypes are represented in our PACO model and thus may provide an explanation for their histopathological and cellular heterogeneity. Genesets for each subtype, based on the PDAssigner, were created and together with the gene-expression data of primary and PACO-DT xenografts used in the Gene Set Enrichment Analysis (GSEA) to test the subtype affiliation of each tumor. Each primary xenograft tumor, for which gene expression data was available, could be unequivocally assigned to a specific subtype with a significant enrichment score (FDR < 0.2). For each subclass we were able to determine individual expression profiles, with regard to the subclass-specific PDAssigner genes previously defined by Collisson *et al*. **(Figure 20A-C)**. From 14 tumors with available gene expression data, we classified five tumors as classical (PT11, PT12, PT24, PT32 and PT38) **(Figure 20A)**, four as QM-PDA (PT3, PT7, PT13 and PT39) **(Figure 20B)** and another five as exocrine-like PDAC (PT8, PT9, PT21, PT25 and PT30) **(Figure 20C)**. Having matched our primary xenografts to individual subtypes, we thus were interested if these associations are retained in the PACO-DT xenografts. Indeed, by applying the same analysis pipeline as for the primary xenografts we were able to confirm that all of the PACO-DT xenografts retained the molecular subtype of their corresponding primary xenograft **(Figure 20A-C, Table 6)**.

As the study of Collisson *et al.* was not able to detect a cell line model for the exocrine-like subtype, we were especially interested if the PACO cultures generated from tumors classified as being of the exocrine-like subtype still displayed this subtype in culture.

Indeed, we found that all four PACO cell lines to be considered - PACO 3, PACO 10, PACO 14 and PACO 18 – could be mapped to the exocrine-like subtype and were therefore shown to stably maintain this subtype in culture after derivation from their original xenografts (**Table 6**). As shown for the exocrine-like subtype, both the classical and QM-PDA subtype were also stably maintained in the corresponding PACO lines (**Table 6**).

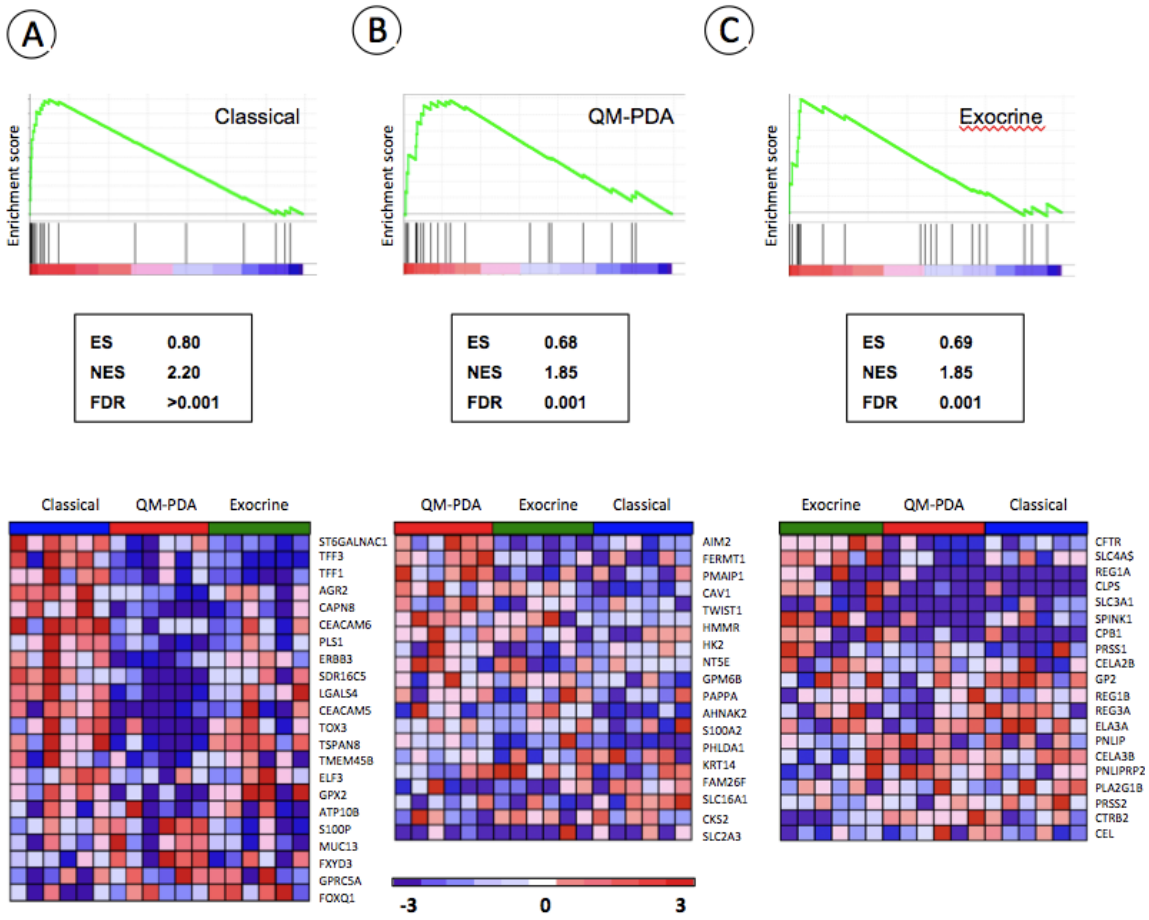

Figure 20 - (A-C) Enrichment plots, statistics and heatmaps generated by GSEA using the PDAssigner 62-gene signature on the expression dataset from corresponding first passage xenografts and PACO-derived tumors for the (A) classical, (B) QM-PDA and (C) exocrine-like subtype. Enrichment score (ES), Normalized Enrichment Score (NES) and False Discovery Rate (FDR) are shown. Expression is displayed as a range of three standard deviations from the mean.

As described above, we noted marked differences in morphology between the individual primary pancreatic tumors and xenografts. The existence of two morphologically different groups of tumors raised the possibility that they could be matched to distinct molecular subtypes. Indeed, we found that tumors of the "poorly differentiated'" group (PT3, 7, 13 and 39) were all classified as QM-PDA, while the morphological class of "well-differentiated

tumors" consisted exclusively of the classical and exocrine-like tumors. Despite the fact that these tumors could not be subdivided based on morphological features, analysis of their growth behavior and *in vivo* clonogenicity identified two biologically different groups of tumors. Interestingly, we found that the slowly proliferating tumors were exclusively classified as exocrine-like subtype (PT8, 9, 21, 25 and 30) while all of the fast-growing tumors could be mapped to the classical subtype (PT11, 12, 24, 32 and 38).

We also analyzed the subtype association of the tumors that so far could not be established in culture for which we so far obtained gene expression data, as we were interested if a certain subtype has a significantly worse capacity to be grown *in vitro*. While PT12 was shown to be of the classical subtype, PT25 was assigned to the exocrine-like subtype (**Table 6** remaining tumors still under investigation). Hence we could not find a tendency that one subtype has a significantly lower potential to grow in our PACO model, given the fact that for both the classical and exocrine-like tumors we observed an 80% (4 out of 5 tumors) *in vitro* engraftment efficiency.

We thus conclude that in our PACO culture, three distinct PDAC subtypes, including the exocrine-like type, can be expanded while retaining their characteristic gene-expression signature. Moreover, orthotopic transplants of PACO cells recapitulate tumors of all three subtypes that maintain the gene-expression patterns of the original xenografts.

Table 6 – Subtype classification of individual primary xenografts, PACO-DT xenografts and PACO cell lines (NES – Normalized enrichment score, FDR – False discovery rate; Statistics calculated by GSEA)

Sample	Subtype	NES	P-Value	FDR
PT3	QM-PDA	1.66	0.012	**0.017**
Paco7	QM-PDA	1.23	0.184	**0.194**
Paco7_DT	QM-PDA	1.22	0.190	**0.199**
PT7	QM-PDA	1.40	0.073	**0.069**
Paco8	QM-PDA	1.24	0.201	**0.190**
Paco8_DT	QM-PDA	1.30	0.133	**0.128**
PT13	QM-PDA	1.80	0.001	**0.003**
Paco9	QM-PDA	1.54	0.025	**0.028**
Paco9_DT	QM-PDA	1.61	0.025	**0.051**
PT39	QM-PDA	1.49	0.048	**0.122**
Paco20	QM-PDA	1.42	0.088	**0.074**
PT8	exocrine-like	1.40	0.083	**0.088**
Paco10	exocrine-like	1.91	> 0.001	**> 0.001**
Paco10_DT	exocrine-like	1.58	0.021	**0.065**
PT9	exocrine-like	1.56	0.028	**0.028**
Paco3	exocrine-like	1.65	0.016	**0.017**
Paco3_DT	exocrine-like	1.77	0.004	**0.008**
PT21	exocrine-like	2.00	> 0.001	**> 0.001**
Paco 14	exocrine-like	1.82	0.002	**0.002**
Paco 14 DT	exocrine-like	1.46	0.065	**0.065**
PT25	exocrine-like	1.98	> 0.001	**> 0.001**
PT30	exocrine-like	1.70	0.014	**0.032**
Paco18_DT	exocrine-like	2.11	> 0.001	**> 0.001**
PT11	classical	2.17	> 0.001	**> 0.001**
Paco2	classical	2.09	> 0.001	**> 0.001**
Paco2_DT	classical	2.11	> 0.001	**> 0.001**
PT24	classical	1.90	> 0.001	**> 0.001**
Paco 16	classical	1.57	0.027	**0.054**
Paco16_DT	classical	2.42	> 0.001	**> 0.001**
PT32	classical	1.89	0.002	**0.003**
Paco 17	classical	2.03	> 0.001	**0.002**
Paco17_DT	classical	2.22	> 0.001	**> 0.001**
PT38	classical	2.13	> 0.001	**> 0.001**
Paco19	classical	1.16	0.26	**0.25**
PT12	classical	2.12	> 0.001	**> 0.001**

Gene-expression analysis predicts substantial differences in pathway activity and drug sensitivities between PDAC subtypes

Having confirmed that the PACO model stably maintains all three reported PDAC subtypes *in vitro*, it allows us for the first time to functionally analyze the complete heterogeneity of this malignancy. In this context we were especially interested in the identification of molecular differences distinct for each subtype. We thus used the gene-expression profiles of the PACO-cultures and their respective primary and derived xenografts to perform a gene-set enrichment analysis, using the Broad Institute's MSig database (v3.82, 10/2011) containing >6700 gene sets [93]. From the data we obtained we exclusively focused on gene sets, both negatively and positively correlated with a subtype of interest, which were shown to be significant, indicated by a FDR < 0.25. Using this cutoff, we found for the QM-PDA subtype a significant positive correlation of 770 gene sets, while conversely 481 gene sets were found negatively correlated with this subtype. For the classical subtype we identified 723 significantly, positively correlated gene sets, as well as 431 negatively correlated gene sets. The exocrine-like subtype displayed the lowest number of positively correlated gene sets (234), while a high number of gene sets (1015) were predicted to be significantly, negatively correlated with this subtype. In order to substantiate the findings from the PACO model, we reduced this dataset by building the intersection with the GSEA results obtained from the respective PACO xenografts (both PT and DT). From this condensed enrichment list, we specifically focused our further studies on gene sets that predict drug sensitivities and targetable pathways and thus have potential therapeutic utility. This approach revealed consistent enrichment of multiple gene signatures associated with activation of the PI3K and mTOR pathways in both, the QM-PDA and classical subtypes **(Figure 21A).**

Both the classical and QM-PDA subtype were also selectively enriched for signatures associated with oncogenic Src-activation [96]. We also found additional indications for therapeutic utility of the Src pathway in both of these subtypes, as several gene sets predicting sensitivity to the Src/Bcr-Abl inhibitors Dasatinib [97,98] and the structurally related Saracatinib [99] was also enriched in the classical and QM-PDA subtype, while conversely a higher resistance was predicted for the exocrine-like subtype. As reported previously, we

detected a significantly lower number of positively correlated gene-sets with the exocrine-like subtype **(Figure 21A)**. None of the above reported genes-sets was found to be enriched in this subtype of PDAC. Therefore we also investigated the negatively correlated gene-sets for potential candidate pathways. Interestingly we found that the gene-expression profile of the exocrine-like subtype cells was significantly, negatively correlated with genes involved in cell-cycle, proliferation and DNA replication **(Figure 21B)**. A finding very well in line with our previous observations of significantly lower proliferative indices and lower frequency of actively cycling cells exclusive to the exocrine-like PACO cells and xenografts.

We also identified several signatures involved in apoptosis or regulation of such, selectively, negatively correlated with the exocrine-like subtype **(Figure 21A)**. This led to the hypothesis that this subtype is putatively enriched for anti-apoptotic molecules. Indeed we found selective enrichment of a gene set predicting sensitivity to the BH3-mimetic ABT-737 [100] only for the exocrine-like subtype, while both other subtypes were predicted to be insensitive to this treatment **(Figure 21A)**.

While we analyzed three models for each subtype we sought to further verify our findings in a larger cohort of patients. We thus applied the same analysis pipeline to two previously generated sets of expression-data of more than 70 PDAC tumor samples [82,101]. The results obtained from this analysis largely confirmed our model-derived data, as most associations we found were present in at least one of the two patient data sets **(Figure 21A)**. The concordance of the data, derived from the PACO model, with those of patient-derived tumors thus indicates that the PACO-lines and xenografts are a clinically relevant model for human PDAC.

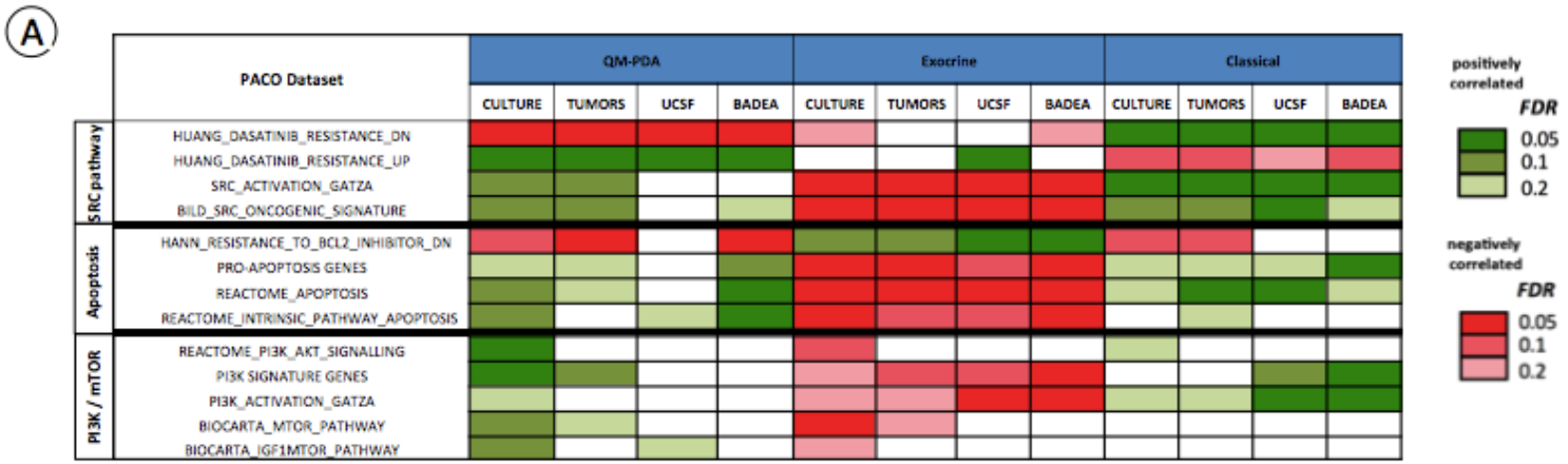

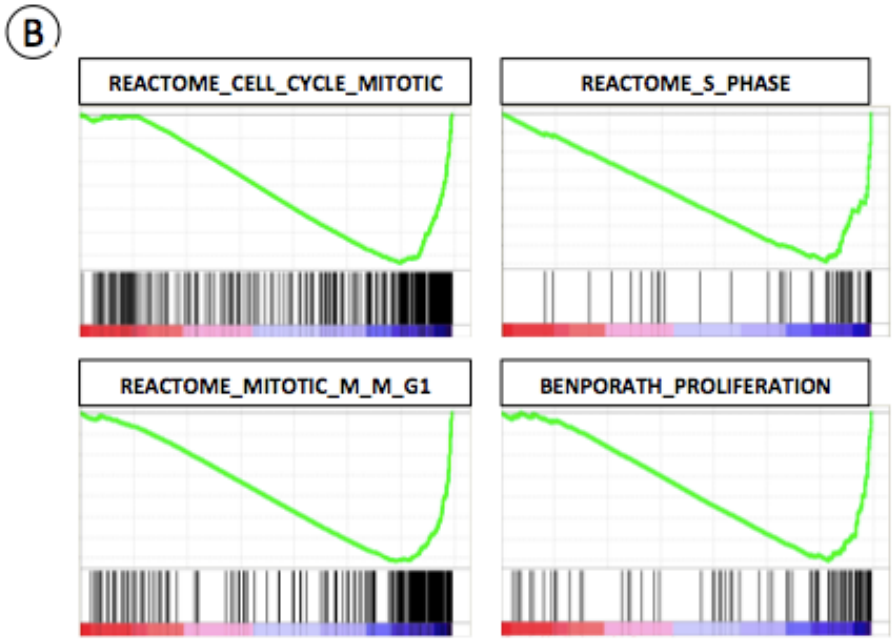

MSigDB SETS	ES	NES	P-Val	FDR
REACTOME_CELL_CYCLE_MITOTIC	-0.63	-2.42	0.000	0.000
REACTOME_S_PHASE	-0.68	-2.27	0.000	0.000
REACTOME_MITOTIC_M_M_G1	-0.63	-2.27	0.000	0.000
BENPORATH_PROLIFERATION	-0.62	-2.20	0.000	0.000
BIOCARTA_CELLCYCLE_PATHWAY	-0.78	-1.97	0.000	0.000
KEGG_DNA_REPLICATION	-0.70	-1.96	0.000	0.000
KEGG_CELL_CYCLE	-0.56	-1.95	0.000	0.000

Figure 21 - (A) Overview of the differentially enriched pathway signatures and drug vulnerabilities as predicted by GSEA for expression data from the PACO culture, the PACO-DT tumors and the two publicly available datasets (UCSF and Badea) (B) The exocrine-like subtype is negatively correlated with several genesets involved in cell cycle and its regulation (statistics calculated by GSEA)

An integrative approach combining multiple *in silico* tools identifies putative subtype-specific markers

Given that only one of the three subtypes could be distinguished by morphological features, we sought to identify immunohistochemical markers for each of the three subtypes to allow patient stratification. We followed a multistep approach to determine and validate candidate marker proteins based upon gene expression profiles of the subtype-specific PACO lines **(Figure 22A)**. An initial list of genes showing strong (> 5 fold) differential subtype-specific expression was established from our gene-expression data. Since we sought to develop immunohistochemical markers, the candidate list was refined using the Protein Atlas database [102]. Assuming that all three subtypes were represented in this database, antibodies were only selected and included in the candidate list, if they specifically stained a subset of all available PDAC specimens. In addition, we used the GSEA motif module [93] to identify putative subtype-specific transcription factor activity. This analysis aims to identify selectively enriched groups of genes, which share a common consensus site for a given transcription factor within a 2kb window from their respective transcription start. This approach revealed an enrichment of genes containing binding-sites for the transcription factors HNF1 homeobox A and B (HNF1) exclusively in the exocrine-like subtype **(Figure 22B,C)**. In concordance with this finding, we found the same association in both primary tumor datasets. Therefore HNF1 was included as a candidate marker for the exocrine-like subtype in the final candidate list **(Table 7)**.

A

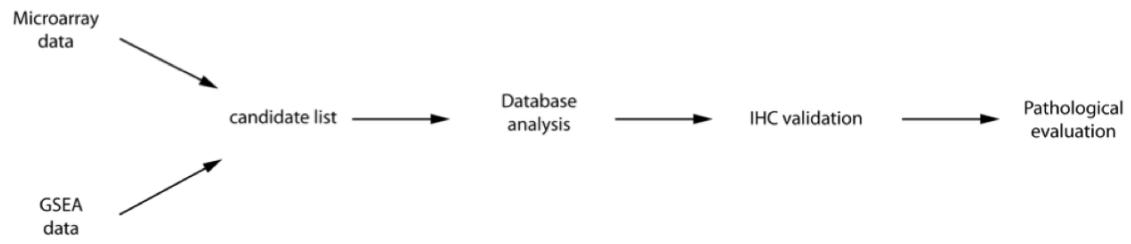

B

MSigDB Set	PACO Dataset	UCSF Dataset	Badea et al. dataset
V$HNF1_Q6	2.06 (*0.033*)	1.98 (*0.011*)	1.48 (*0.370*)
V$HNF1_C	1.99 (*0.037*)	1.54 (*0.222*)	1.33 (*0.495*)
V$HNF1_01	1.89 (*0.063*)	2.14 (*0.001*)	1.46 (*0.351*)

C

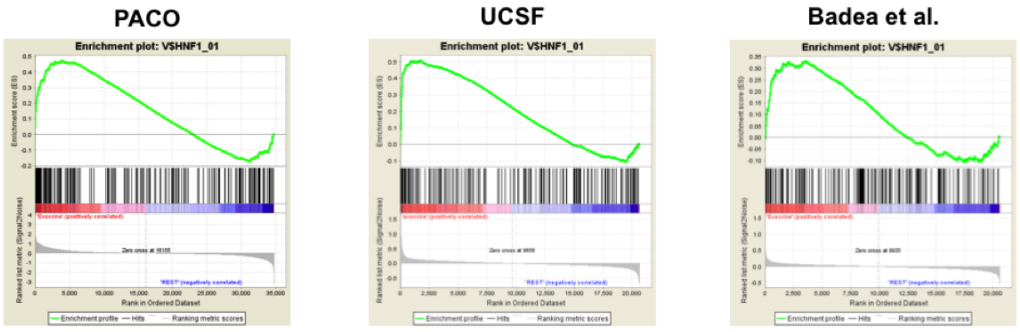

Figure 22 - (A) Outline of the marker identification strategy (B) GSEA motif search identifies HNF-1 as putative regulator in the exocrine-like subtype – Overview of analyses performed on the PACO dataset, the UCSF and Badea datasets using HNF-1 motif sets present in the MSigDB. Numbers indicated Normalized Enrichment Score (NES) with the FDR in brackets. (C) Enrichment plots of the motif set V$HNF1-01 are exemplarily displayed for all three datasets.

Table 7 - Final candidate list of subtype-specific markers. Two independent pathologists evaluated staining quality and quantity of each antibody on tumors of each subtype

Marker	Designated for subtype	QM-PDA	Classical	Exocrine	Note
CEACAM3	*Classical*	-	-	-	Ab did not stain
CEACAM6	*Classical*	+/-	-	+	Diffuse staining in few cells
S100P	*Classical*	-	-	-	Ab did not stain
S100A1	*Classical*	+/-	++	+/-	Ab gave a nuclear staining only in the classical subtype
TFF3	*Classical*	+	-	-	In patient tumors Ab did not stain exclusively
SLC2A3	*QM-PDA*	-	-	-	Ab did not stain
AIM2	*QM-PDA*	+/-	-	-	diffuse staining in PACO8 DT, rest did not stain
SMAD4	*QM-PDA*	+/-	+/-	+/-	Ab stained isolated ductal structures in all tumors tested
VIM	*QM-PDA*	++	-	-	Ab did neither stain classical nor exocrine tumors
CFTR	*Exocrine*	-	-	-	Ab did not stain
SLC4A4	*Exocrine*	-	-	-	Ab did not stain
REG1A	*Exocrine*	+	-	+	Weak, cytoplasmatic staining
CEL3A	*Exocrine*	-	-	-	Ab did not stain
SPINK1	*Exocrine*	++	++	++	Ab gave a strong cytoplasmic staining in all tumors
HNF1	*Exocrine*	-	+/-	++	Ab stained isolated ducts in classical tumors

++ strong staining
+ weak staining
+/- diffuse staining / unspecific staining
- no staining

Analysis of subtype-specific pathway activity

We next tested whether the predicted subtype specific pathway activation was reflected on the protein level in the PACO cells. To that end, lysates from model lines for each of the subtypes were prepared and the expression levels and phosphorylation status of key proteins were analyzed by Western blot. For both the QM-PDA and classical subtype our analysis predicted a selective activity of the Src-family kinases (SFK). The activity of SFK members is regulated by an activating phosphorylation at Tyrosine (Tyr)^{419}, while phosphorylation at inactivating site Tyr^{527} abrogates protein function [103].

Western blot analysis showed that the level of Tyr^{527} phosphorylation was significantly higher in the exocrine-like subtype cells as compared to both the classical and QM-PDA subtypes **(Figure 23)**. Additionally, we detected a high level of the Tyr^{419} activating phosphorylation in two out of three classical PACO lines while being lower in the remaining samples. However we were not able to identify a strict, subtype-specific association of Tyr^{419} phosphorylation status. Taken together, this data on the one hand confirms our *in silico* prediction that the SFKs are not active in the exocrine-like subtype, as indicated by the exclusive presence of the inactivating phosphorylation site in this subtype, but on the other hand does not provide conclusive data for a confirmation of the enrichment of several Src-activity signatures.

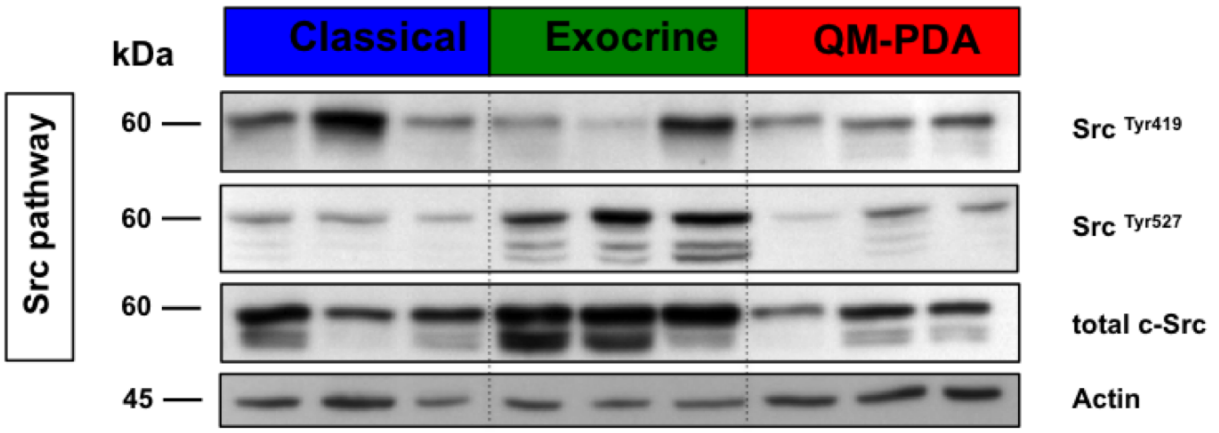

Figure 23 - Lysates from nine model PACO lines representing three of each subtype were analyzed by immunoblot for the expression and phosphorylation-status of members of the oncogenic SRC family kinases.

Furthermore, GSEA analysis predicted selective activity of both the mTOR and PI3K pathway in the QM-PDA and classical subtype. We analyzed the expression of several members of the PI3K and mTOR pathway by immunoblot. There we found no significant different expression levels of the p110 family members among the three subtypes. Interestingly we found a higher expression of the mTOR complex 1 regulatory protein raptor in cells of the QM-PDA subtype, while conversely expression of the mTOR complex 2 regulatory protein rictor was lowest in this subtype **(Figure 24)**. The classical subtype on the other hand expressed higher levels of rictor and a low level of raptor. Additionally we observed a significantly higher expression of the PI3K class III in both the QM-PDA and classical subtype **(Figure 24)**.

We also investigated the activation of these pathways by analyzing the phosphorylation status of the upstream kinases (mTOR, p85) and downstream substrates (p70S6K, eIF4 and S6RP) [104]. In line with our predictions from the GSEA, we found strong phosphorylation of these proteins in all six cell lines of the classical and the QM-PDA subtypes, while the exocrine-like PACO lines showed significantly lower or absent phosphorylation levels **(Figure 24)**. Interestingly we detected a stronger mTOR Tyr^{2448} staining in the classical subtype relative to the total mTOR level. Besides that we also found selective activation of PI3K pathway as indicated by Tyr^{458} phosphorylation of the upstream regulatory kinase p85, which was strongest in the QM-PDA while being almost absent in the exocrine-like cells. Along the same line, phosphorylation of Akt on its two activating sites Ser^{473} and Thr^{308} was strongest in the QM-PDA subtype **(Figure 24)**.

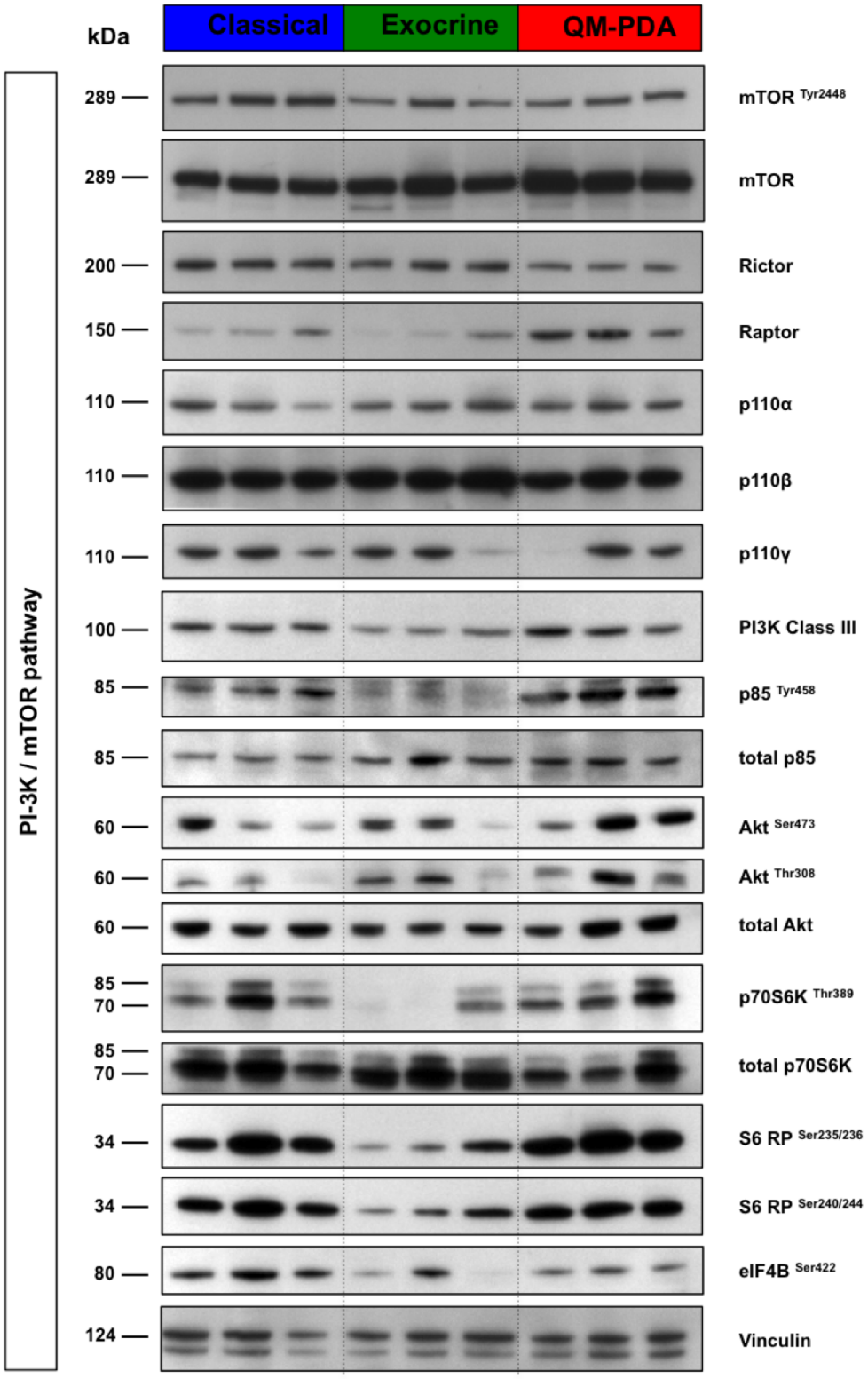

Figure 24 - Lysates from nine model PACO lines representing three of each subtype were analyzed by immunoblot for the expression and phosphorylation-status of members of the PI3K/mTOR pathway. (Note the two bands present for Vinculin represent Metavinculin (upper band) and Vinculin (lower band))

These data confirm the previously described predictions of a subtype-specific activity of the PI3K/mTOR pathway selectively in both the QM-PDA and classical subtype.

We further investigated if a specific member of the Bcl-2 family is selectively enriched in the exocrine-like subtypes, which might explain the predicted negative enrichment for apoptotic pathways and signatures. Many of the proteins we tested (Bad, Mcl-1 and Bcl-XL) were broadly expressed across all lines tested. Bcl-2 stained strongest in one exocrine-like cell line, however both other lines only showed weak or absent staining **(Figure 25)**.

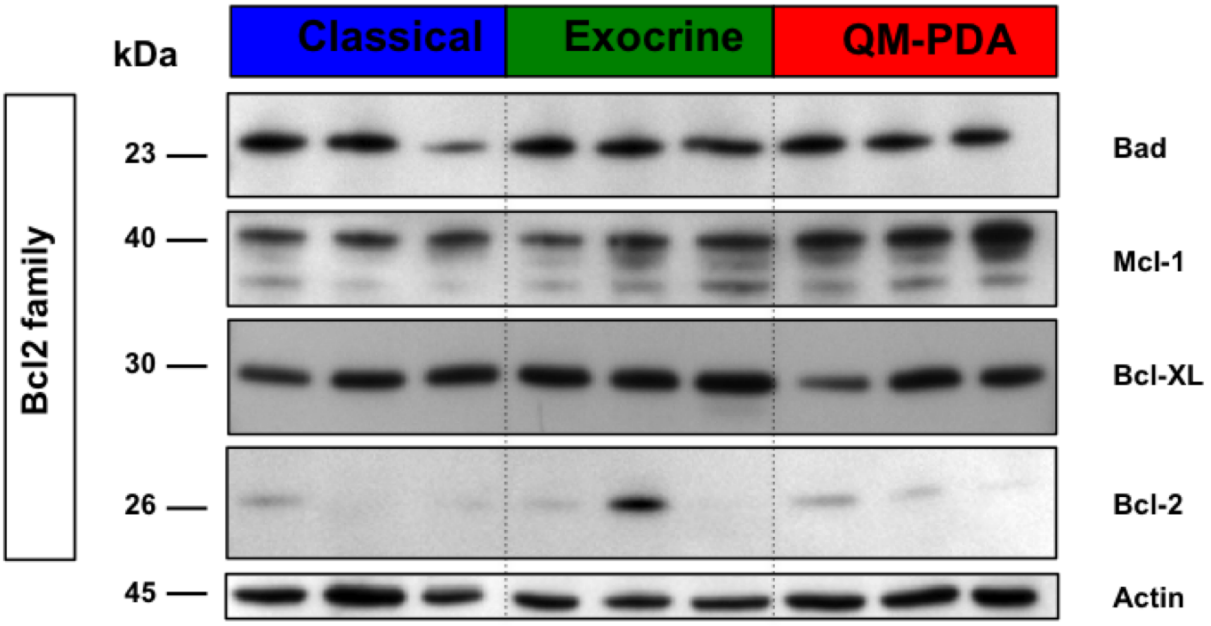

Figure 25 - Lysates from nine model PACO lines representing three of each subtype were analyzed by immunoblot for the expression of members of the Bcl-2 family.

As our culture conditions might influence the activation of signaling pathways, we wanted to investigate if we could detect a similar and selective pattern of pathway activity in our PACO xenografts. Staining of tumors representative for each subtype, confirmed a subtype-specific activation of key pathway effectors. Strong staining for S6RP$^{Ser235/236}$, S6RP$^{Ser240/244}$ and p70S6K^{Thr389} was found in tumors of the classical and QM-PDA subtype, while being weak or absent in the exocrine-like tumors **(Figure 26)**.

Conversely, staining for Src^{Tyr419}, was detected both in tumors of the QM-PDA and classical subtype. As already seen for the *in vitro* cultured PACOs of the exocrine-like subtype, their corresponding tumors did not show SFK activity **(Figure 26)**.

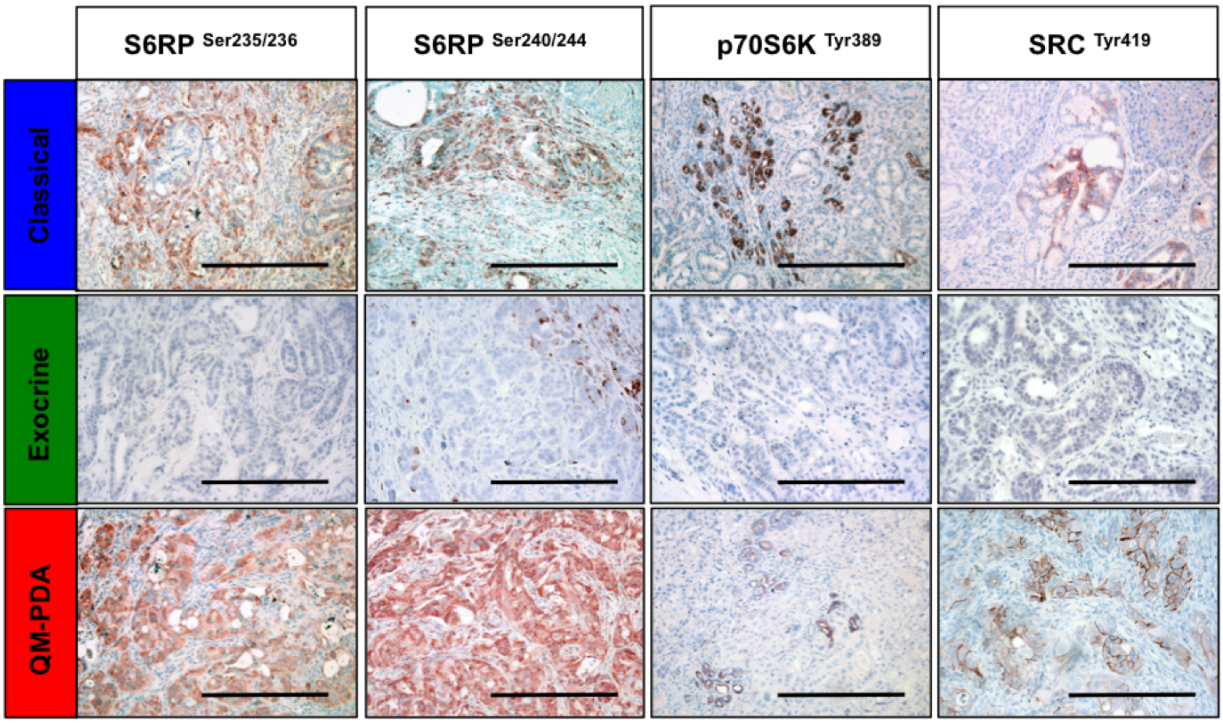

Figure 26 - Immunohistochemical detection of the indicated phospho-proteins in sections of the PACO-derived xenografts PACO2-DT (classical), PACO3-DT (exocrine-like) and PACO7-DT (QM-PDA) (Scale bars 100 µm).

Taken together, this shows that the predictions of our combined *in silico* approach, can be validated to a great extend both *in vitro* and *in vivo*. Our approach may thus be used to predict and analyze the biology of the different subtypes of PDAC.

Subtype specific markers

Validation of *in silico* predicted candidates reveals a two-marker set capable of stratifying PDAC patients according subtype

Application of the analysis pipeline depicted above **(Figure 22A)** resulted in a candidate list of 15 markers with high potential for subtype-specificity. In total five proteins were analyzed for specificity for the classical subtype, four for the QM-PDA subtype and six for the exocrine-like subtype **(Table 7)**. Some of the markers have been either already reported to be associated with pancreatic cancer (e.g. SMAD4, CEACAM6) or are even part of the initially published PDAssigner (CEACAM3, CEACAM6, TFF3, CFTR, SLC4A4, REG2A, CEL3A, AIM2). Others have not been associated with PDAC before (e.g. HNF1, KRT81).

The expression of all candidates was tested by immunohistochemistry on sections of the entire panel of PACO-derived xenografts using specific antibodies derived from the Human Protein Atlas **(Table 7)**. Our analysis also included the markers reported by Collisson et al. to be specific for the exocrine-like subtype, CFTR and ELA3A. In our hands, using the identical antibodies, both markers did not stain in any of the sections of our panel. Many of our markers did either not stain at all (SLC4A4, SLC2A3, S100P, CEACAM3), stained only a subset of tumors albeit not with strict subtype specificity (CEACAM6, AIM2), or stained all of the tumors under investigation (SPINK1, SMAD4).

Exclusion of these unspecific markers reduced our list to five proteins with strict subtype specificity. Staining for HNF1 was specific for nuclei of tumor cells of the exocrine-like subtype, consistent with its function as a transcription factor, while both Vimentin (VIM) and Keratin-81 (KRT81) staining was limited to tumors of the QM subtype **(Figure 27A** and data not shown). Staining of TFF3 was only detected in tumors of the classical subtype, whereas S100A1 was found to stain all tumors, however, only in classical tumors displayed a nuclear localization. We then sought to validate these markers on the corresponding primary tumors in order to exclude cross-reactivity with non-tumor cells, since the stromal compartment in our xenografts is of murine origin. This analysis further reduced the initial list of five

candidates to a final list of two markers, HNF1 for the exocrine-like subtype and KRT81 for the QM-PDA subtype. Both markers exclusively detected tumor cells and we confirmed their subtype specificity and suitability for being used in clinical histopathology **(Figure 27B)**. Though we tested two potential marker-candidates for the classical subtype (S100A1 and TFF3), none of them specifically and consistently stained tumors of the classical subtype when verified on a panel of human tumor sections (**Table 7** and data not shown). However as tumors of the classical subtype were negative for both HNF1 and KRT81 **(Figure 27A,B)** we defined this subtype as KRT81/HNF1 double-negative (DN). Taken together, this data suggest that a set of two markers can be used to stratify PDAC patients according to one of the three described subtypes.

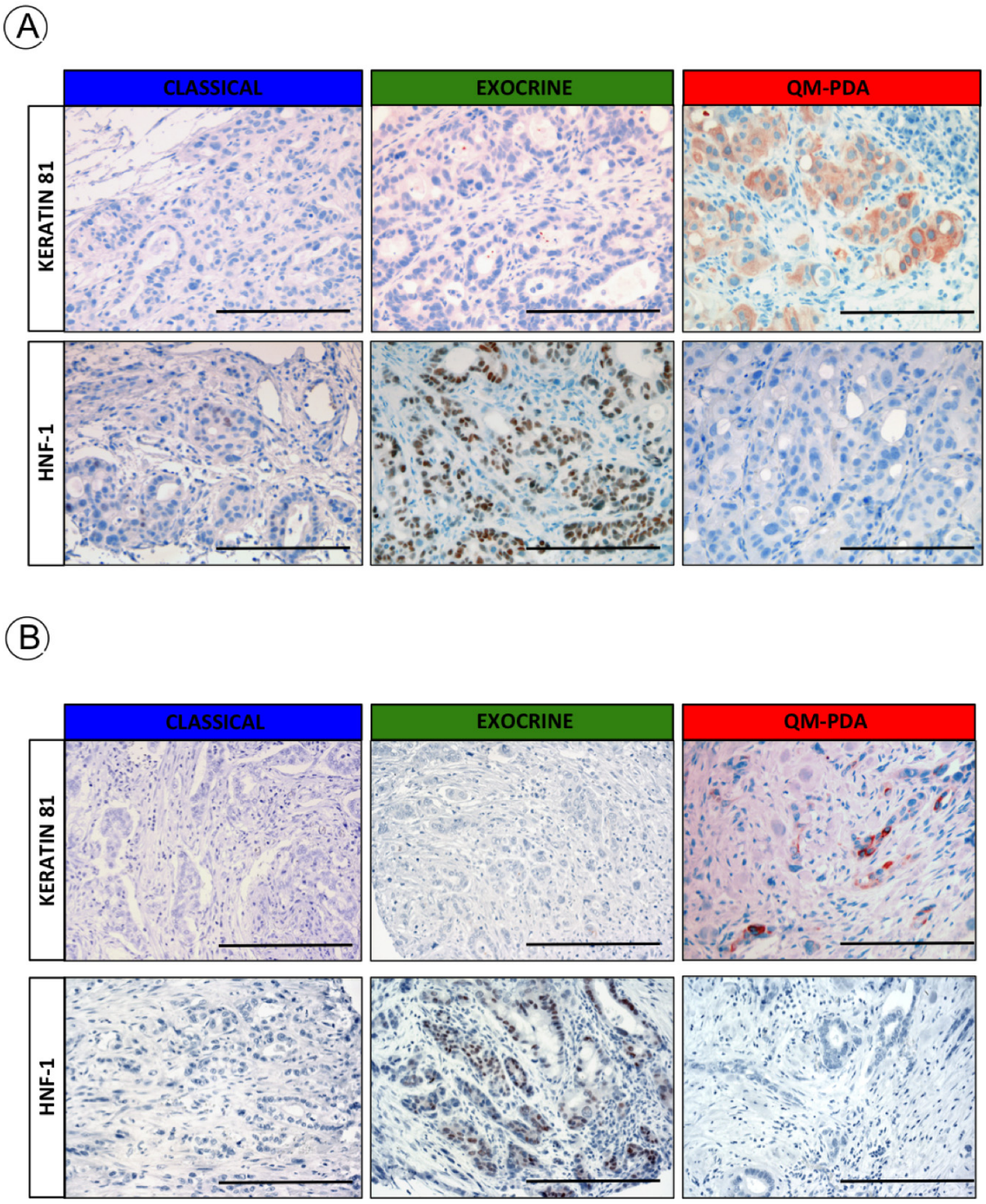

Figure 27 - (A) Immunohistochemical staining of representative experimental tumors of the different subtypes for KRT81 (top row) and HNF-1 (bottom row). Tumors depicted are PACO2-DT (classical), PACO3-DT (exocrine-like) and PACO7-DT (QM-PDA) (B) Immunohistochemical staining of the corresponding primary tumors PT11 (classical), PT9 (exocrine-like) and PT3 (QM-PDA) for KRT81 (top row) and HNF-1 (bottom row). (Scale bars 100 µm)

Stratification of PDAC patients reveals significant survival differences between subtypes

Having identified a set of markers that has been shown to be subtype-specific, we asked whether such marker-based stratification of PDAC patients could reveal subtype-specific differences in clinical outcome. To this end we analyzed a cohort of 252 human invasive PDAC tumors (patient information in **Appendix Table 2**). Staining of this tissue microarray (TMA) for HNF1 and KRT81 confirmed the specificity of these markers as exclusively tumor cells were stained. Additionally we found only 11 (4.4%) samples positive for both markers, which further substantiates the strict subtype-specificity of both markers. For our analysis, we defined patients with KRT81 expression as QM-PDA, while patients with HNF1 positivity were defined as exocrine-like subtype type and double-negative patients were of the classical type **(Figure 28A)**. Patients staining for both markers (11) were excluded from our further analyses. Analysis of the frequency of each subtype revealed 44% classical, 35% QM-PDA and 21% exocrine-like tumors in the patient cohort under investigation **(Table 8)**. We next investigated a potential subtype-specific association with clinical outcome.

Survival data was available for 217 of the classifiable patients and the analysis revealed significant differences according to subtype as defined by our markers. Whereas patients suffering from exocrine-like PDAC had a mean survival time of 43.5 months, the mean survival of patients with classical PDAC was 26.3 months. Finally, the group of patients with QM-PDA had the worst overall prognosis with a mean survival of 16.5 months **(Figure 28B, Table 8)**. These data demonstrate not only that our set of two markers can be used to stratify PDAC patients according to subtype, but also demonstrates significant differences in clinical outcome that might direct future therapeutic approaches.

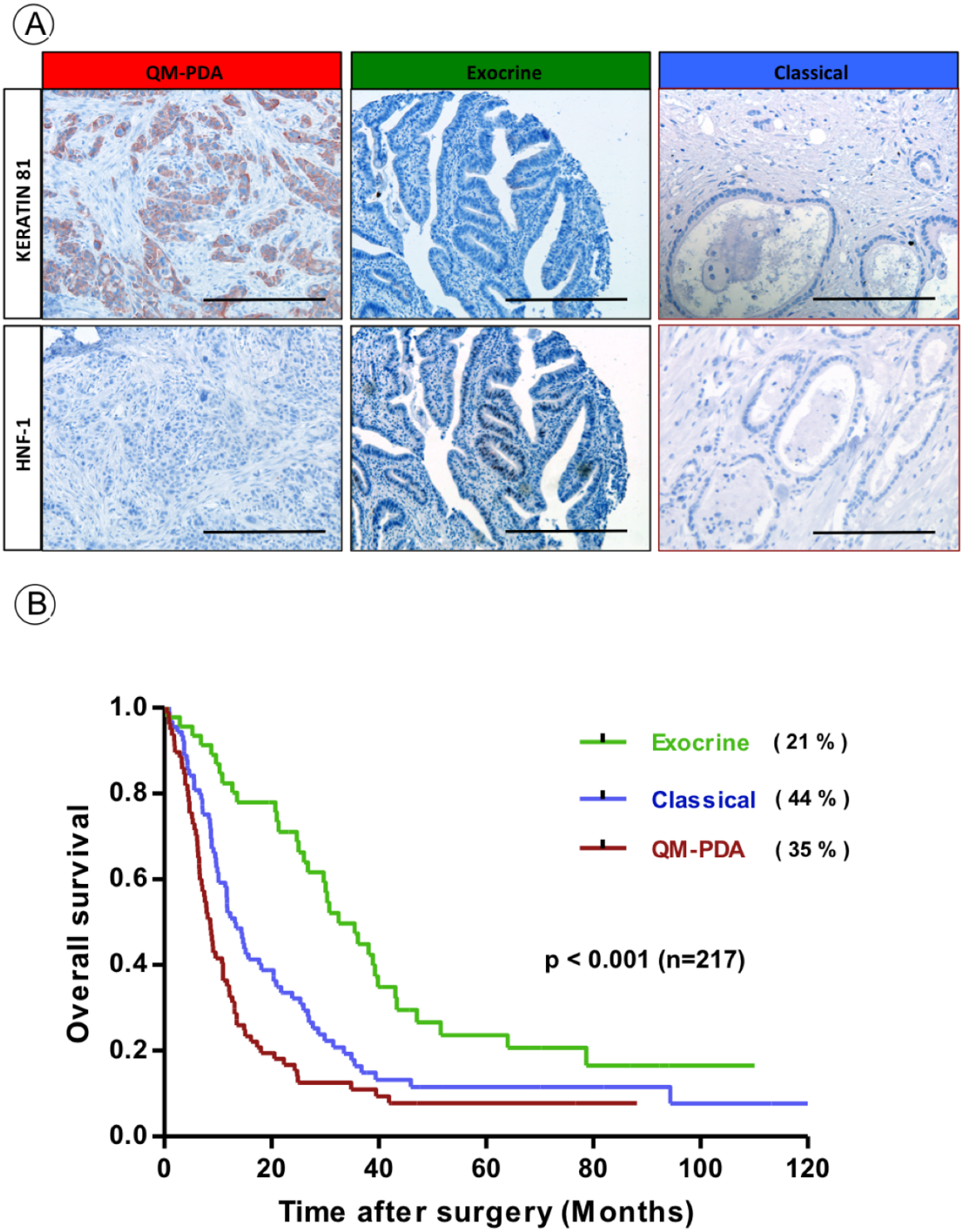

Figure 28 - (A) Representative and corresponding staining for KRT81 and HNF-1 on tissue-microarray containing samples from 252 PDAC patients (Scale bars 100 µm). (B) Kaplan-Meier survival curve for 217 PDAC patients according to marker-defined subtypes. Significance was calculated with the Log-rank (Mantel-Cox) Test.

Table 8 – Distribution frequency of the different subtypes and overall survival data of the patients included in the TMA (DN – double-negative)

Marker	Subtype	Cases	% of total	Mean survival (months)
HNF1	Exocrine-like	46	21	43.5
KRT81	QM-PDA	79	36	16.5
DN	Classical	92	42	26.3
Total		**217**	**100**	

Drug screening

In vitro drug screens guided by in silico predictions reveal novel subtype-specific treatment options

The differential activation of signaling pathways **(Figure 21)** suggests that the subtypes might also differ in their drug-responsiveness, especially to molecules that target such specific signaling pathways. To this end, we first evaluated if such differences could also be reflected in the responsiveness to a variety of compounds targeting multiple, different kinases. First of all we could show that the PACO system enables small-scale drug screening with robust results, indicated by a Z-value of 0.76. Thus the cells may be utilized in miniaturized drug discovery screens in order to identify novel lead compounds for each of the different subtypes **(Figure 29A)**. Interestingly we observed, as predicted by the molecular analyses, a significantly higher potency of PI3K/mTOR inhibitors in both QM-PDA and classical subtypes, when compared to the exocrine subtype **(Figure 29B)**. We further observed, that the exocrine-like subtype only responded to a minority of compounds, while displaying a selective resistance to the majority of compounds evaluated. Intriguingly, some of the tested compounds even resulted in an adverse effect, i.e. promotion of cell growth instead of inhibition **(Figure 29A)**.

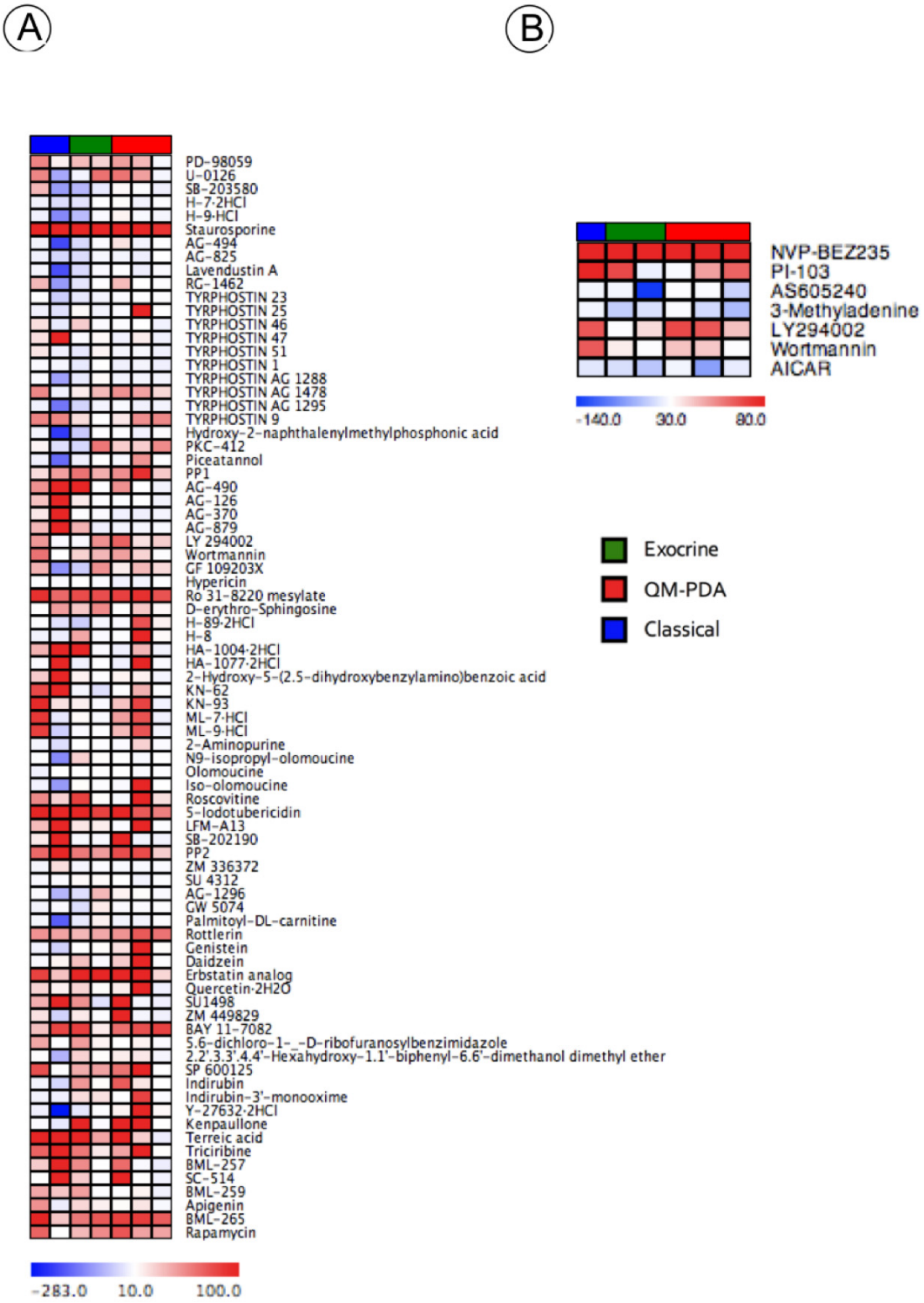

Figure 29 - (A) Small-scale drug screen of a Kinase Inhibitor Library targeting multiple, different human kinases (B) Analysis of the compounds targeting the PI3K/mTOR pathway reveals that they are more potent in QM-PDA and classical PACO cells (scale bar denotes percent inhibition by a given compound in relation to negative and positive control; Z-value of the screen was 0.76)

Having shown the suitability of our model to obtain reliable results from small-scale drug screens when next wanted to validate some of the findings from this initial screen as it was conducted at a fixed concentration. We thus determined the individual IC_{50} values for each PACO line for a set of compounds targeting predicted and already validated drug candidates for each of the subtypes. We also included the currently available frontline therapeutic options for PDAC, Gemcitabine and the tyrosine-kinase inhibitor Erlotinib. While both the QM-PDA and classical PACO lines were similarly sensitive to Gemcitabine **(Figure 30A)**, treatment with Erlotinib was more effective in the classical subtype **(Figure 30B)**, in line with previous results [82]. The exocrine-like subtype cells however displayed marked resistance towards both compounds **(Figure 30A,B)**.

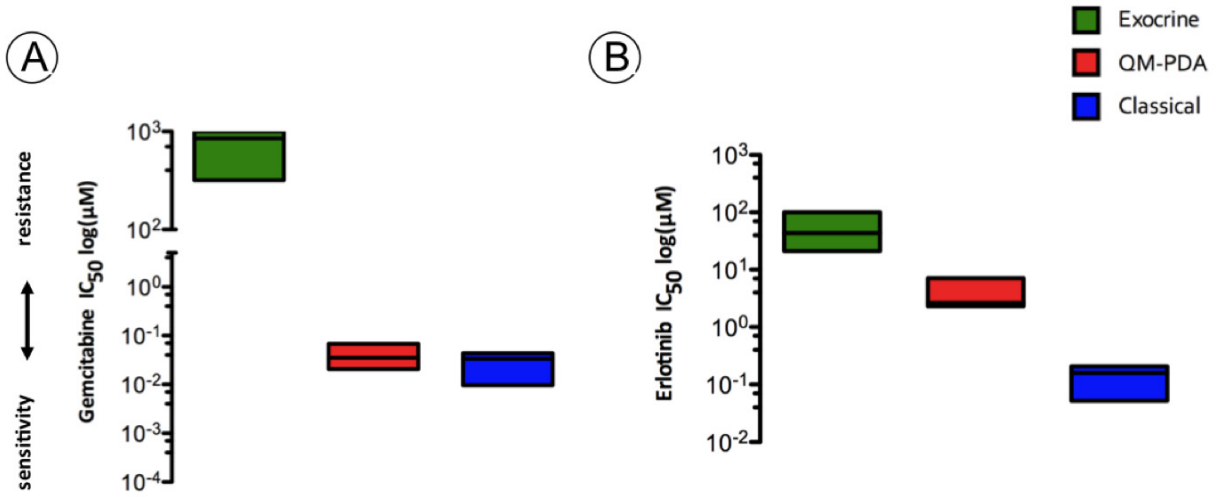

Figure 30 - Min-max plots of IC_{50} values for the two currently available front-line therapeutics for PDAC (A) Gemcitabine and (B) Erlotinib representative for three PACO lines of each subtype. Horizontal bar depicts median value (legend indicates sensitivity/resistance of the respective subtype to a compound).

Inhibition of the PI3K by LY294002 and mTOR pathway by Rapamycin and Torin1 targeted both the QM-PDA and classical subtype **(Figure 31A-C)**. These data thus confirm the predicted sensitivity of both the QM-PDA and classical subtype to treatment with Rapamycin and show that the selectively active PI3K pathway can be inhibited in these subtypes. The median IC_{50} value for some of these compounds however was lower in the QM-PDA as compared to the classical subtype (6,2E-05 µM versus 3,1E-04 µM for Rapamycin and 5,8 µM versus 9,2 µM for LY294002), suggesting a higher efficacy of those compounds in QM-PDA tumor cells **(Figure 31A,B)**.

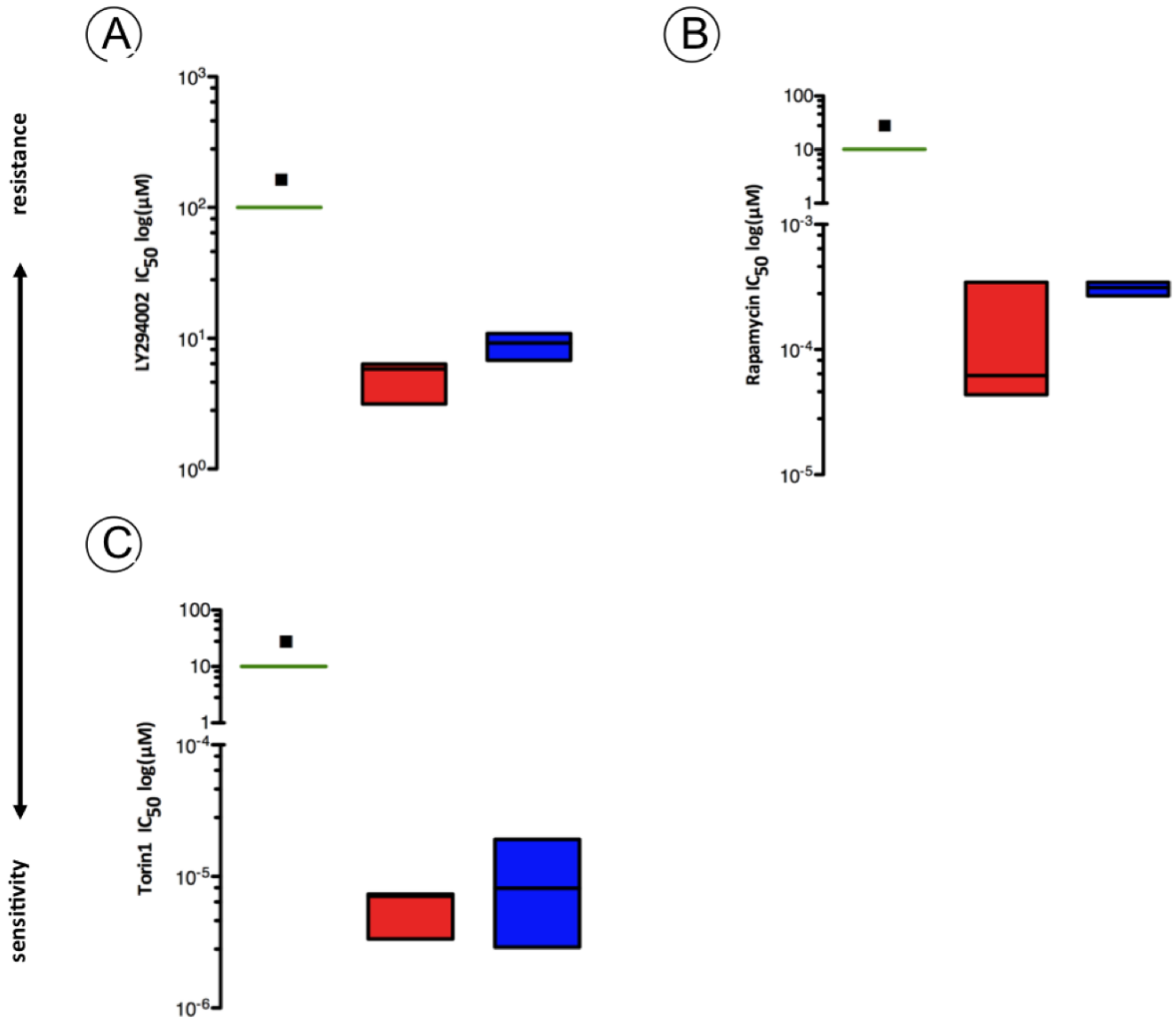

Figure 31 - Min-max plots of IC_{50} values for compounds targeting the PI3K/mTOR pathway, (A) LY294002, (B) Rapamycin and (C) Torin1, representative for three PACO lines of each subtype. Horizontal bar depicts median value. ■ indicates that the cells were resistant up to the maximum solubility of the respective compound (legend indicates sensitivity/resistance of the respective subtype to a compound).

This analysis also provides compelling evidence that both exocrine-like and QM-PDA cells are relatively resistant to Dasatinib, whereas the classical subtype showed a $>10^4$ fold lower median IC_{50} value, which is within the range that has been previously reported to be therapeutically relevant [105] **(Figure 32A)**. We found the same subtype-specific trend, albeit with a smaller difference in absolute sensitivity, for the Dasatinib-related compound Saracatinib. Again cells of the classical subtype showed the highest sensitivity towards this inhibitor, while both exocrine-like and QM-PDA cells were relatively resistant towards Saracatinib treatment **(Figure 32B)**. This indicates that such treatment has selective potency in cells of the classical subtype.

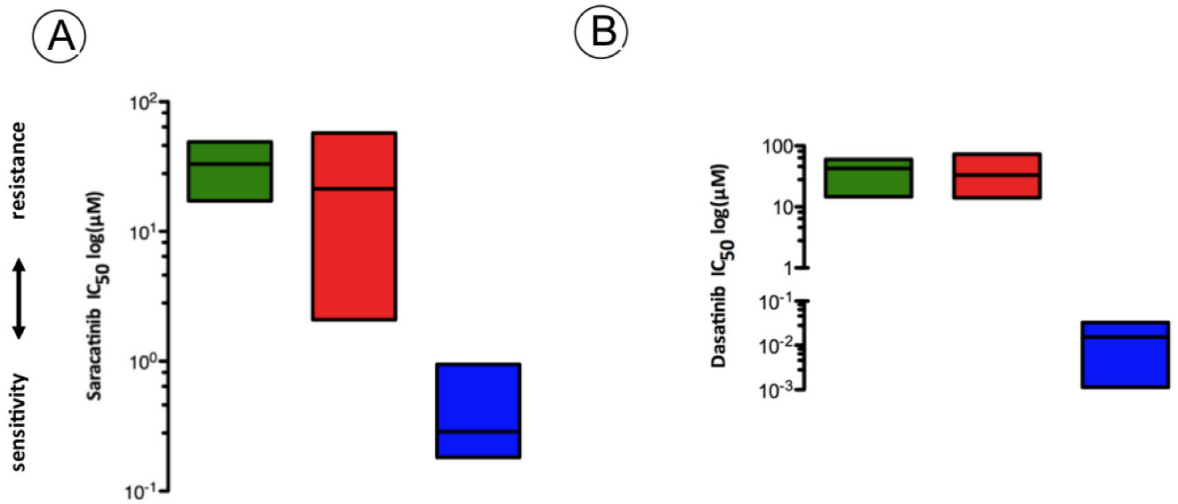

Figure 32 - Min-max plots of IC_{50} values for two compounds targeting the oncogenic Src pathway (A) Saracatinib and (B) Dasatinib representative for three PACO lines of each subtype. Horizontal bar depicts median value (legend indicates sensitivity/resistance of the respective subtype to a compound).

The exocrine-like subtype was significantly more resistant to all compounds tested, including the currently used frontline treatments for PDAC, Gemcitabine and Erlotinib, as compared to both other subtypes. In our gene-expression analysis a signature predicting sensitivity to the BH3 mimetic ABT-737 was selectively enriched in tumors and PACO cells of the exocrine-like subtype **(Figure 21A)**. Determination of the IC_{50} for ABT-737 revealed that the exocrine-like PACO lines were up to 10^3 times more sensitive to this compound compared to the other two subtypes **(Figure 33)**. These results confirm the initial prediction of exocrine-specific sensitivity towards ABT-737, providing a rationale for further exploration of its potential in treating exocrine-like PDAC.

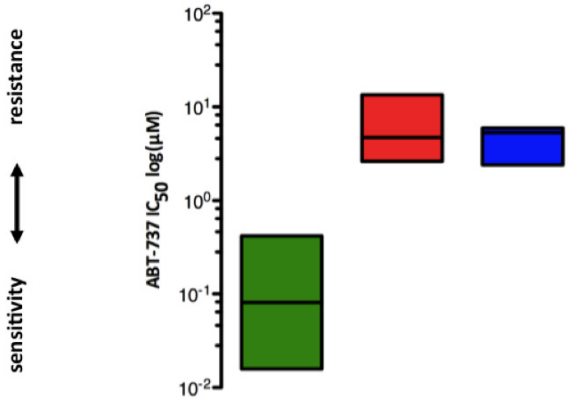

Figure 33 - Min-max plot of IC_{50} values for ABT-737 representative for three PACO lines of each subtype. Horizontal bar depicts median value (legend indicates sensitivity/resistance of the respective subtype to a compound)

Additionally we tested if Dasatinib for the classical subtype and ABT-737 for the exocrine-like subtype increases the *in vitro* potency of Gemcitabine. To test this, we evaluated the IC_{50} of Gemcitabine in a cytotoxic assay on PACO cells treated either in combination with a fixed concentration of either drug or with vehicle alone.

This showed that a fixed dose of 5 µM Dasatinib decreased the median IC_{50} of Gemcitabine of all the classical lines tested by at least 600 fold **(Figure 34A)**. Interestingly we also found a significant effect of this combination treatment in cells of the exocrine-like subtype, while it had no additive effect on QM-PDA cells.

Furthermore, we found a similar trend for the combination of ABT-737 and Gemcitabine. For all exocrine-like cells tested, the IC_{50} for Gemcitabine decreased by > 500 fold when we added a fixed dose of 4 µM ABT-737 **(Figure 34B)**. Again we also detected similar effects in another PACO line although not as profound as for the exocrine-like subtype.

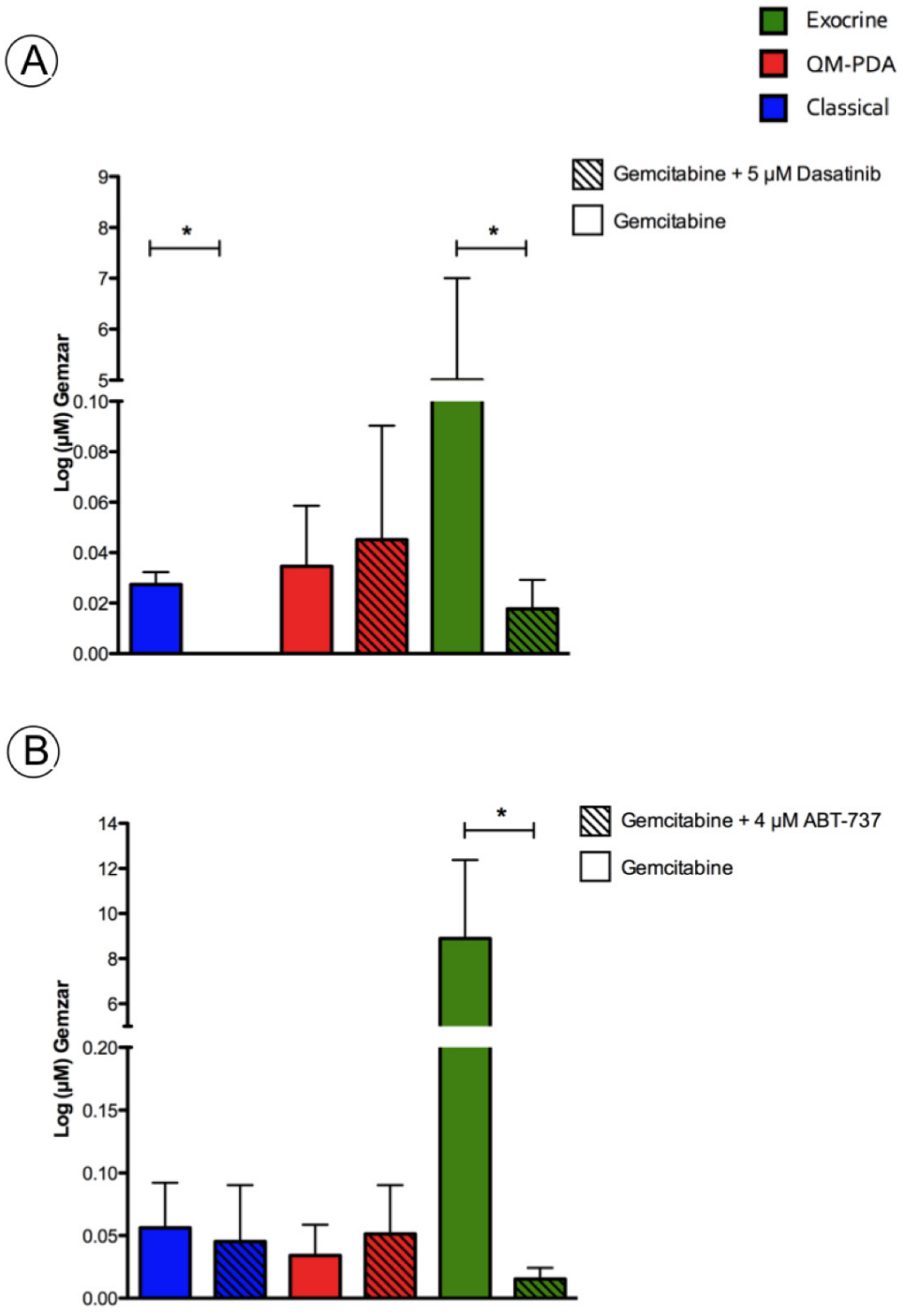

Figure 34 - In vivo efficacy of a combination of (A) Dasatinib and (B) ABT-737 with the standard chemotherapeutic Gemcitabine showed that both compounds selectively potentiated the efficacy of the chemotherapeutic drug. Note that Dasatinib treatment also increased Gemcitabine efficacy in the exocrine-like cells; Displayed are individual mean IC50 values + SEM for Gemcitabine, determined w/ or w/o addition of a fixed concentration of either Dasatinib (A) or ABT-737(B), fixed concentration of either drug represents the median IC50 for this drug across all PACO lines, * $p < 0.05$.

In summary, the data reveal that PDAC subtypes differ widely in their drug sensitivity profiles and demonstrate, for the first time, resistance of the exocrine-like subtype to most drugs tested. Our PACO-model enables the identification of novel subtype-specific drugs, guided by *in silico* analysis. Most importantly, we identified ABT-737 and Dasatinib as drugs with a strong subclass-specific efficacy, which have shown to increase the potency of standard chemotherapy *in vitro*. Those findings thus provide the rationale for patient stratification in PDAC and our model system is a valid tool to discover subtype-specific drugs.

Dasatinib shows strong subtype-specific potency in vivo

Having validated the predicted, differential drug sensitivities in an *in vitro* screen, we were interested if we could validate this strict subtype-specific drug efficacy *in vivo*. Therefore we used three model PACO lines of different subtypes to generate a cohort of mice bearing subcutaneous tumors for treatment. After tumor establishment, mice were randomized to individual groups and treated according to the scheme depicted in **Figure 35**. We included the current standard of care, Gemcitabine, both as a single treatment and as combination treatment with Dasatinib, to evaluate if Gemcitabine potentiates the effects of Dasatinib *in vivo*.

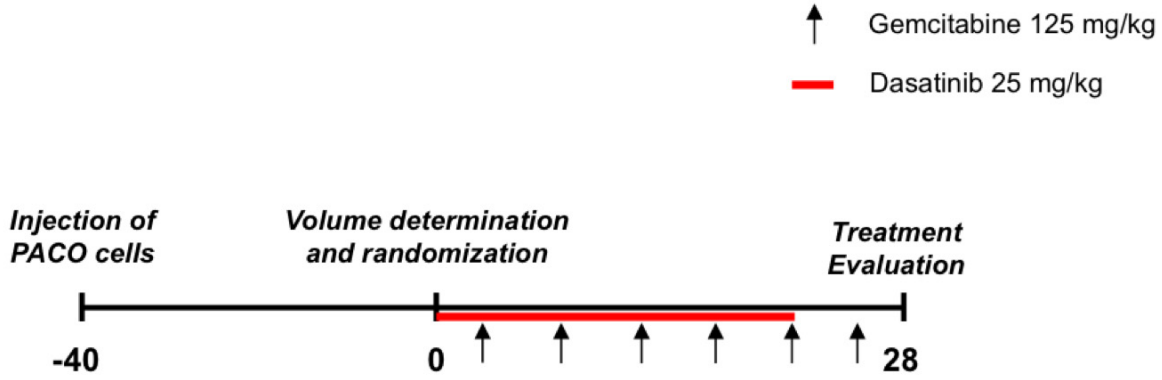

Figure 35 - Schematic overview of the treatment schedule for testing the *in vivo* efficacy of Dasatinib treatment

While we found Dasatinib to be effective as a monotherapy in two independent tumors of the classical subtype (PACO 2 and PACO 17), thereby significantly delaying primary tumor growth (2-way ANOVA $p<0.05$) (**Figure 36A,B**), both the exocrine-like and the QM-PDA subtype tumors were not significantly inhibited in their growth (**Figure 36C,D**). For the exocrine-like tumors (PACO 3) we even observed that the single-treated tumors grew significantly better than the control tumors ($p<0.05$). In tumors of the QM-PDA subtype (PACO 8) Dasatinib mono-therapy did not significantly enhance or decrease tumor growth ($p>0.05$). For all subtypes we observed that single treatment with Gemcitabine significantly delayed tumor growth in our observation period ($p<0.05$), with a higher potency in tumors of the classical subtype, decreasing tumor growth by roughly 5-fold compared to the control.

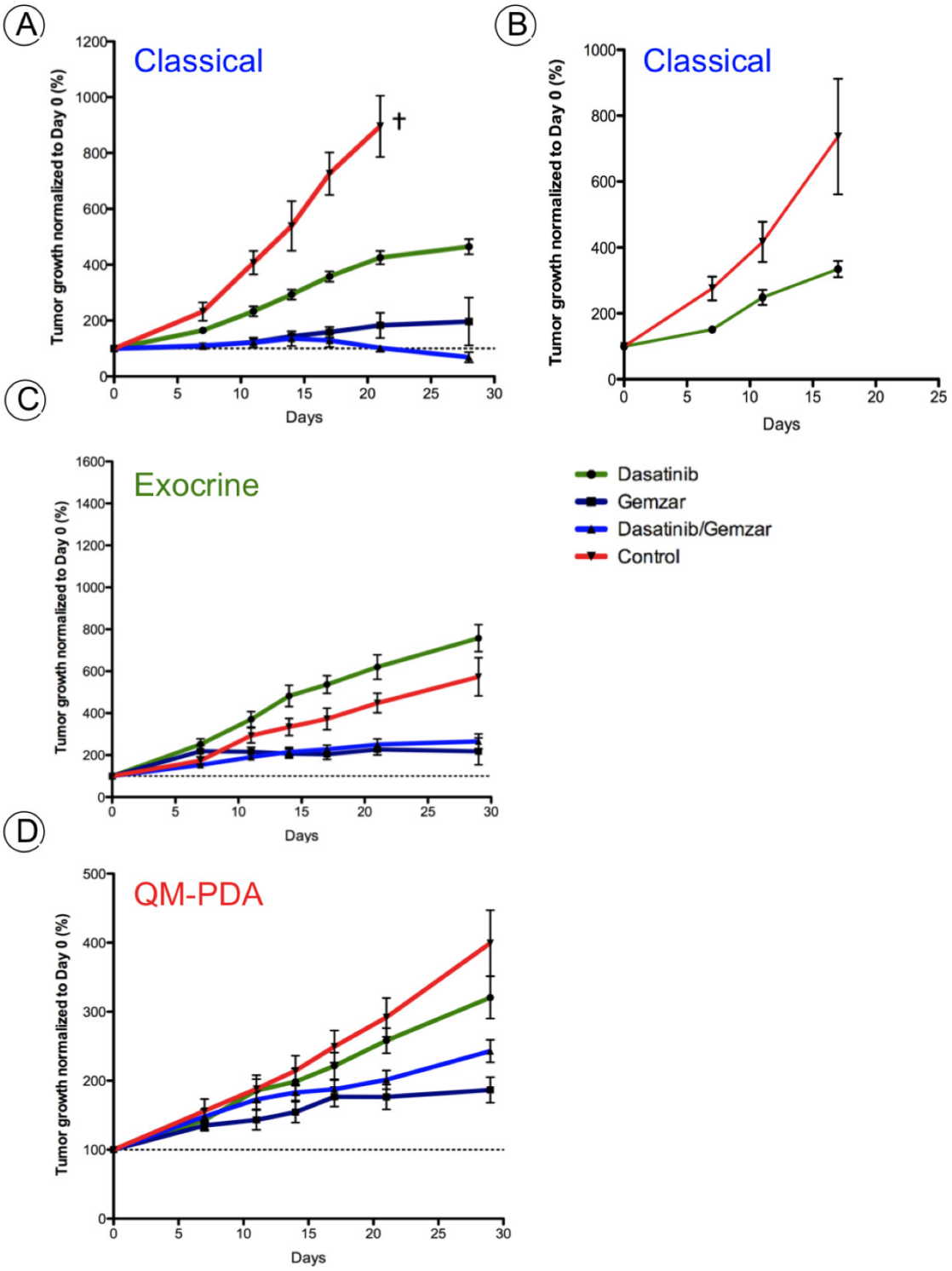

Figure 36 - Tumor growth curves for the respective treatment groups of tumors of the classical subtype (A,B), the exocrine-like subtype (C) and QM-PDA subtype (D) indicated that Dasatinib treatment both as single and combination with Gemcitabine is selectively effective in classical tumors, while both other subtype only marginally (D) or even adversely (C) responded to Dasatinib treatment (data are displayed as mean ± SEM, n = 10 for each group).

The combinatorial treatment of Gemcitabine and Dasatinib showed no additive effects in tumors of the exocrine-like and QM-PDA subtype (**Figure 36B,C**). Tumor growth in the combinatory treated group was inhibited to a comparable extend as with Gemcitabine treatment alone. Tumors of the classical subtype however, as shown for the *in vitro* treatment, responded to the combination treatment with a significantly inhibited primary tumor growth in mice, as compared to mono-treatment with either Dasatinib or Gemcitabine **(Figure 36A)**.

End point analysis of the individual tumors confirmed these results. We observed significantly lower tumor masses in all treatment groups of the classical subtype tumors (PACO 17). Interestingly, we also found a significant difference ($p<0.05$) in tumor mass between the Gemcitabine and Gemcitabine/Dasatinib treated classical subtype tumors confirming the effectiveness of the combined treatment in these tumors **(Figure 37A)**.
Furthermore this analysis confirmed the effectiveness of Gemcitabine treatment in tumors of the exocrine-like subtype (PACO 3). We also observed, that the combination of Gemcitabine and Dasatinib has no significant, additive effect to that of Gemcitabine alone **(Figure 37B)**. Even though we observed a difference in the median tumor mass between Dasatinib treated tumors (0.61 g) and vehicle treated tumors (0.42 g), this difference did not reach statistical significance ($p>0.05$).
The tumors of the QM-PDA subtype responded to treatment with Gemcitabine, although this difference was not statistically significant ($p>0.05$). Our analysis furthermore confirmed that neither the treatment with Dasatinib, nor the combination of Dasatinib and Gemcitabine showed any significant effects in tumors of this subtype **(Figure 37C)**.
Taken together this shows that Dasatinib, either as mono-therapy or in combination with Gemcitabine, selectively inhibits growth of tumors of the classical subtype, while showing no or even inverse effects on tumors of both other subtypes.

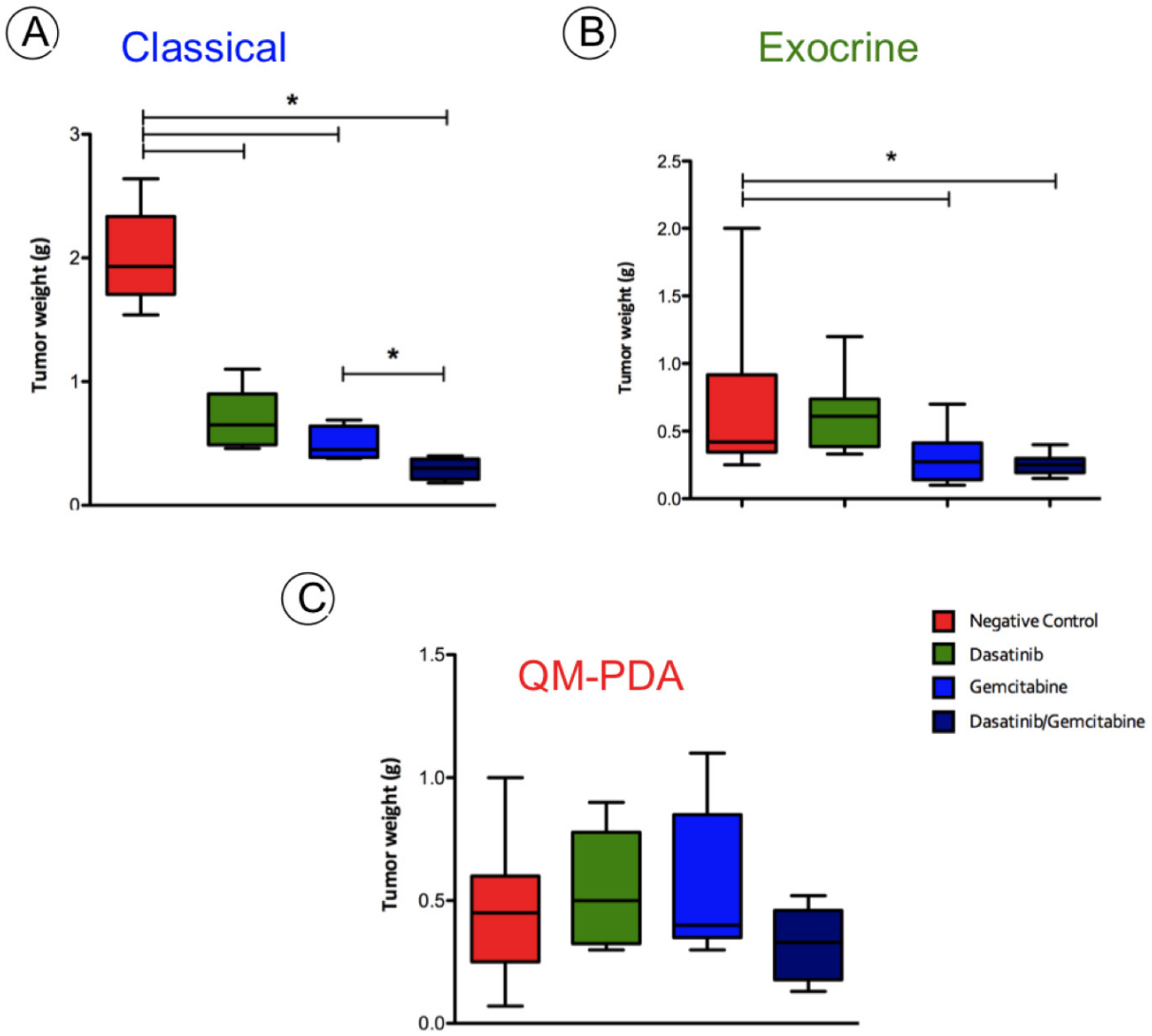

Figure 37 - Tumor weight determined for each treatment group after end of the treatment scheme depicted in Figure for each subtype (A) Classical (B) Exocrine (C) QM-PDA.(Data are displayed as Box plots ± SEM; * denotes $p < 0.05$ determined by ANOVA)

6 Discussion

In summary, we show the establishment and a first exploration of a novel pancreatic cancer model system termed PACO, which allows generating primary cell line models from patient tumors via an intermediate xenograft step. Importantly, orthotopic transplantation of PACO cells re-initiates patient similar tumors, making the PACO system a very versatile tool for the discovery of novel subtype specific markers and drugs. The power of this system is demonstrated by the identification of the first markers (KRT81 and HNF1) useful for stratification of three subtypes of PDAC (QM-PDA, classical and exocrine-like) by histopathology. Application of those markers identified significant differences in overall survival between the three subtypes. Moreover, our data suggest Dasatinib and ABT-737 as first drugs that show high specificity and efficacy for PDAC cells of the classical and exocrine-like subtype respectively. The observed differences in drug sensitivity within the individual PACO subclasses underscore the need to introduce molecular stratification of pancreatic cancer patients followed by subclass-specific therapies. This work and the PACO system may contribute to the development of improved diagnostics and therapeutics for the benefit of patients suffering from this devastating cancer.

Establishment and evaluation of a novel pancreatic cancer model to study the heterogeneity of the disease

In this study, we established a novel, primary pancreatic cancer model (PACO), which recapitulates the original tumor histology and preserves subtype-specific gene-expression patterns. Our model is based on an intermediate xenograft step to enrich for tumor cells, allowing us to furthermore assess the quality of the obtained clinical specimen. Several studies have shown that direct xenografts of human tumor specimens preserve the phenotype of the original tumors [47,106]. Comparison of the histopathology of our primary xenograft tumors with the corresponding patient tumors confirmed that all characteristic features of the primary tumor are retained in the xenograft in line with previous reports [106]. Xenograft models have been demonstrated to be suitable for drug testing [107,108] and some have already successfully predicted the clinical response to therapy [109,110]. However the use of direct xenografts has its limitations. The inherent heterogeneity of tumor specimens renders the reproducible generation of larger groups of animals difficult. Further, high-throughput drug screening for the discovery of novel compounds is also exacerbated by the complexity of the technique [106]. Also, since in almost all cases immune-compromised mice are used for xenografts, the lack of a functional immune system inhibits analyses on the tumor-host interaction.

To partly overcome such limitations, genetically engineered mouse models have been developed that accurately recapitulate the human disease. A major advantage of such models is the development of a host-matching tumor microenvironment. Moreover, genetically engineered mice are fully immune-competent and thus allow the study on the interaction between tumor cells, the microenvironment and the host immune system. Several different GEMs exist for PDAC, which have previously been used to advance our understanding of the development and biology of PDAC [39], with many of them also being used for pre-clinical testing of therapeutics [111].

Even though these GEMs closely mirror human cancerogenesis, several studies already revealed that many of the molecular and genetic alterations occurring secondary to the initial, genetically introduced alteration are not found in the human disease (M.Barbacid DKFZ joint lecture). The initiating KRAS mutation has been targeted to multiple compartments of the pancreas, e.g. the ductal lineage, acinar cells or endocrine cells, however it is still debated, which of the human counterparts gives rise to the founding mutated clone [3,5,6]. Also targeting of additional loci like e.g. *SMAD4*, *INK4/ARF* already provides the pre-cancerous cells with a fixed set of driver mutations thereby limiting and at the same time impairing the *de novo* acquisition of equivalent or novel genetic aberrations. Therefore studies on GEMs in every case have to be considered with caution, as findings in the murine setting cannot be easily transferred to the human disease [106]. Additionally, any compound or antibody tested in such models needs to be validated with respect to the human disease [106]. Thus, identification and validation of anticancer drugs requires both *in vitro* and *in vivo* models that accurately represent the original human malignancy.

Historically, *in vitro* tumor culture is perceived as cultivation of primary tumor cells in media supplemented with fetal calf serum [112]. As for other cancers, major insights into the biology of pancreatic cancer have been gained by using such models [74]. However, FCS-cultured cell lines upon xeno-transplantation frequently result in tumors that phenotypically do not resemble the originating tumor [35]. One of the most evident issues here is that many of them lost the capacity to develop the characteristic stromal compartment [113]. Indeed we found that orthotopic xenografts of two prominent PDAC cell lines, BxPC3 and PANC1, either completely lacked (PANC1) or sparsely developed (BxPC3) a desmoplastic reaction **(Figure 16B)**. Furthermore, serial passage in FCS leads to the acquisition of secondary mutations over time as well as outgrowth of tumor subclones, which are not found in the primary tumor [114]. Although multiple studies have tried to tackle this problem by establishing novel pancreatic cancer lines [115,116], the underlying problem of this culture technique remains.

In order to establish an improved culture system we adapted serum-free culture techniques that previously have been successful in preserving the phenotype of multiple tumor entities [35,59,60].

Tumor cells derived from our primary xenograft tumors were used to develop adherent *in vitro* cultures, which upon re-injection in secondary recipient mice form tumors that recapitulate the original tumor's histopathology. Our model thus retains the phenotypic diversity of the corresponding primary tumors suggesting that it enables the propagation of the full heterogeneity of human PDAC.

However, we cannot rule out a selective bias towards certain PDAC subtypes in our model, which might have been introduced by factors inherent to either the model itself or the integrity of primary tumor specimens. We found that a total of 44% of PDAC specimen did not form xenografts. Many aspects might contribute to an unsuccessful engraftment like compromised quality of the tumor sample obtained, a small quantity of viable tumor cells, failure to recapitulate crucial tumor-microenvironment interaction or inability of a specific type of human PDAC to engraft *in vivo*. Another limiting factor in our model is the vast heterogeneity of primary tumors. Several studies have shown that tumors are not only displaying inter-heterogeneity but also intra-heterogeneity [64]. Yachida et al. analyzed serial sections of pancreata from diseased patients and could show that multiple clones with heterogeneous mutational spectra exist within a primary pancreatic tumor [7]. Given these data we cannot ascertain that the primary tumor specimens in our study represent the complete clonal complexity of the corresponding tumors. Therefore any conclusions being made about a specific tumor xenograft might not hold true for the entire corresponding primary tumor.

We evaluated a number of combinations of different substrates and growth factors to determine the optimal conditions for the culture of primary pancreatic tumor cells. At the beginning we compared adherent versus suspension culture.

We found the suspension culture to be inferior in many aspects. On the one hand it circumvents the critical factor that cells in a tissue very rarely exist as free-floating aggregates, but in almost every case need a substrate to grow in order to evade anoikis.

Additionally, the uniform access to growth factors in the adherent culture model impairs any potential spontaneous differentiation. Several studies report this phenomenon occurring in spheroid culture due to the low perfusion of spheres with such factors [35,60].

Furthermore, large-scale high-throughput screens e.g. for discovery of novel drugs are not possible with spheroid culture. Above all we found, at least in our hands, that spheroid culture also extends a significant number of fibroblast-like cells, which we were not able to remove that easily as in the adherent culture setting. However, adherent culture also has its limitations, as spheroids can, at least to some extend, mirror the 3D environment of cells, thereby mimicking a microenvironment within the culture dish.

Even though several studies reported the successful expansion of primary PDAC cells as spheroids we chose adherent conditions for our culture model.

Additionally we tested a number of different coatings (FCS, Matrigel and Collagen) together with additional growth factors (Shh, Jagged1) in the basic SCM. As we did not observe enhanced growth of tumor cells through the use of a specific coating or growth factor **(Table 2)**, we decided for the most practical culture method, i.e. culture of primary PDAC cells on Primaria flasks with basic stem cell medium. However it remains to be determined if any of the tumor cells not growing in the basic stem cell medium (PT12, PT25) additionally need any of the two tested growth factors or even other growth factors not tested, for expansion *in vitro*.

All of the PACO cultures we established using these conditions could be stably propagated for at least 20 passages and retain tumorigenicity throughout culture.

Although our PACO cultures consist of 100% human, epithelial cells **(Figure 13)** they still retain the capacity to develop the stromal compartment reminiscent of its primary tumor **(Figure 16A)**. However the microenvironment of our tumors is limited to the stromal compartment as NSG mice fail to trigger an immune reaction as seen in human PDAC [117]. Hence the tumors generated by our PACO model fail to recapitulate the complete extend of tumor-microenvironment interaction, therefore largely impairing analyses on such. Additionally, the fact that the tumor microenvironment present in the PACO-DT as well as in the initial xenografts is derived from the murine host might also induce changes in the tumor cells that are not present in the primary human tumor.

Above all we also cannot rule out that the culture method itself introduces a selective bias thereby only favoring the selective outgrowth of distinct clones present in an otherwise heterogeneous primary xenograft. Not every cell, embedded in a 3-D microenvironment of neighboring tumor cells and adjacent stromal cells is capable of growing in a 2-D environment. Thus our otherwise heterogeneous xenograft cannot be mirrored completely by our *in vitro* culture technique. However from analyses on the respective tumors' gene expression data we can conclude that the expression profile of both primary xenograft and corresponding PACO DT xenograft shows a significant correlation in all cases studied (R^2 > 0.8) **(Figure 19B)**. Another example is the lack of CD133 expression in both PACO2 and PACO8, while both corresponding xenografts express this marker. Conversely the respective PACO-DT xenografts both re-express CD133 at levels comparable to the primary xenograft **(Table 5)**. Taken together, our data suggests that the PACO model introduces several selection steps, e.g. *in vivo* xenograft, *in vitro* culture, and that the cell lines display intra-culture homogeneity. However our model still retains the capability to fully recapitulate the heterogeneous expression and marker profile characteristic for the corresponding primary xenograft.

Despite the limitations of our model system, it nevertheless resolves some of the major issues inherent to the direct xenograft model, however preserving its advantages. The PACO model also maintains genetic stability within individual cell lines and heterogeneity across different lines, thereby resolving the biggest disadvantage of conventional cell culture methods.

Thus this new system significantly extends the repertoire of human pre-clinical models that are available to both develop biomarkers and to test novel therapeutic approaches.

The PACO model preserves all molecular PDAC subtypes and confirms exocrine-like PDAC as a distinct subtype

Historically, pancreatic adenocarcinoma was perceived as one disease and as such treated uniformly. Even though molecular subtypes have been defined for a number of different carcinomas [71,118,119], some of them are already guiding clinical therapy [67], the identification of pancreatic cancer subtypes based on molecular features is complicated by the lack of reliable, cancer-related gene expression data. So far, pancreatic cancer has been subclassified in many studies correlating histopathological marker expression or mutational status with overall survival [120,121]. Yet, none of these studies have stimulated therapeutic or diagnostic advances in pancreatic cancer.

In 2011, the study of Collisson and colleagues provided the first evidence that PDAC is comprised of at least three distinct molecular subtypes. They based their analysis on gene-expression signatures derived from micro-dissected pancreatic tumors and termed the three identified subtypes quasi-mesenchymal (QM), classical and exocrine-like pancreatic adenocarcinoma [122]. Although both conventional human PDAC cell lines and cell lines derived from GEMs, were shown to represent the classical and QM-PDA subtype *in vitro*, none of the available and tested pancreatic cell lines were of the exocrine-like subtype. As the signature for this subtype contains many genes usually expressed by acinar cells, the possibility was raised that the exocrine signature may have been caused by contamination of tumor cells with normal exocrine pancreas.

In our study we confirmed the findings from Collisson and colleagues, as we identified in our cohort of pancreatic cancer xenografts, five tumors of the classical subtype, four of the QM-PDA subtype and five of the exocrine-like subtype.

Interestingly we found that the three molecularly distinct groups of tumors could not be discriminated based on morphological features. Only tumors belonging to the QM-PDA subtype could be well distinguished as they exclusively displayed a poorly differentiated histology. However, it was remarkable that both classical and exocrine-like tumors are indistinguishable at the histopathological level.

Interestingly the observed morphological differences in pancreatic adenocarcinomas have been described before [95] and are very well known among pathologists (personal communication Wilko Weichert). However no study yet concluded a strict subtype-specific association from this morphological divergence.

As we were able to develop *in vitro* PACO models from 12 primary PDAC xenografts, we investigated if the primary cell lines retain the subtype associations of their corresponding xenografts. Indeed we found that all lines derived from QM-PDA and classical PDAC xenografts stably retained these subtypes *in vitro*, thereby confirming previous findings [82] **(Figure 20)**. In this respect we were especially interested if the PACO cells lines derived from exocrine-like xenografts still represent this subtype *in vitro*. Indeed we could show that all four PACO lines derived from exocrine-like tumors still retain the subtype-specific expression profiles *in vitro* **(Table 6)**. Additionally, upon transplantation of these PACO cells in secondary recipients, the PACO derived tumors closely mirror the gene expression of the originating xenografts thereby preserving the exocrine-like specific profile even after *in vitro* culture. We thus show for the first time that the exocrine-like subtype is a distinct subtype of pancreatic cancer and provide, to our knowledge, the first *in vitro* and *in vivo* model for studying this PDAC subtype.

We found that we were only able to develop PACO lines from 12 out of 16 primary xenografts generated, from which PT19 and PT36 is still under investigation. Interestingly there was no significant association for that a specific subtype had a worse capability to be propagated *in vitro*, as one of these tumors was classified as classical (PT12) while the other one was found to be of the exocrine-like subtype (PT25). There are multiple, possible explanations for the failure of these tumor cells to grow *in vitro.* They might depend on specific growth factors, which are not provided in our media or they need a specific substrate or microenvironment in order to grow *in vitro*. This observation might also hint at the existence at additional subtypes of PDAC that cannot be propagated by our PACO culture model.

Having shown that all previously reported subtypes can be propagated *in vitro*, the inherent biological differences observed both *in vitro* and *in vivo* also raises the possibility of the existence of additional PDAC subtypes. For example one QM-PDA line (PACO 8) displayed a higher *in vivo* clonogenicity than the other cell lines of this subtype. Also the differences in metastatic capacity, e.g. PACO 8 of the QM-PDA subtype metastasizes to the liver, while all other QM-PDA tumors did not develop macroscopic metastases, argues in favor of additional, biologically different types of QM-PDA. Recent large-scale molecular analyses on over 2000 breast cancer specimen have already provided compelling evidence that based on such molecular profiles, the established breast cancer subtypes can be further subclassified [69].

As noted above, many genes usually expressed in the exocrine compartment of the pancreas comprise the exocrine-like signature. This might hint at different cells of origin for the individual PDAC subtypes. While the exocrine-like PDAC potentially develops in the exocrine compartment hence retaining much of the tissue-specific gene expression, both the QM-PDA and classical subtype possibly develop in different pancreatic compartments. This might be a reasonable explanation as tumors, which developed in GEMs that target the initial KRAS mutation to different pancreatic compartments are indistinguishable at the histopathological level [8].

The finding that QM-PDA tumors exclusively present with an almost complete loss of differentiation, while both classical and exocrine-like tumors display a well-differentiated histology might also argue in favor of a putative PDAC progression model. In such, both exocrine-like and classical PDAC could be the early forms of pancreatic cancer, as they still retain many of the morphological characteristics of the tissue of origin. As the tumor progresses, it de-differentiates thereby losing any remnants of ductal morphology and thus develops in a QM-PDA tumor. It is tempting to speculate that the QM-PDA subtype can be further subclassified into a QM-exocrine-PDA, tumors that developed from an exocrine-like PDAC, and a QM-classical-PDA, which advanced from an initially classical subtype PDAC.

Interestingly such a model of subtype conversion has recently been described in the case of lung cancer, where several tumors of the non-small cell type developed into a small-cell type lung cancer [123]. Our data indeed contains several observations that substantiate a hypothesis of two biologically distinct QM-PDA entities.

Analysis of the gene expression profiles revealed that two QM-PDA cell lines (PACO 9 and 20) cluster together with the classical tumors, while both other lines (PACO 7 and 8) exhibit a greater accordance with the profiles of the exocrine-like tumors (data not shown). Above all, one of the principal investigators of the study that initially devised the three PDAC subtypes confirmed the existence of a fourth PDAC subtype, which subdivides the QM-PDA (A. Sadanandam, personal communication). In this perspective, genetically engineered mouse models can be used to answer many of these unsolved questions. Analysis on PDAC tumor samples at different time points of development could substantiate either a parallel or linear subtype progression model. Furthermore lineage-tracing analyses will allow to identify the cells of origin for the different subtypes of PDAC.

Novel subtype-specific markers allow stratification of patients

Patient stratification is becoming increasingly important to discern patients that will benefit from a given therapy from those who won't. Current clinical standard in diagnosis is the evaluation of specific marker expression by immunohistochemistry. In breast cancer for example, the status of estrogen, progesterone and HER2 receptors are identified by histopathology and are subsequently used to guide specific treatments. The overall prognosis of breast cancer patients has significantly increased since the introduction of this sub classification [1], as it discriminates patients who need to be treated more aggressively (e.g. triple-negative breast cancer [124]) from those who benefit from targeted therapy (e.g. HER2+ breast cancer [125]).

Despite extensive research and numerous studies proposing several novel marker candidates for PDAC [3,9,15], none of these markers translated into clinical practice. Pancreatic cancer is mostly diagnosed based on morphological features determined by histology rather than specific protein marker expression (personal communication Wilko Weichert).

We have shown that only two of the three reported pancreatic cancer subtypes could be categorized by such an approach, as classical and exocrine-like tumors are indistinguishable at the histopathological level **(Figure 11)**. Thus, to introduce unbiased PDAC subtyping into clinical practice, markers are needed, which allow discriminating subtypes via analysis of histological sections.

To this end, we followed a multistep approach by combining multiple bioinformatic tools, which yielded a list of putative marker candidates that was refined by evaluating the specificity and reliability of their respective marker staining in the Human Protein Atlas. This resulted in a list of 15 marker proteins with the potential to discriminate between PDAC subtypes **(Table 7)**.

Among the six markers we tested for the exocrine-like subtype, we identified an antibody targeting the transcription-factor HNF1 exclusively staining tumor cells of this subtype. So far, expression of HNF1 was discovered in both endo- and exocrine cells of the developing pancreas, while no expression could be detected in the adult pancreas [126]. Gidekel et al. suggested that chronic inflammation could alter the fate of insulin-expressing cells of the endocrine pancreas to serve as cell of origin for exocrine neoplasia [127]. The observed, selective re-expression of HNF1 in exocrine-like tumor cells would be consistent with a potential endocrine cell of origin with an altered cellular fate responsible for this subtype of PDAC. Interestingly this finding substantiates our observation of a selective enrichment of several liver-specific genes like e.g. aldo-keto reductases, alcohol dehydrogenases etc., as well as enrichment for liver-specific gene sets in the tumors and cells of the exocrine-like subtype, as many of these genes are directly regulated by HNF1 [128,129].

For the QM-PDA subclass we evaluated a panel of four markers and found two of them to be exclusively staining tumors of this subtype – Vimentin and Keratin-81 (KRT81). The QM-PDA subtype is characterized by the expression of several genes associated with epithelial-to-mesenchymal transition (EMT), e.g. *TWIST1* is part of the QM-PDA classifier, and furthermore displays a mesenchymal-like morphology both *in vitro* and *in vivo*. Additionally we found QM-PDA tumors and cells to be enriched for several gene sets associated with EMT, metastasis and induction of such (data not shown).

Thus our finding that both markers are exclusive for the QM-PDA subtype is supported by these observations as well as by previous reports [82].

The intermediary filament Vimentin is a marker of mesenchymal cells and used as the most widely accepted marker for tumor cells undergoing EMT. It is furthermore associated with metastatic dissemination in many types of cancer, including PDAC [130-132].

Expression of Keratin-81 is usually found in hair follicles [133]. Recent studies however reported a correlation of KRT81 expression with pulmonary metastasis in breast cancer as well as an increased risk of recurrence in lung cancer and multiple myeloma [134-136]. Taken together both of the identified markers support the notion of a mesenchymal-like state of the QM-PDA tumors and further substantiate our data on a potentially active EMT in these cells. As noted, both markers Keratin-81 and Vimentin have been previously associated with an increased metastatic capability [130,134]. However analyzing the capacity of developing spontaneous metastases in our four QM-PDA model lines, we only found metastases occurring in xenografts of one of these lines (PACO 8), which is an apparent contradiction to the observed and reported increased metastatic capacity of cells with active EMT. Possible explanations are that our culture selects for the non-metastatic clones of the QM-PDA subtype or that specific growth factors, substrates or micro-environmental influences are needed to support the metastatic capacity of these cells. It is also possible that the cells are lacking specific micro-environmental cues *in vivo,* like e.g. external stimuli from parts of the immune system, which are not present in our NSG model. Also the observation that only 1 out of 4 QM-PDA cell lines develops spontaneous metastases hints at the existence of additional subtypes, further subdividing the QM-PDA subtype into highly aggressive QM-PDA (PACO 8) and less aggressive QM-PDA (PACO 7, 9, 20). Of course we cannot rule out that at time of necropsy, mice with QM-PDA xenografts already had microscopically detectable metastases, which could be detected by serially sectioning the liver or lung of these animals.

As we validated both markers on the corresponding patient tumor sections, we observed massive background expression of Vimentin in the stromal compartment. Since this is the major constituent of human PDAC tumors [137], with tumor cells being scattered among it, a marker which additionally stains this predominant part of the cancer will not prove useful in

clinical practice. Hence even though expression of Vimentin can still be considered as being subtype-specific, our data showed that it is not tumor-specific.

The classical subtype is characterized by the expression of genes that are commonly associated with the ductal cells of the pancreas, such as keratins and CEACAMs [9], which might hint at a ductal cell of origin for the classical PDAC subtype. However, the common expression of those genes rendered the discovery of specific markers difficult. From a set of five potential markers, we identify two, nuclear localized S100A1 and TFF3 to be exclusive for tumor cells of the classical subtype in our xenografts. However, when we validated these markers on corresponding primary tumor slides, we observed staining in multiple tumors not classified as being of the classical subtype. Despite testing of several marker candidates none of those showed specific expression when assayed on the corresponding patient tumors. A potential explanation might be that even though the difference in expression level for the candidate marker proteins was shown to be significant, the other two subtypes still express enough protein to be detected by IHC. Hence future approaches to identify a marker specific for the classical subtype should exclude genes commonly expressed in the pancreas in order to focus on PDAC-specific genes, thereby minimizing the potential of unspecific staining.

As we identified HNF1 to be specific for the exocrine-like subtype and KRT81 expression to be exclusive for the QM-PDA tumors, we designated classical tumors as double negative (DN), i.e. staining for neither of these markers **(Figure 27)**.

We thus investigated if our set of two markers can unambiguously identify all three PDAC subtypes in a larger group of patients. Application of those markers to a cohort of 258 PDAC patients confirmed a largely non-overlapping staining (96% stained exclusively for one or neither of the two markers); demonstrating the robustness of our two marker-set. This allowed us to stratify patients according marker staining into three groups, HNF1 positive (exocrine-like), KRT81 positive (QM-PDA) and DN (classical). Interestingly, we found a significant difference of overall survival (OS) between the three groups. KRT81-positive patients had the worst prognosis (mean OS=16.5 months), which we found to be coherent with findings from Campayo et al. and de Larrea et al., which both reported a significant

correlation of KRT81 expression and decreased overall survival in both lung cancer and multiple myeloma.

HNF1 positive patients had the best outcome in our analysis (mean OS=43.5 months), which could be explained by the low proliferative index of the respective tumors as compared to both the other two subtypes. Patients with a double negative tumor designated as being of the classical subtype displayed intermediate overall survival when compared to both other subtypes (mean OS=26.3 months) **(Figure 28)**.

Taken together the clinical demonstration that the QM-PDA subtype is the most aggressive type of tumor supports the finding of Collisson and colleagues [82] as well as our observations that these tumors are exclusively associated with gene-sets predicting active EMT and a high metastatic capacity. However, as already stated above, this data contradicts our observation that QM-PDA tumor cells have a lower clonogenic potential both *in vivo* and *in vitro* when compared to both other subtypes. Potential reasons for this apparent conflict are possibly inherent to our model system and have been stated earlier on.

As noted above we also found a total of 11 patient tumors staining for both markers HNF1 and KRT81. There are several potential explanations for this observation. On the one hand this might support the notion of a potential conversion of subtypes in a way that tumors staining for both markers are currently undergoing transition from one type to the other. On the other hand, as tumors are heterogeneous in nature, the observation of a double staining might be explained by the presence of two different clones within the same tumor that belong to different PDAC subtypes. As the tumor progresses one clone might get outcompeted by the other therefore the majority of the tumors only display single marker or absent staining. Of course, as mentioned earlier, as the biopsies present on a tissue microarray are only representative for the very part of the tumor from which they were derived from, one cannot make statements about the entireness of the respective tumor.

Until now, subtyping of PDAC required the analysis of the gene expression profile of respective tumors. Until now, only a small set of patient tumors on the TMA (10%) has been analyzed by gene expression analysis in order to investigate the concordance of subtype association by marker staining and expression profile. Thereby we found that both protein

marker and gene expression profile classified >60% of tumors accordingly (ongoing work). Protein marker expression is in general more robust than gene expression as sample processing and fixation can alter the gene expression in tissues [138].

Furthermore, profiling of formalin-embedded fixed samples is still an erroneous technique. Therefore, histopathological staining for a set of markers, which can be easily incorporated into clinical routine diagnostics, is more favorable than gene expression profiling in order to determine the subtype of a given tumor sample.

We thus identified a set of markers that unambiguously classifies the three subtypes of PDAC in a clinically relevant setting. Furthermore we have shown that our markers, for the first time allow a clinically meaningful stratification of PDAC patients.

Different pancreatic subtypes show distinct pathway activation signatures

Several pathways, which are deregulated in PDAC, have been described, including PI3K, Hedgehog, mTOR, SRC [139-141]. The efficacies of some drugs that target those pathways have been investigated for their potency in PDAC, however with limited success [9]. We here show a strict subtype-specific association of some of those pathways. *De novo* predictions using molecular pathway analysis in our PACO model coupled with validation of pathway activity *in vitro* and *in vivo*, provided powerful insights into the mechanisms that may be involved in growth, aggressiveness and therapy-resistance of the individual subtypes.

In our molecular analysis we found strong enrichment of multiple signatures predicting a selective activity of the PI3K/mTOR pathway in both the classical and QM-PDA subtype **(Figure 21A)**. The PI3K/mTOR pathway is one of the major signaling pathways involved in cancerogenesis and has been reported to be play a central role in a variety of human cancers [142]. Aberrant activation of this pathway can either be caused by hyperactive, upstream receptor tyrosine kinases or by mutations and amplifications of major pathway components [142]. The PI3K and mTOR pathway are interdependent pathways by either sharing common substrates, negative feedback loops, or direct activation mechanism, and as such have been previously associated with functions like the regulation of growth, proliferation, migration,

survival, and angiogenesis [143,144]. Atypical PI3K/mTOR signaling was also found to be a prominent feature in PDAC [144,145]. Alterations in regulators of this pathway such as K-ras mutations, increased expression of receptor tyrosine kinases like EGFR, and loss of PTEN, are potential effectors of inadequate PI3K/mTOR pathway activity in pancreatic cancer [146,147]. It is also tempting to speculate that selective activation of this pathway in QM-PDA and classical subtype PDAC suggests different cells of origin for both of these subtypes as compared to the exocrine-like PDAC. However sparse data is available on the involvement of PI3K/mTOR signaling in the developing or adult pancreas [148].

Several studies showed that activated PI3K downstream effector Akt/PKB identifies a subgroup of pancreatic cancer patients with a significantly worse overall survival [149,150]. We showed in our TMA analysis that both QM-PDA and classical patients had a significantly worse overall survival compared to exocrine-like patients, which is in line with the reported differences in overall survival considering Akt activity **(Figure 28)**.

We could also validate these findings on a larger patient cohort, revealing selective PI3K/mTOR pathway activity in a dataset of >80 human PDAC tumors. Histopathological analysis of sections of xenograft tumors also confirmed a selective and subtype-specific activity of p70S6K, restricted to classical and QM-PDA tumors.

Taken together our findings confirm that the PI3K/mTOR pathway is a major pathway in pancreatic cancer biology albeit with strict subtype-specific activity. Previous studies that analyzed the PI3K/mTOR pathway in pancreatic cancer are predominantly based on conventional FCS-based cell lines. Therefore this crucial selective pathway activity was missed, as none of the studied lines represented the exocrine-like subtype. Hence conclusions on widespread activity of this pathway in PDAC should be re-considered under the premise that only two out of three PDAC subtypes were investigated.

We also detected significant enrichment of several signatures predicting oncogenic Src activity in both the QM-PDA and classical subtype **(Figure 21A)**. The family of Src kinases (SFK) was one of the earliest established families of oncogenes. Overexpression or hyperactivity of SFK members have been reported for a number of different epithelial cancers [151], including pancreatic adenocarcinoma [152]. Elevated SFK levels have been reported

for over 70% of the patients, with roughly 60% of pancreatic tumors showing increased SFK activity. This would partly agree with the data from our TMA, where classical and QM-PDA patients constitute 78% of the total cohort. Two independent studies showed that high SFK activity in primary tumor specimen is an independent prognostic marker for patient overall survival. Both studies concluded that patients with an elevated SFK activity had a poorer overall survival as compared to patients with low SFK activity [153,154]. We detected considerable activity of SFK members only in cell lines and tumors of the classical and QM-PDA subtype. Staining for the activating phosphorylation site Tyr^{419} was exclusively detected in PACO cells and tumors of these very subtypes. Interestingly, we observed strong phosphorylation of the inhibitory site Tyr^{527} exclusively in the cells of the exocrine-like subtype. These findings confirmed our initial prediction of a selective SFK activity in the QM-PDA and classical subtype cells. Furthermore, as for the PI3K/mTOR pathway, the observation that patients with high SFK activity have a significantly lower overall survival is in agreement with the data from our TMA analysis, where patients with QM-PDA or classical subtype tumors have a significantly worse overall survival **(Figure 28)**.

The exocrine-like subtype displayed enrichment for a significantly lower number of gene sets than any of the other subtypes **(Figure 21A)**. Besides that we so far did not detect a pathway specifically activated in this subtype. However we found several gene sets to be negatively correlated, involved in cell cycle progression, DNA synthesis and replication **(Figure 21B)**. Our observations that these cells have the lowest proliferative index both *in vitro* and *in vivo*, as well as the that patients with exocrine-like PDAC survive the longest, might explain, at least to some extend, the prediction of a diminished cell cycle profile. Several explanations might be possible, why we couldn't find significant enrichment for specific pathway activities. One of the most apparent is since the absolute number of exocrine-like tumors were low both in our and the public datasets, any genesets predicting selective pathway activity failed to reach statistical significance. Also it might be possible that the existence of further subclasses of the exocrine-like subtype resulted in a heterogeneous gene expression signature, which then failed to predict any subtype-specific pathway activity with statistical significance.

As we validated all our findings both on expression data from a larger patient cohort and by histopathological demonstration of selective pathway activity, we confirmed that our culture model did not introduce the subtype-specific differences seen.

Taken together we showed that molecular analyses on improved models representing the full heterogeneity of PDAC could be used to predict subtype-specific pathway dependencies. Furthermore, past and future studies have to be reconsidered with respect to the different PDAC subtypes in order to make meaningful conclusions, as we have found selective pathway activation in several subtypes of this cancer.

PDAC subtypes exhibit differences in drug sensitivities to both targeted and cytotoxic agents

Current treatment options for pancreatic cancer patients are limited to Gemcitabine and Erlotinib, which extend the overall survival of patients by only a few months [3]. Several promising drug candidates for PDAC recently failed in Phase III trials [155]. As these trials have been performed in unselected cohorts of patients, one potential reason for these failures could be that subtype-specific efficacies of these drugs are diluted by patients of the opposing subtypes that do not respond. Our PACO model thus allows not only to investigate subtype-specific drug sensitivities in a pre-clinical setting, but also to predict novel therapeutic targets by a combination of *in silico*, *in vitro* and *in vivo* tools. Analyzing the gene expression data of our PACO model, we identified several subtype-specific pathway activation and drug vulnerabilities. Some of those have already been associated with pancreatic cancer and several pre-clinical trials have tested the efficacy of compounds targeting these pathways.

We confirmed a selective activation of the PI3K/mTOR pathway in the QM-PDA and classical subtype both in our *in vitro* models and in the derived xenografts **(Figure 24, Figure 26)**. Aberrant activity of the PI3K/mTOR pathway is a prominent feature of pancreatic cancer and many studies evaluated the efficacy of distinct inhibitors of this pathway both in pre-clinical [147,156] and clinical trials [145] (NLM Identifiers NCT01337765, NCT00560963 and NCT00499486). Cao et al. tested the dual PI3K/mTOR inhibitor NVP-BEZ235 for efficacy in primary human

PDAC xenografts. In the five primary xenografts they analyzed, only three tumors responded to treatment, one with a modest response, while tumor growth in two xenograft tumors was not significantly inhibited by NVP-BEZ235 [147].

These observations are in line with the findings from our PACO model. We found that only cells of the QM-PDA and classical subtype responded to PI3K/mTOR inhibition either with LY290042 or Rapamycin/Torin1 at comparable dosage, whereas the exocrine-like cells were resistant to both agents **(Figure 31)**. Our findings thus may provide a reasonable explanation for the partial response of the xenografts in the study of Cao and colleagues. Having shown that only QM-PDA and classical tumors respond to PI3K/mTOR inhibition, this suggests that the NVP-BEZ235-insensitive xenografts could have been of the exocrine-like subtype. Our findings are further substantiated by another study, which reported efficacy of NVP-BEZ235 in a panel of four conventional cell lines [156]. However, the critical resistance of the exocrine-like subtype to PI3K/mTOR inhibitors revealed by us and observed in the study of Cao et al. is missed by Awashti and colleagues, as conventional cell lines fail to mirror this subtype [82]. Hence, our data suggests that future evaluation of PI3K/mTOR inhibitors should consider their subtype-specific efficacy.

Gene expression analysis also predicted a selective sensitivity of the classical and QM-PDA subtypes to the BCR/ABL and Src inhibitor Dasatinib. However we found that only PACO cells of the classical like subtype responded to treatment with Dasatinib or the related Saracatinib **(Figure 32)**. We currently do not know the basis for this selective sensitivity however several potential explanations exits why the predicted sensitivity to Dasatinib only holds true in the classical subtype. The Dasatinib susceptibility signature, which we used, was generated from breast cancer cell lines, which due to the inherent biological differences between breast and pancreatic cancer might not accurately predict susceptibility of PDAC tumors to this treatment. Another potential issue could be the fact that Huang and colleagues used FCS-based cell lines, which already diverged substantially from what is observed in human tumors and as such fail to mirror the patient situation.

Moreover our data proposes that the family of SRC kinases might not be the prime target of Dasatinib and Saracatinib in the classical subtype cells, as both QM-PDA and classical subtype

PACO cells showed comparable activity levels of SFK **(Figure 23)**, however only the classical subtype cells are inhibited upon treatment. Several reports already evaluated additional targets of Dasatinib other than the SFK members [157,158]. Future studies should therefore aim to identify the target shared by Dasatinib and Saracatinib, which serve as the main target of both inhibitors in the classical subtype cells.

SFK inhibitors already showed promising results in several pre-clinical studies [153,159-161] and are therefore currently evaluated in phase II clinical trials for advanced PDAC (NLM Identifiers NCT00544908, NCT00735917). However, our data suggests that only a subset of patients is likely to benefit from Dasatinib respectively Saracatinib treatment. We showed in our *in vivo* treatment model, that only xenograft tumors of the classical subtype responded with a significant growth inhibition to treatment with Dasatinib both as mono-therapy and in combination with Gemcitabine **(Figure 36A,B, Figure 37A)**. This would be in agreement with studies that analyzed the efficacy of several SFK-inhibitors on human xenografts, revealing that only a fraction of the patient-derived tumors responded to this treatment [160,161]. Surprisingly we found that Dasatinib mono-therapy even promoted the growth of the exocrine-like xenografts when compared to the control **(Figure 36C)**. This might argue that in some tumors, treatment with Dasatinib might even have adverse effects. Similar observations have already been made on primary PDAC xenografts [160,161], underscoring the need of stratifying patients prior to treatment in order to minimize unwanted or even adverse treatment effects. In contrast to our observation *in vitro*, we did not see that the combination of Dasatinib and Gemcitabine resulted in a significant combinatorial effect in xenografts of the exocrine-like subtype. There are several explanations for this, the most apparent is that the *in vitro* culture lacks major parts of the tumor microenvironment and as such cannot predict the impact of this crucial constituent of PDAC with respect to treatment efficacy. Another possible explanation might be that either the concentration at which Dasatinib exhibits additive effects on Gemcitabine is not reached in the tumor due to the huge stromal compartment, which limits perfusion of the tumor with the drug, or not reached at all, as it would be toxic to the animal.

Additionally, as the tumors have been placed subcutaneously and not at the orthotopic site, this might have induced changes in proliferation or gene-expression, which made the tumors insensitive towards treatment.

Previous to our study, it was not possible to study the drug-sensitivity profile of the exocrine-like subtype due to the absence of any cell line model. The exocrine-like subtype showed the most resistant nature among all three subtypes to the tested compounds including Gemcitabine, Erlotinib, LY294002, Rapamycin and Dasatinib **(Figures 31- 33)**.

One possible explanation can be found in the expression profile of exocrine-like cells and tumors. As described above we found selective enrichment of several liver-specific genes, including aldo-ketoreductases, alcohol dehydrogenases and alike, as well as enrichment of cytochrome P signatures and genes. Taken together, this suggests that the exocrine-like cells possess a set of drug metabolizing enzymes similar to that of the liver and as such have the capacity to modify and thus mitigate the potency of many xenobiotics. Another explanation might me the low proliferative index of these cells both *in vitro* and *in vivo*. As most cytotoxic drugs affect rapidly cycling cells, the exocrine-like cells might just grow slow enough to escape most of the cytotoxic effects of such drugs.

Conversely, even though we observed significantly higher tolerance of exocrine-like cells towards Gemcitabine *in vitro*, the corresponding xenografts responded in a similar manner to Gemcitabine as the xenografts of both other subtypes **(Figure 36)**. One of the possibilities explaining this contradiction might lie in the inability of our *in vitro* model to mimic the influence of the microenvironment on the tumor cells. Another aspect, which already has been shown to crucially impact treatment response in xenograft models, is the location of the tumor. As we decided to generate subcutaneous tumors in order to follow tumor response to treatment over time, we introduced a selective bias in our treatment model. Several studies have shown that subcutaneous tumors both of human and murine origin develop significantly higher mean vessel densities, thus promoting accumulation of active gemcitabine triphosphate to a degree not observed in orthotopic respectively primary tumors [44,162,163].

Orthotopic tumors might thus better recapitulate the patient situation, however it remains to be determined if exocrine-like tumors at orthotopic sites respond to Gemcitabine as the corresponding PACO cultures *in vitro*.

Interestingly we showed that in our TMA, patients suffering from exocrine-like PDAC displayed a significantly higher median overall survival (43.5 months) than both other tumor subtypes **(Figure 28B, Table 8)**. This observation is clearly inconsistent with our data showing that this subtype of PDAC exhibits marked resistance to any type of cytotoxic and targeted drug we tested. One would expect that the most resistant type of tumor is also the most aggressive. However several arguments might explain this apparent conflict. The exocrine-like tumor, in a progression model of PDAC, might be one of the earliest forms of PDAC, demonstrated also by the expression of several markers of the developing pancreas e.g. HNF family members. As such, if resected early, it did not yet acquire the aggressive nature inherent to the classical and QM-PDA subtype tumors, did not yet metastasize and hence patients life longer. However when analyzing the TMN classification and grades of the exocrine-like tumors in relation to both other subtypes, we could not find a significant enrichment of low grade (G1/2) or low stage (T1/2) tumors in our cohort of exocrine-like PDAC. As the exocrine-like tumors were shown to proliferate significantly slower than any of the other two subtypes, the exocrine-like tumors might grow slower in the patient, therefore explaining the observed survival benefit.

The gene-expression analysis predicted that inhibition of Bcl-2 function by the BH3-mimetic ABT-737 [164] might provide a novel treatment option for exocrine-like subtype PDAC. Determination of the differential sensitivities to ABT-737 indeed confirmed those predictions in an *in vitro* assay **(Figure 33)**.

Overexpression of pro-survival Bcl-2 family members was reported for many tumor entities. Hence drugs mimicking the function of their pro-apoptotic counterparts, the BH3-only proteins, hold large promise as novel anticancer strategies [165].

Several studies showed that BH3-mimetics are effective as single agents and have the power to potentiate conventional chemotherapy and radiotherapy [165]. ABT-737 has already been evaluated in several Phase I/II clinical trials, which showed that Bcl-2 inhibition is a valid therapeutic option both as mono- and combination therapy in treating a multitude of malignancies such as lymphomas, small-cell and non-small cell lung cancers as well as leukemia [166-169]. We investigated the expression of several pro- and anti-apoptotic Bcl-2 family members in the three subtypes, however we could not find selective enrichment for a specific member in the exocrine-like cells **(Figure 25)**. However many studies reported that the mechanism-of-action of these BH3-mimetics is still unresolved und under investigation [165]. Despite this, the application of BH3-mimetics and similar drugs [170] may provide a novel treatment possibility for exocrine-like PDAC, which should be further explored in the future.

In sum, these findings show that efficacy studies on any novel compound require pre-clinical models that accurately represent the heterogeneity of human PDAC. While i*n vivo* xenograft models are well suited for this purpose, their complexity and difficult handling impairs large-scale screening approaches. Thus our PACO model complements the available *in vitro* and *in vivo* models, enabling large-scale screening of novel drugs as a first step towards personalized medicine.

Concluding remarks and outlook

The primary culture model for human PDAC, which we developed in this study, preserves the full molecular and morphological heterogeneity of pancreatic cancer and demonstrates for the first time that the exocrine-like subtype is a *bona-fide* PDAC entity. Significant differences in pathway activity and drug sensitivities were found between the subtypes. Based upon these findings we revealed novel therapeutic approaches with strict subtype-specificity. This includes Dasatinib for the classical subtype, mTOR/PI3K inhibitors for the QM-PDA subtype and BH3-mimetics for the exocrine-like subtype. Furthermore, we identified two markers, HNF1 and KRT81 that unambiguously classify pancreatic tumors into the three subtypes and demonstrated that the overall survival in a large cohort of patients differs significantly between subtypes.

Future studies will need to elucidate the molecular basis of the differential drug sensitivities to better understand and improve targeted therapies. This could allow predicting the efficacy of novel combinatorial drug treatments while minimizing side effects. Finally, mechanisms of acquired resistance might also differ between subtypes and an in-depth analysis could help to improve treatment schemes in order to prevent therapy resistance. Based on our findings that the classical subtype displays selective sensitivity to Dasatinib – a compound already approved for treatment – clinical trials can be launched evaluating potential subtype specificity in a large cohort of patients. Furthermore it will be interesting to investigate the specific target of Dasatinib in the classical subtype cells, as our data provides the rationale that the SFK might not be the primary target of Dasatinib in these cells.

Our PACO model can also be easily used for high-throughput drug screens, as already demonstrated in this work. Ongoing work encompasses screening of libraries of FDA-approved drugs and drugs that are already in clinical trials. This focused approach allows for fast transition into clinical trials with promising candidates.

Given that many of the pathway activities and drug susceptibilities we analyzed have already been evaluated for their efficacy in pancreatic cancer, however with limiting success, our data proposes that stratification of patients according subtype is a necessity when evaluating treatment success of novel therapies. The here presented set of markers can easily be integrated into the clinical routine and be utilized for stratifying patients prior to treatment or even in retrospective. Ongoing work will focus on the identification of additional subtype-specific markers in order to further refine our marker set. Additionally with regard to the potential existence of additional subtypes, more than two markers are needed to stratify pancreatic tumors.

Moreover, it will be crucial to determine the specific mutational spectrum and epigenetic profile of the individual subtypes. By combining such data with our subtype-specific expression profiles, a deeper understanding about driver mutations and affected pathways can be gained, which will then allow to specifically target central driving pathways in individual subtypes. Along these lines, genetically engineered mouse models can now be utilized to investigate the origin of the different subtypes. It will be important to determine if, as hypothesized earlier, the different subtypes stem from distinct cells of origin or the subtypes may converge and follow a progression model, in which subtypes change as the tumor progresses. Such studies could for example change the way pancreatic cancer is treated in the future. If tumor subtypes result from different cells of origin it is very likely that the molecular profile of such tumors still resembles the tissue of origin. These molecular differences might already provide cues for the efficacy of several therapies.
Furthermore these investigations might also provide novel insights that will lead to a more efficient early diagnosis of PDAC. If it can be shown that pancreatic tumors progress from a less-malignant (e.g. exocrine) to a more malignant (classical or QM) tumor, it would be crucial to catch the disease before it progresses, thereby minimizing the chance of metastatic spread.

As already discussed, studies have shown that multiple mutant clones can co-exist within the same pancreatic tumor. It would be interesting to investigate if these molecularly distinct clones can be classified as different subtypes. Such discovery would have a major impact on the way PDAC will be treated and diagnosed in the future. Any subtyping method would need to consider the entireness of the tumor rather than only a specific and probably regionally limited specimen. Additionally, treatment schemes of such tumors will have to recognize the differential drug sensitivities of individual subtypes.

Furthermore we observed morphological and molecular heterogeneity within the three individual subtypes, prompting that a further sub-classification might be needed to understand the full molecular heterogeneity of PDAC.

In summary, it will be important to classify each individual tumor according to mutational spectrum, gene and marker expression to determine the optimal treatment strategy. This will be of benefit of for the individual patient, as pancreatic cancer is currently still treated as one disease.

Appendix

Tumor ID	Cell Line ID	Age	Sex	Tumor	Nodal	Metastasis	Grade	R-Class	Pathological Diagnosis
PT1		65	Männlich	T3	N1	Mx	G2		Adenocarcinom ductal
PT2		77	Männlich						Autoimmun-Pankreatitis des Schweregrades 4
PT3 *	**Paco 7**	45	Männlich	T3	N1	Mx	G2		Adenocarcinom ductal
PT4		42	Männlich	T3	N1	Mx	G2		Adenocarcinom ductal
PT5		74	Weiblich	T3	N1	M0	G2		Adenocarcinom ductal
PT6		72	Männlich	T3	N1	M0			Adenocarcinom ductal
PT7 *	**Paco 8**	71	Weiblich	T3	N1	Mx	G3		Adenocarcinom ductal
PT8 *	**Paco 10**	61	Männlich	T3	N1	Mx	G3		Adenocarcinom ductal
PT9 *	**Paco 3**	77	Weiblich	T3	N0	Mx	G2		Adenocarcinom ductal
PT10 *		69	Männlich	T3	N1	Mx	G3		Adenosquamöses Carcinom
PT11 *	**Paco 2**	60	Weiblich	T3	N1	M1	G2		Adenocarcinom ductal
PT12 *		86	Männlich	T3	N1	M0	G2		Adenocarcinom ductal
PT13 *	**Paco 9**	52	Männlich	T3	N1	Mx	G2		Adenocarcinom ductal
PT14		45	Weiblich	T4	N1	M1	G2		muzinöses Adenocarcinom
PT15		73	Männlich	T3	N1	Mx	G2		neuroendokrines Carcinom
PT16		84	Weiblich	T4	N1	Mx	G2		muzinöses Adenocarcinom
PT17		66	Weiblich	T3	N1	Mx	G2		Gallengangscarcinom
PT18		70	Weiblich	T3	N1	Mx	G4		undifferenziertes, anaplastisches Pankreas-Carcinom
PT19 *		64	Männlich	T2	N0	Mx	G2		Adenocarcinom ductal
PT20		57	Männlich	T3	N1	M0			Adenocarcinom ductal
PT21 *	**Paco 14**	65	Weiblich	T3	N1	M1			Adenocarcinom ductal
PT22		61	Weiblich	T3	N0	M0		R1	Adenocarcinom ductal (auch szirrhöses)
PT23		57	Weiblich	T3	N0	M0	G2	R1	Adenocarcinom ductal
PT24 *	**Paco 16**	48	Männlich	T3	N1	M0	G3	R1	Adenocarcinom mit squamöser Komponente
PT25 *		81	Weiblich	T3	N1	M0	G3	R1	Adenocarcinom ductal (auch szirrhöses)
PT26		67	Weiblich	T3	N1	M0	G2	R0	Adenocarcinom ductal (auch szirrhöses)
PT27		60	Weiblich	T3	N0	M0	G2	R1	Adenocarcinom ductal (auch szirrhöses)
PT28		53	Männlich	T3	N1	M0	G3	R0	Azinuszellcarcinom
PT29		56	Weiblich	T3	N1	M0	G3	R1	Azinuszellcarcinom
PT30 *	**Paco 18**	62	Männlich	T3	N1	M0	G3	R1	Adenocarcinom ductal (auch szirrhöses)
PT31		70	Männlich	T3	N1	M0	G2	R1	Adenocarcinom ductal (auch szirrhöses)
PT32 *	**Paco 17**	65	Männlich	T3	N1	M0	G3	R1	Adenocarcinom ductal (auch szirrhöses)
PT33		65	Weiblich						IPMN benigne
PT34		76	Weiblich						Cystadenom (muzinös)
PT35		64	Weiblich	T3	N1	M0	G2	R1	Adenocarcinom ductal (auch szirrhöses)
PT36 *		53	Weiblich	T3	N0	M0	G4	R0	Adenocarcinom ductal (auch szirrhöses)
PT37		74	Männlich	T3	N1	M0	G3	R1	Adenocarcinom o.n.A.
PT38 *	**Paco 19**	49	Männlich	T3	N1	M0	G3	R1	Adenocarcinom ductal (auch szirrhöses)
PT39 *	**Paco 20**	37	Weiblich	T3	N1	M0	G2	R1	Adenocarcinom ductal (auch szirrhöses)

Appendix Table 1 – Patient characteristics of primary tumors (PT) obtained during the period of May 09 – May 12; * denotes successful xenograft

Patient TMA		
Age (mean)	64,7 years	
Sex		Cases (% of total)
	Male	136 (54)
	Female	116 (46)
T stage		
	T1	2 (0,8)
	T2	48 (19)
	T3	189 (75)
	T4	13 (5,2)
N stage		
	N0	67 (26,6)
	N1	185 (73,4)
Grade		
	G1	10 (4)
	G2	139 (55,2)
	G3	103 (40,9)

Appendix Table 2 – Patient characteristics of tumors present on the tumor microarray

Acknowledgements

First of all I would like to thank my supervisor **Andreas Trumpp** for assigning me with this very interesting and daring project. I am indebted to you for that you offered me a PhD position in your lab even though I am not a major in biology; well I sure don't regret my decision to join your lab, I hope you don't either ☺. I am grateful for all your inspiration, patience and for your never-ending encouragement. I have learned a lot during the past years thanks to all the opportunities your lab, the DKFZ and Heidelberg offers. It has sure been an amazing time if I look back on the past 3 ½ years! Considering that I initially joined the lab with around 10 members and now having expanded to almost 50, things sure have changed but you still remained the open-minded and kick-ass boss, which I met in the middle of the DKFZ construction site in 2009.
Thank you a lot for the trust you put in me and for the freedom you gave to me in order to become the scientist I am now!

Another big thank you goes to **Martin Sprick**, who joined the lab during a time of change and who greatly helped me in focusing on parts of my PhD project, which resulted in this interesting and amazing story. You have helped me a lot to become the critical and interested scientist I am now. Thank you for supporting me in times when I didn't think that there was an easy solution to a problem…well most of the time there wasn't but at least you supported me along the rocky way ☺ And as you told me that a wall of text is just annoying the reader I stop right here :D Thanks a lot for all the trust you put in me and for all the possibilities you opened up to me!

I would also like to thank my second referee, TAC committee member and collaborator **Jens Werner**. Without you this thesis would not have been possible. Thank you for promoting our fruitful cooperation from the very beginning of my thesis and for hanging on to it ☺

You were of great help throughout my thesis and always had an open ear in case of troubled times! Thank you very much for the confidence you put into my work!

I would also like to express my gratitude to the third member of my Thesis Advisory Committee, **Hanno Glimm**. Thanks for your critical review of my work and the valuable input you provided during all the discussions we had in these meetings!

I would also like to express my gratitude to our prime pathologists **Wilko Weichert** and **Albrecht Stenzinger**. Thank you for our very fruitful cooperation, help and support throughout my entire work. It has been a real pleasure working with you, Jens and you both made me revert my statement that there are no cool clinicians out there ☺ Well there are! Thank you so much!

Thank you to the members of the core facilities, especially to **Sabine Henze** and **Oliver Heil** of the Genomics Core facility, who supported me a lot during my work, and to **Steffen Schmidt**, **Klaus Hexel**, **Gelo de la Cruz** and **Jens Hertwig** of the Flow Cytometry Facility. Special thanks to Klaus and Steffen for sharing their wisdom and secrets about flow cytometry, you have been amazing! Thanks to Klaus I can now set up an Influx system blindfolded :D

It is hard to find words for the gratitude I would like to express to our superwoman **Corinna.** Without you, major parts of my thesis would not have been possible. Thank your for being every possible help I needed in troubled times! You have been consultant, kindergarten teacher, cheerleader, Mc Guyver, Chuck Norris and much more all in one! Thank you for joining the METICS back then and for being keeping the group together and running. Thank you Corambo ☺

I would also like to thank our princess of darkness aka **Vanessa**! After you joined the METICS group in 2011 we finally were told how histology really works ;) Thanks a lot for all the help you provided and of course for all the nice stainings you have contributed to my thesis and paper! I really hope that we finally can find a date to party together ☺

Thank you to all the members of the METICS group for making our little subgroup the most outstanding group within the A010/HI-STEM department. Thank you **Thomas** aka Tombo aka Tombine for proving that even medical doctors can rock hard! It was an amazing time with you, thanks for all the discussion, help and support you gave me and a big thank you for every critical review during my entire work!

You have become a true friend during our seemingly endless discussions and head-bang sessions in the cell culture ☺

Thanks to **Steve** aka Steviboy aka Patient Null for joining our fantastic and crazy group in 2010. You have been a great help throughout my thesis, thank you for supporting me in many of the parts of this thesis. Also thank you for your critical and reflective thoughts in case I didn't know what to do! Thank you for the amazing time we had during all the parties I mean conferences at various places ☺

Nobody ever thought that I would be able to supervise fellow scientists but I sure proved them wrong ☺ Thanks to **Jan** aka Jane Fonda, my first guniea pig master student for bearing with me despite occasional freak-outs! It has been amazing to work with you, thanks for all the help you provided in times I needed it most! Thanks as well to my second master student **Franzi** for taking a chance on me ☺ I hope we will still have an amazing time in the lab, all the best to you in the future!

Lastly I would like to express my biggest gratitude to our METICS wonder woman **Teresa** aka Schereeez. Thank you for your never-ending support, help, motivation and criticism from the very moment you joined our little group. You have not only been of great help but also became a good friend during the past few months!

I probably cursed several hundred times while I was reading your comments on my paper, thesis or any kind of publication, however I am more than just grateful for every critical review and for every input that you provided to my work. Additionally you are probably the only one (except me) who read the masterpiece thesis several times from top to bottom :D Thanks for that!

Oh and of course thanks for being the character counterpart which helps me to remain grounded every day :D

Thanks to **Massimo** and **Corinna** for joining our crazy crowd, you certainly won't regret it! Another big thank goes to our favorite lab wizard **Marina** aka Mareeenaaa. Thank you a lot for your happiness and spirit you brought to our group, for the amazing organization talent. In any case I didn't start the day with a smile, after having prepared my first coffee in your office my mood improved dramatically ☺ Thank you for that!

Thanks to **Armin, Stephan, Anja, Irène, Marieke, Andrea Kuck**, **Meike and Raphi** for helping me settle in Heidelberg. You've been of great help during my first months!

Thanks to **HBIGS** for providing me with the rich opportunities to develop substantial knowledge in non-science related fields. Thanks for offering the chance to get internationally recognized certificates in business administration as well as project management. Thanks to **Rolf**, **Claudia**, **Sandra** and all the rest of the HBIGS team!

Thanks to all the members of **HI-STEM** and **A010** for making the lab such an amazing work environment!

Der meiste Dank gebührt allerdings meinen Eltern und meiner Schwester ohne deren Hilfe diese Arbeit niemals möglich gewesen wäre. Danke für euer immer offenes Ohr in Zeiten als ich Hilfe und Unterstützung nötig hatte. Ihr wart mir in meiner ganzen bisherigen Karriere die allergrößte Stütze, ihr wusstet immer Rat, wenn ich nicht mehr weiter wusste. Vielen Dank dafür!

Acknowledgements

Most importantly the biggest thank you goes to the most amazing immunologist I got to know in Heidelberg. Her biggest achievement yet is to bear with me despite my very pronounced Franconian phenotype ☺ There are barely any words that can describe my gratitude for your seemingly endless support and strength :*

Sorry to all I forgot!

7 References

1 Siegel, R., Naishadham, D. & Jemal, A. Cancer statistics, 2012. *CA: a cancer journal for clinicians* **62**, 10-29, doi:10.3322/caac.20138 (2012).

2 Iodice, S., Gandini, S., Maisonneuve, P. & Lowenfels, A. B. Tobacco and the risk of pancreatic cancer: a review and meta-analysis. *Langenbeck's archives of surgery / Deutsche Gesellschaft fur Chirurgie* **393**, 535-545, doi:10.1007/s00423-007-0266-2 (2008).

3 Vincent, A., Herman, J., Schulick, R., Hruban, R. H. & Goggins, M. Pancreatic cancer. *Lancet* **378**, 607-620, doi:10.1016/S0140-6736(10)62307-0 (2011).

4 Ghaneh, P., Costello, E. & Neoptolemos, J. P. Biology and management of pancreatic cancer. *Postgraduate medical journal* **84**, 478-497, doi:10.1136/gut.2006.103333 (2008).

5 Hruban, R. H. & Adsay, N. V. Molecular classification of neoplasms of the pancreas. *Human pathology* **40**, 612-623, doi:10.1016/j.humpath.2009.01.008 (2009).

6 Maitra, A. & Hruban, R. H. Pancreatic cancer. *Annual review of pathology* **3**, 157-188, doi:10.1146/annurev.pathmechdis.3.121806.154305 (2008).

7 Yachida, S. *et al.* Distant metastasis occurs late during the genetic evolution of pancreatic cancer. *Nature* **467**, 1114-1117, doi:10.1038/nature09515 (2010).

8 Mazur, P. K. & Siveke, J. T. Genetically engineered mouse models of pancreatic cancer: unravelling tumour biology and progressing translational oncology. *Gut*, doi:10.1136/gutjnl-2011-300756 (2011).

9 Hidalgo, M. Pancreatic cancer. *The New England journal of medicine* **362**, 1605-1617, doi:10.1056/NEJMra0901557 (2010).

10 Lemoine, N. R. *et al.* Ki-ras oncogene activation in preinvasive pancreatic cancer. *Gastroenterology* **102**, 230-236 (1992).

11 Schutte, M. *et al.* Abrogation of the Rb/p16 tumor-suppressive pathway in virtually all pancreatic carcinomas. *Cancer research* **57**, 3126-3130 (1997).

12 Redston, M. S. *et al.* p53 mutations in pancreatic carcinoma and evidence of common involvement of homocopolymer tracts in DNA microdeletions. *Cancer research* **54**, 3025-3033 (1994).

13 Hahn, S. A. *et al.* DPC4, a candidate tumor suppressor gene at human chromosome 18q21.1. *Science* **271**, 350-353 (1996).

14 Jones, S. *et al.* Core signaling pathways in human pancreatic cancers revealed by global genomic analyses. *Science* **321**, 1801-1806, doi:10.1126/science.1164368 (2008).

15 Yeo, T. P. *et al.* Pancreatic cancer. *Current problems in cancer* **26**, 176-275 (2002).

16 Edge, S. B. & American Joint Committee on Cancer. *AJCC cancer staging manual*. 7th edn, (Springer, 2010).

17 Bilimoria, K. Y. *et al.* National failure to operate on early stage pancreatic cancer. *Annals of surgery* **246**, 173-180, doi:10.1097/SLA.0b013e3180691579 (2007).

18 Neoadjuvant chemotherapy in invasive bladder cancer: a systematic review and meta-analysis. *Lancet* **361**, 1927-1934 (2003).

19 Herreros-Villanueva, M., Hijona, E., Cosme, A. & Bujanda, L. Adjuvant and neoadjuvant treatment in pancreatic cancer. *World journal of gastroenterology : WJG* **18**, 1565-1572, doi:10.3748/wjg.v18.i14.1565 (2012).

20 Gillen, S., Schuster, T., Meyer Zum Buschenfelde, C., Friess, H. & Kleeff, J. Preoperative/neoadjuvant therapy in pancreatic cancer: a systematic review and meta-analysis of response and resection percentages. *PLoS medicine* **7**, e1000267, doi:10.1371/journal.pmed.1000267 (2010).

21 Roeder, F. *et al.* Clinical phase I/II trial to investigate neoadjuvant intensity-modulated short term radiation therapy (5 x 5 Gy) and intraoperative radiation therapy (15 Gy) in patients with primarily resectable pancreatic cancer - NEOPANC. *BMC cancer* **12**, 112, doi:10.1186/1471-2407-12-112 (2012).

22 Kalser, M. H. & Ellenberg, S. S. Pancreatic cancer. Adjuvant combined radiation and chemotherapy following curative resection. *Arch Surg* **120**, 899-903 (1985).

23 Burris, H. A., 3rd *et al.* Improvements in survival and clinical benefit with gemcitabine as first-line therapy for patients with advanced pancreas cancer: a randomized trial. *Journal of clinical oncology : official journal of the American Society of Clinical Oncology* **15**, 2403-2413 (1997).

24 Oettle, H. *et al.* Adjuvant chemotherapy with gemcitabine vs observation in patients undergoing curative-intent resection of pancreatic cancer: a randomized controlled trial. *JAMA : the journal of the American Medical Association* **297**, 267-277, doi:10.1001/jama.297.3.267 (2007).

25 Herrmann, R. *et al.* Gemcitabine plus capecitabine compared with gemcitabine alone in advanced pancreatic cancer: a randomized, multicenter, phase III trial of the Swiss Group for Clinical Cancer Research and the Central European Cooperative Oncology Group. *Journal of clinical oncology : official journal of the American Society of Clinical Oncology* **25**, 2212-2217, doi:10.1200/JCO.2006.09.0886 (2007).

26 Cunningham, D. *et al.* Phase III randomized comparison of gemcitabine versus gemcitabine plus capecitabine in patients with advanced pancreatic cancer. *Journal of clinical oncology : official journal of the American Society of Clinical Oncology* **27**, 5513-5518, doi:10.1200/JCO.2009.24.2446 (2009).

27 Bernier, J., Hall, E. J. & Giaccia, A. Radiation oncology: a century of achievements. *Nature reviews. Cancer* **4**, 737-747, doi:10.1038/nrc1451 (2004).

28 Hazard, L. The role of radiation therapy in pancreas cancer. *Gastrointestinal cancer research : GCR* **3**, 20-28 (2009).

29 Moore, M. J. *et al.* Erlotinib plus gemcitabine compared with gemcitabine alone in patients with advanced pancreatic cancer: a phase III trial of the National Cancer Institute of Canada Clinical Trials Group. *Journal of clinical oncology : official journal of the American Society of Clinical Oncology* **25**, 1960-1966, doi:10.1200/JCO.2006.07.9525 (2007).

30 Hidalgo, M. & Maitra, A. The hedgehog pathway and pancreatic cancer. *The New England journal of medicine* **361**, 2094-2096, doi:10.1056/NEJMcibr0905857 (2009).

31 Xiong, H. Q. *et al.* Phase 2 trial of oxaliplatin plus capecitabine (XELOX) as second-line therapy for patients with advanced pancreatic cancer. *Cancer* **113**, 2046-2052, doi:10.1002/cncr.23810 (2008).

32 Saif, M. W. New developments in the treatment of pancreatic cancer. Highlights from the "44th ASCO Annual Meeting". Chicago, IL, USA. May 30 - June 3, 2008. *JOP : Journal of the pancreas* **9**, 391-397 (2008).

33 House, M. G. & Choti, M. A. Palliative therapy for pancreatic/biliary cancer. *The Surgical clinics of North America* **85**, 359-371, doi:10.1016/j.suc.2005.01.022 (2005).

34 Bachmann, J., Michalski, C. W., Martignoni, M. E., Buchler, M. W. & Friess, H. Pancreatic resection for pancreatic cancer. *HPB : the official journal of the International Hepato Pancreato Biliary Association* **8**, 346-351, doi:10.1080/13651820600803981 (2006).

35 Lee, J. *et al.* Tumor stem cells derived from glioblastomas cultured in bFGF and EGF more closely mirror the phenotype and genotype of primary tumors than do serum-cultured cell lines. *Cancer cell* **9**, 391-403, doi:10.1016/j.ccr.2006.03.030 (2006).

36 Deer, E. L. *et al.* Phenotype and genotype of pancreatic cancer cell lines. *Pancreas* **39**, 425-435, doi:10.1097/MPA.0b013e3181c15963 (2010).

37 Voskoglou-Nomikos, T., Pater, J. L. & Seymour, L. Clinical predictive value of the in vitro cell line, human xenograft, and mouse allograft preclinical cancer models. *Clinical cancer research : an official journal of the American Association for Cancer Research* **9**, 4227-4239 (2003).

38 Stathis, A. & Moore, M. J. Advanced pancreatic carcinoma: current treatment and future challenges. *Nature reviews. Clinical oncology* **7**, 163-172, doi:10.1038/nrclinonc.2009.236 (2010).

39 Frese, K. K. & Tuveson, D. A. Maximizing mouse cancer models. *Nature reviews. Cancer* **7**, 645-658, doi:10.1038/nrc2192 (2007).

40 Hingorani, S. R. *et al.* Preinvasive and invasive ductal pancreatic cancer and its early detection in the mouse. *Cancer cell* **4**, 437-450 (2003).

41 Aguirre, A. J. *et al.* Activated Kras and Ink4a/Arf deficiency cooperate to produce metastatic pancreatic ductal adenocarcinoma. *Genes & development* **17**, 3112-3126, doi:10.1101/gad.1158703 (2003).

42 Hingorani, S. R. *et al.* Trp53R172H and KrasG12D cooperate to promote chromosomal instability and widely metastatic pancreatic ductal adenocarcinoma in mice. *Cancer cell* **7**, 469-483, doi:10.1016/j.ccr.2005.04.023 (2005).

43 Izeradjene, K. *et al.* Kras(G12D) and Smad4/Dpc4 haploinsufficiency cooperate to induce mucinous cystic neoplasms and invasive adenocarcinoma of the pancreas. *Cancer cell* **11**, 229-243, doi:10.1016/j.ccr.2007.01.017 (2007).

44 Olive, K. P. *et al.* Inhibition of Hedgehog signaling enhances delivery of chemotherapy in a mouse model of pancreatic cancer. *Science* **324**, 1457-1461, doi:10.1126/science.1171362 (2009).

45 Cook, N. *et al.* Gamma secretase inhibition promotes hypoxic necrosis in mouse pancreatic ductal adenocarcinoma. *The Journal of experimental medicine* **209**, 437-444, doi:10.1084/jem.20111923 (2012).

46 Flanagan, S. P. 'Nude', a new hairless gene with pleiotropic effects in the mouse. *Genetical research* **8**, 295-309 (1966).

47 Kim, M. P. *et al.* Generation of orthotopic and heterotopic human pancreatic cancer xenografts in immunodeficient mice. *Nature protocols* **4**, 1670-1680, doi:10.1038/nprot.2009.171 (2009).

48 Bosma, G. C., Custer, R. P. & Bosma, M. J. A severe combined immunodeficiency mutation in the mouse. *Nature* **301**, 527-530 (1983).

49 Ito, M. *et al.* NOD/SCID/gamma(c)(null) mouse: an excellent recipient mouse model for engraftment of human cells. *Blood* **100**, 3175-3182, doi:10.1182/blood-2001-12-0207 (2002).

50 Rubio-Viqueira, B. *et al.* An in vivo platform for translational drug development in pancreatic cancer. *Clinical cancer research : an official journal of the American Association for Cancer Research* **12**, 4652-4661, doi:10.1158/1078-0432.CCR-06-0113 (2006).

51 Rajeshkumar, N. V. *et al.* MK-1775, a potent Wee1 inhibitor, synergizes with gemcitabine to achieve tumor regressions, selectively in p53-deficient pancreatic cancer xenografts. *Clinical cancer research : an official journal of the American Association for Cancer Research* **17**, 2799-2806, doi:10.1158/1078-0432.CCR-10-2580 (2011).

52 Rajeshkumar, N. V. *et al.* A combination of DR5 agonistic monoclonal antibody with gemcitabine targets pancreatic cancer stem cells and results in long-term disease control in human pancreatic cancer model. *Molecular cancer therapeutics* **9**, 2582-2592, doi:10.1158/1535-7163.MCT-10-0370 (2010).

53 Gage, F. H., Ray, J. & Fisher, L. J. Isolation, characterization, and use of stem cells from the CNS. *Annual review of neuroscience* **18**, 159-192, doi:10.1146/annurev.ne.18.030195.001111 (1995).

54 Rietze, R. L. & Reynolds, B. A. Neural stem cell isolation and characterization. *Methods in enzymology* **419**, 3-23, doi:10.1016/S0076-6879(06)19001-1 (2006).

55 Dontu, G. *et al.* In vitro propagation and transcriptional profiling of human mammary stem/progenitor cells. *Genes & development* **17**, 1253-1270, doi:10.1101/gad.1061803 (2003).

56 Singh, S. K. *et al.* Identification of human brain tumour initiating cells. *Nature* **432**, 396-401, doi:10.1038/nature03128 (2004).

57 Ricci-Vitiani, L. *et al.* Identification and expansion of human colon-cancer-initiating cells. *Nature* **445**, 111-115, doi:10.1038/nature05384 (2007).

58 Hermann, P. C. *et al.* Distinct populations of cancer stem cells determine tumor growth and metastatic activity in human pancreatic cancer. *Cell stem cell* **1**, 313-323, doi:10.1016/j.stem.2007.06.002 (2007).

59 Vermeulen, L. *et al.* Single-cell cloning of colon cancer stem cells reveals a multi-lineage differentiation capacity. *Proceedings of the National Academy of Sciences of the United States of America* **105**, 13427-13432, doi:10.1073/pnas.0805706105 (2008).

60 Pollard, S. M. *et al.* Glioma stem cell lines expanded in adherent culture have tumor-specific phenotypes and are suitable for chemical and genetic screens. *Cell stem cell* **4**, 568-580, doi:10.1016/j.stem.2009.03.014 (2009).

61 Pollard, S. M., Conti, L., Sun, Y., Goffredo, D. & Smith, A. Adherent neural stem (NS) cells from fetal and adult forebrain. *Cereb Cortex* **16 Suppl 1**, i112-120, doi:10.1093/cercor/bhj167 (2006).

62 Visvader, J. E. Cells of origin in cancer. *Nature* **469**, 314-322, doi:10.1038/nature09781 (2011).

63 Tlsty, T. D. & Coussens, L. M. Tumor stroma and regulation of cancer development. *Annual review of pathology* **1**, 119-150, doi:10.1146/annurev.pathol.1.110304.100224 (2006).

64 Marusyk, A. & Polyak, K. Tumor heterogeneity: causes and consequences. *Biochimica et biophysica acta* **1805**, 105-117, doi:10.1016/j.bbcan.2009.11.002 (2010).

65 Prat, A., Ellis, M. J. & Perou, C. M. Practical implications of gene-expression-based assays for breast oncologists. *Nature reviews. Clinical oncology* **9**, 48-57, doi:10.1038/nrclinonc.2011.178 (2012).

66 Reis-Filho, J. S. & Pusztai, L. Gene expression profiling in breast cancer: classification, prognostication, and prediction. *Lancet* **378**, 1812-1823, doi:10.1016/S0140-6736(11)61539-0 (2011).

67 Goldhirsch, A. *et al.* Strategies for subtypes--dealing with the diversity of breast cancer: highlights of the St. Gallen International Expert Consensus on the Primary Therapy of Early Breast Cancer 2011. *Annals of oncology : official journal of the European Society for Medical Oncology / ESMO* **22**, 1736-1747, doi:10.1093/annonc/mdr304 (2011).

68 Harris, T. J. & McCormick, F. The molecular pathology of cancer. *Nature reviews. Clinical oncology* **7**, 251-265, doi:10.1038/nrclinonc.2010.41 (2010).

69 Curtis, C. *et al.* The genomic and transcriptomic architecture of 2,000 breast tumours reveals novel subgroups. *Nature*, doi:10.1038/nature10983 (2012).

70 Chang, H. H., Dreyfuss, J. M. & Ramoni, M. F. A transcriptional network signature characterizes lung cancer subtypes. *Cancer* **117**, 353-360, doi:10.1002/cncr.25592 (2011).

71 Integrated genomic analyses of ovarian carcinoma. *Nature* **474**, 609-615, doi:10.1038/nature10166 (2011).

72 Passegue, E., Wagner, E. F. & Weissman, I. L. JunB deficiency leads to a myeloproliferative disorder arising from hematopoietic stem cells. *Cell* **119**, 431-443, doi:10.1016/j.cell.2004.10.010 (2004).

73 Dirks, P. B. Cancer's source in the peripheral nervous system. *Nature medicine* **14**, 373-375, doi:10.1038/nm0408-373 (2008).

74 Hezel, A. F., Kimmelman, A. C., Stanger, B. Z., Bardeesy, N. & Depinho, R. A. Genetics and biology of pancreatic ductal adenocarcinoma. *Genes & development* **20**, 1218-1249, doi:10.1101/gad.1415606 (2006).

75 Stanger, B. Z. & Dor, Y. Dissecting the cellular origins of pancreatic cancer. *Cell Cycle* **5**, 43-46 (2006).

76 Means, A. L. *et al.* Pancreatic epithelial plasticity mediated by acinar cell transdifferentiation and generation of nestin-positive intermediates. *Development* **132**, 3767-3776, doi:10.1242/dev.01925 (2005).

77 Lee, C. J., Dosch, J. & Simeone, D. M. Pancreatic cancer stem cells. *Journal of clinical oncology : official journal of the American Society of Clinical Oncology* **26**, 2806-2812, doi:10.1200/JCO.2008.16.6702 (2008).

78 Van Cutsem, E. *et al.* Phase III trial of gemcitabine plus tipifarnib compared with gemcitabine plus placebo in advanced pancreatic cancer. *Journal of clinical oncology : official journal of the American Society of Clinical Oncology* **22**, 1430-1438, doi:10.1200/JCO.2004.10.112 (2004).

79 Laheru, D. *et al.* Integrated preclinical and clinical development of S-trans, trans-farnesylthiosalicylic acid (FTS, Salirasib) in pancreatic cancer. *Investigational new drugs*, doi:10.1007/s10637-012-9818-6 (2012).

80 da Cunha Santos, G. *et al.* Molecular predictors of outcome in a phase 3 study of gemcitabine and erlotinib therapy in patients with advanced pancreatic cancer: National Cancer Institute of Canada Clinical Trials Group Study PA.3. *Cancer* **116**, 5599-5607, doi:10.1002/cncr.25393 (2010).

81 Wang, H., Han, H. & Von Hoff, D. D. Identification of an agent selectively targeting DPC4 (deleted in pancreatic cancer locus 4)-deficient pancreatic cancer cells. *Cancer research* **66**, 9722-9730, doi:10.1158/0008-5472.CAN-05-4602 (2006).

82 Collisson, E. A. *et al.* Subtypes of pancreatic ductal adenocarcinoma and their differing responses to therapy. *Nature medicine* **17**, 500-503, doi:10.1038/nm.2344 (2011).

83 Gottesman, M. M. Mechanisms of cancer drug resistance. *Annual review of medicine* **53**, 615-627, doi:10.1146/annurev.med.53.082901.103929 (2002).

84 Gillet, J. P. & Gottesman, M. M. Mechanisms of multidrug resistance in cancer. *Methods Mol Biol* **596**, 47-76, doi:10.1007/978-1-60761-416-6_4 (2010).

85 Szakacs, G., Paterson, J. K., Ludwig, J. A., Booth-Genthe, C. & Gottesman, M. M. Targeting multidrug resistance in cancer. *Nature reviews. Drug discovery* **5**, 219-234, doi:10.1038/nrd1984 (2006).

86 Singh, S. K. *et al.* Identification of a cancer stem cell in human brain tumors. *Cancer research* **63**, 5821-5828 (2003).

87 Bednar, F. & Simeone, D. M. Pancreatic cancer stem cell biology and its therapeutic implications. *Journal of gastroenterology* **46**, 1345-1352, doi:10.1007/s00535-011-0494-7 (2011).

88 Trumpp, A., Essers, M. & Wilson, A. Awakening dormant haematopoietic stem cells. *Nature reviews. Immunology* **10**, 201-209, doi:10.1038/nri2726 (2010).

89 Cortes, J., O'Brien, S. & Kantarjian, H. Discontinuation of imatinib therapy after achieving a molecular response. *Blood* **104**, 2204-2205, doi:10.1182/blood-2004-04-1335 (2004).

90 Gottesman, M. M., Fojo, T. & Bates, S. E. Multidrug resistance in cancer: role of ATP-dependent transporters. *Nature reviews. Cancer* **2**, 48-58, doi:10.1038/nrc706 (2002).

91 Fulda, S. Apoptosis pathways and their therapeutic exploitation in pancreatic cancer. *Journal of cellular and molecular medicine* **13**, 1221-1227, doi:10.1111/j.1582-4934.2009.00748.x (2009).

92 Wang, Z. *et al.* Pancreatic cancer: understanding and overcoming chemoresistance. *Nature reviews. Gastroenterology & hepatology* **8**, 27-33, doi:10.1038/nrgastro.2010.188 (2011).

93 Subramanian, A. *et al.* Gene set enrichment analysis: a knowledge-based approach for interpreting genome-wide expression profiles. *Proceedings of the National Academy of Sciences of the United States of America* **102**, 15545-15550, doi:10.1073/pnas.0506580102 (2005).

94 Weichert, W. *et al.* Overexpression of Polo-like kinase 1 is a common and early event in pancreatic cancer. *Pancreatology* **5**, 259-265, doi:10.1159/000085280 (2005).

95 Bosman, F. T., World Health Organization. & International Agency for Research on Cancer. *WHO classification of tumours of the digestive system*. 4th edn, (International Agency for Research on Cancer, 2010).

96 Bild, A. H. *et al.* Oncogenic pathway signatures in human cancers as a guide to targeted therapies. *Nature* **439**, 353-357, doi:10.1038/nature04296 (2006).

97 Huang, F. *et al.* Identification of candidate molecular markers predicting sensitivity in solid tumors to dasatinib: rationale for patient selection. *Cancer research* **67**, 2226-2238, doi:10.1158/0008-5472.CAN-06-3633 (2007).

98 Nunoda, K. *et al.* Identification and functional signature of genes regulated by structurally different ABL kinase inhibitors. *Oncogene* **26**, 4179-4188, doi:10.1038/sj.onc.1210179 (2007).

99 Gautschi, O. *et al.* Regulation of Id1 expression by SRC: implications for targeting of the bone morphogenetic protein pathway in cancer. *Cancer research* **68**, 2250-2258, doi:10.1158/0008-5472.CAN-07-6403 (2008).

100 Hann, C. L. *et al.* Therapeutic efficacy of ABT-737, a selective inhibitor of BCL-2, in small cell lung cancer. *Cancer research* **68**, 2321-2328, doi:10.1158/0008-5472.CAN-07-5031 (2008).

101 Badea, L., Herlea, V., Dima, S. O., Dumitrascu, T. & Popescu, I. Combined gene expression analysis of whole-tissue and microdissected pancreatic ductal adenocarcinoma identifies genes specifically overexpressed in tumor epithelia. *Hepato-gastroenterology* **55**, 2016-2027 (2008).

102 Uhlen, M. *et al.* A human protein atlas for normal and cancer tissues based on antibody proteomics. *Molecular & cellular proteomics : MCP* **4**, 1920-1932, doi:10.1074/mcp.M500279-MCP200 (2005).

103 Thomas, S. M. & Brugge, J. S. Cellular functions regulated by Src family kinases. *Annual review of cell and developmental biology* **13**, 513-609, doi:10.1146/annurev.cellbio.13.1.513 (1997).

104 Huang, S. & Houghton, P. J. Targeting mTOR signaling for cancer therapy. *Current opinion in pharmacology* **3**, 371-377 (2003).

105 Christopher, L. J. *et al.* Metabolism and disposition of dasatinib after oral administration to humans. *Drug metabolism and disposition: the biological fate of chemicals* **36**, 1357-1364, doi:10.1124/dmd.107.018267 (2008).

106 Richmond, A. & Su, Y. Mouse xenograft models vs GEM models for human cancer therapeutics. *Disease models & mechanisms* **1**, 78-82, doi:10.1242/dmm.000976 (2008).

107 Garrido-Laguna, I. *et al.* Tumor engraftment in nude mice and enrichment in stroma-related gene pathways predict poor survival and resistance to gemcitabine in patients with pancreatic cancer. *Clinical cancer research : an official journal of the American Association for Cancer Research* **17**, 5793-5800, doi:10.1158/1078-0432.CCR-11-0341 (2011).

108 Jimeno, A. *et al.* A direct pancreatic cancer xenograft model as a platform for cancer stem cell therapeutic development. *Molecular cancer therapeutics* **8**, 310-314, doi:10.1158/1535-7163.MCT-08-0924 (2009).

109 Davis, D. W. *et al.* Regional effects of an antivascular endothelial growth factor receptor monoclonal antibody on receptor phosphorylation and apoptosis in human 253J B-V bladder cancer xenografts. *Cancer research* **64**, 4601-4610, doi:10.1158/0008-5472.CAN-2879-2 (2004).

110 Hurwitz, H. *et al.* Bevacizumab plus irinotecan, fluorouracil, and leucovorin for metastatic colorectal cancer. *The New England journal of medicine* **350**, 2335-2342, doi:10.1056/NEJMoa032691 (2004).

111 Ocana, A., Pandiella, A., Siu, L. L. & Tannock, I. F. Preclinical development of molecular-targeted agents for cancer. *Nature reviews. Clinical oncology* **8**, 200-209, doi:10.1038/nrclinonc.2010.194 (2011).

112 Dobrynin, Y. V. Establishment and Characteristics of Cell Strains from Some Epithelial Tumors of Human Origin. *Journal of the National Cancer Institute* **31**, 1173-1195 (1963).

113 Mahadevan, D. & Von Hoff, D. D. Tumor-stroma interactions in pancreatic ductal adenocarcinoma. *Molecular cancer therapeutics* **6**, 1186-1197, doi:10.1158/1535-7163.MCT-06-0686 (2007).

114 McQueen, H. A., Wyllie, A. H., Piris, J., Foster, E. & Bird, C. C. Stability of critical genetic lesions in human colorectal carcinoma xenografts. *British journal of cancer* **63**, 94-96 (1991).

115 Ku, J. L. *et al.* Establishment and characterization of four human pancreatic carcinoma cell lines. Genetic alterations in the TGFBR2 gene but not in the MADH4 gene. *Cell and tissue research* **308**, 205-214, doi:10.1007/s00441-001-0510-y (2002).

116 Ruckert, F. *et al.* Five primary human pancreatic adenocarcinoma cell lines established by the outgrowth method. *The Journal of surgical research* **172**, 29-39, doi:10.1016/j.jss.2011.04.021 (2012).

117 Pandol, S., Edderkaoui, M., Gukovsky, I., Lugea, A. & Gukovskaya, A. Desmoplasia of pancreatic ductal adenocarcinoma. *Clinical gastroenterology and hepatology : the official clinical practice journal of the American Gastroenterological Association* **7**, S44-47, doi:10.1016/j.cgh.2009.07.039 (2009).

118 Perou, C. M. *et al.* Molecular portraits of human breast tumours. *Nature* **406**, 747-752, doi:10.1038/35021093 (2000).

119 Barbieri, C. E. *et al.* Exome sequencing identifies recurrent SPOP, FOXA1 and MED12 mutations in prostate cancer. *Nature genetics* **44**, 685-689, doi:10.1038/ng.2279 (2012).

120 Russo, S. M., Ove, R. & Saif, M. W. Identification of prognostic and predictive markers in pancreatic adenocarcinoma. Highlights from the "2011 ASCO Gastrointestinal Cancers Symposium". San Francisco, CA, USA. January 20-22, 2011. *JOP : Journal of the pancreas* **12**, 92-95 (2011).

121 Iacobuzio-Donahue, C. A. *et al.* DPC4 gene status of the primary carcinoma correlates with patterns of failure in patients with pancreatic cancer. *Journal of clinical oncology : official journal of the American Society of Clinical Oncology* **27**, 1806-1813, doi:10.1200/JCO.2008.17.7188 (2009).

122 Collisson, E. A. *et al.* Subtypes of pancreatic ductal adenocarcinoma and their differing responses to therapy. *Nat Med* **17**, 500-U140, doi:10.1038/nm.2344 (2011).

123 West, L. *et al.* A novel classification of lung cancer into molecular subtypes. *PloS one* **7**, e31906, doi:10.1371/journal.pone.0031906 (2012).

124 Lehmann, B. D. *et al.* Identification of human triple-negative breast cancer subtypes and preclinical models for selection of targeted therapies. *The Journal of clinical investigation* **121**, 2750-2767, doi:10.1172/JCI45014 (2011).

125 Romond, E. H. *et al.* Trastuzumab plus adjuvant chemotherapy for operable HER2-positive breast cancer. *The New England journal of medicine* **353**, 1673-1684, doi:10.1056/NEJMoa052122 (2005).

126 Nammo, T. *et al.* Expression profile of MODY3/HNF-1alpha protein in the developing mouse pancreas. *Diabetologia* **45**, 1142-1153, doi:10.1007/s00125-002-0892-8 (2002).

127 Gidekel Friedlander, S. Y. *et al.* Context-dependent transformation of adult pancreatic cells by oncogenic K-Ras. *Cancer Cell* **16**, 379-389, doi:S1535-6108(09)00338-9 [pii]10.1016/j.ccr.2009.09.027 (2009).

128 Baumhueter, S., Courtois, G., Morgan, J. G. & Crabtree, G. R. The role of HNF-1 in liver-specific gene expression. *Annals of the New York Academy of Sciences* **557**, 272-278, discussion 279 (1989).

129 Ozeki, T. *et al.* Co-operative regulation of the transcription of human dihydrodiol dehydrogenase (DD)4/aldo-keto reductase (AKR)1C4 gene by hepatocyte nuclear factor (HNF)-4alpha/gamma and HNF-1alpha. *The Biochemical journal* **355**, 537-544 (2001).

130 Valastyan, S. & Weinberg, R. A. Tumor metastasis: molecular insights and evolving paradigms. *Cell* **147**, 275-292, doi:10.1016/j.cell.2011.09.024 (2011).

131 Kalluri, R. & Weinberg, R. A. The basics of epithelial-mesenchymal transition. *J Clin Invest* **119**, 1420-1428, doi:10.1172/JCI39104 (2009).

132 Nakajima, S. *et al.* N-cadherin expression and epithelial-mesenchymal transition in pancreatic carcinoma. *Clinical cancer research : an official journal of the American*

Association for Cancer Research **10**, 4125-4133, doi:10.1158/1078-0432.CCR-0578-03 (2004).

133 Rogers, M. A. *et al.* Sequences and differential expression of three novel human type-II hair keratins. *Differentiation; research in biological diversity* **61**, 187-194, doi:10.1046/j.1432-0436.1997.6130187.x (1997).

134 Dydensborg, A. B. *et al.* GATA3 inhibits breast cancer growth and pulmonary breast cancer metastasis. *Oncogene* **28**, 2634-2642, doi:10.1038/onc.2009.126 (2009).

135 Campayo, M. *et al.* A dual role for KRT81: a miR-SNP associated with recurrence in non-small-cell lung cancer and a novel marker of squamous cell lung carcinoma. *PloS one* **6**, e22509, doi:10.1371/journal.pone.0022509 (2011).

136 de Larrea, C. F. *et al.* Impact of MiRSNPs on Survival and Progression in Patients with Multiple Myeloma Undergoing Autologous Stem Cell Transplantation. *Clinical cancer research : an official journal of the American Association for Cancer Research*, doi:10.1158/1078-0432.CCR-12-0191 (2012).

137 Korc, M. Pancreatic cancer-associated stroma production. *American journal of surgery* **194**, S84-86, doi:10.1016/j.amjsurg.2007.05.004 (2007).

138 Chung, J. Y. *et al.* Factors in tissue handling and processing that impact RNA obtained from formalin-fixed, paraffin-embedded tissue. *The journal of histochemistry and cytochemistry : official journal of the Histochemistry Society* **56**, 1033-1042, doi:10.1369/jhc.2008.951863 (2008).

139 Hanlon, L. *et al.* Notch1 functions as a tumor suppressor in a model of K-ras-induced pancreatic ductal adenocarcinoma. *Cancer Res* **70**, 4280-4286, doi:0008-5472.CAN-09-4645 [pii]10.1158/0008-5472.CAN-09-4645 (2010).

140 Mazur, P. K. *et al.* Notch2 is required for progression of pancreatic intraepithelial neoplasia and development of pancreatic ductal adenocarcinoma. *Proc Natl Acad Sci U S A* **107**, 13438-13443, doi:10.1073/pnas.1002423107 (2010).

141 Miyamoto, Y. *et al.* Notch mediates TGF alpha-induced changes in epithelial differentiation during pancreatic tumorigenesis. *Cancer Cell* **3**, 565-576 (2003).

142 Engelman, J. A. Targeting PI3K signalling in cancer: opportunities, challenges and limitations. *Nature reviews. Cancer* **9**, 550-562, doi:10.1038/nrc2664 (2009).

143 Hennessy, B. T., Smith, D. L., Ram, P. T., Lu, Y. & Mills, G. B. Exploiting the PI3K/AKT pathway for cancer drug discovery. *Nature reviews. Drug discovery* **4**, 988-1004, doi:10.1038/nrd1902 (2005).

144 Willems, L. *et al.* PI3K and mTOR signaling pathways in cancer: new data on targeted therapies. *Current oncology reports* **14**, 129-138, doi:10.1007/s11912-012-0227-y (2012).

145 Falasca, M., Selvaggi, F., Buus, R., Sulpizio, S. & Edling, C. E. Targeting phosphoinositide 3-kinase pathways in pancreatic cancer--from molecular signalling to clinical trials. *Anti-cancer agents in medicinal chemistry* **11**, 455-463 (2011).

146 Edling, C. E. *et al.* Key role of phosphoinositide 3-kinase class IB in pancreatic cancer. *Clinical cancer research : an official journal of the American Association for Cancer Research* **16**, 4928-4937, doi:10.1158/1078-0432.CCR-10-1210 (2010).

147 Cao, P., Maira, S. M., Garcia-Echeverria, C. & Hedley, D. W. Activity of a novel, dual PI3-kinase/mTor inhibitor NVP-BEZ235 against primary human pancreatic cancers grown as orthotopic xenografts. *British journal of cancer* **100**, 1267-1276, doi:10.1038/sj.bjc.6604995 (2009).

148 Rachdi, L., Aiello, V., Duvillie, B. & Scharfmann, R. L-leucine alters pancreatic beta-cell differentiation and function via the mTor signaling pathway. *Diabetes* **61**, 409-417, doi:10.2337/db11-0765 (2012).

149 Yamamoto, S. *et al.* Prognostic significance of activated Akt expression in pancreatic ductal adenocarcinoma. *Clinical cancer research : an official journal of the American Association for Cancer Research* **10**, 2846-2850 (2004).

150 Chadha, K. S. *et al.* Activated Akt and Erk expression and survival after surgery in pancreatic carcinoma. *Annals of surgical oncology* **13**, 933-939, doi:10.1245/ASO.2006.07.011 (2006).

151 Irby, R. B. & Yeatman, T. J. Role of Src expression and activation in human cancer. *Oncogene* **19**, 5636-5642, doi:10.1038/sj.onc.1203912 (2000).

152 Shields, D. J. *et al.* Oncogenic Ras/Src cooperativity in pancreatic neoplasia. *Oncogene* **30**, 2123-2134, doi:10.1038/onc.2010.589 (2011).

153 Morton, J. P. *et al.* Dasatinib inhibits the development of metastases in a mouse model of pancreatic ductal adenocarcinoma. *Gastroenterology* **139**, 292-303, doi:10.1053/j.gastro.2010.03.034 (2010).

154 Nagaraj, N. S., Smith, J. J., Revetta, F., Washington, M. K. & Merchant, N. B. Targeted inhibition of SRC kinase signaling attenuates pancreatic tumorigenesis. *Molecular cancer therapeutics* **9**, 2322-2332, doi:10.1158/1535-7163.MCT-09-1212 (2010).

155 Philip, P. A. *et al.* Consensus report of the national cancer institute clinical trials planning meeting on pancreas cancer treatment. *Journal of clinical oncology : official journal of the American Society of Clinical Oncology* **27**, 5660-5669, doi:10.1200/JCO.2009.21.9022 (2009).

156 Awasthi, N., Yen, P. L., Schwarz, M. A. & Schwarz, R. E. The efficacy of a novel, dual PI3K/mTOR inhibitor NVP-BEZ235 to enhance chemotherapy and antiangiogenic response in pancreatic cancer. *Journal of cellular biochemistry* **113**, 784-791, doi:10.1002/jcb.23405 (2012).

157 Li, J. *et al.* A chemical and phosphoproteomic characterization of dasatinib action in lung cancer. *Nature chemical biology* **6**, 291-299, doi:10.1038/nchembio.332 (2010).

158 Bantscheff, M. *et al.* Quantitative chemical proteomics reveals mechanisms of action of clinical ABL kinase inhibitors. *Nature biotechnology* **25**, 1035-1044, doi:10.1038/nbt1328 (2007).

159 Trevino, J. G. *et al.* Inhibition of SRC expression and activity inhibits tumor progression and metastasis of human pancreatic adenocarcinoma cells in an orthotopic nude mouse model. *The American journal of pathology* **168**, 962-972, doi:10.2353/ajpath.2006.050570 (2006).

160 Rajeshkumar, N. V. *et al.* Antitumor effects and biomarkers of activity of AZD0530, a Src inhibitor, in pancreatic cancer. *Clinical cancer research : an official journal of the*

American Association for Cancer Research **15**, 4138-4146, doi:10.1158/1078-0432.CCR-08-3021 (2009).

161 Messersmith, W. A. *et al.* Efficacy and pharmacodynamic effects of bosutinib (SKI-606), a Src/Abl inhibitor, in freshly generated human pancreas cancer xenografts. *Molecular cancer therapeutics* **8**, 1484-1493, doi:10.1158/1535-7163.MCT-09-0075 (2009).

162 Jacobetz, M. A. *et al.* Hyaluronan impairs vascular function and drug delivery in a mouse model of pancreatic cancer. *Gut*, doi:10.1136/gutjnl-2012-302529 (2012).

163 Komar, G. *et al.* Decreased blood flow with increased metabolic activity: a novel sign of pancreatic tumor aggressiveness. *Clinical cancer research : an official journal of the American Association for Cancer Research* **15**, 5511-5517, doi:10.1158/1078-0432.CCR-09-0414 (2009).

164 van Delft, M. F. *et al.* The BH3 mimetic ABT-737 targets selective Bcl-2 proteins and efficiently induces apoptosis via Bak/Bax if Mcl-1 is neutralized. *Cancer cell* **10**, 389-399, doi:10.1016/j.ccr.2006.08.027 (2006).

165 Labi, V., Grespi, F., Baumgartner, F. & Villunger, A. Targeting the Bcl-2-regulated apoptosis pathway by BH3 mimetics: a breakthrough in anticancer therapy? *Cell death and differentiation* **15**, 977-987, doi:10.1038/cdd.2008.37 (2008).

166 Oltersdorf, T. *et al.* An inhibitor of Bcl-2 family proteins induces regression of solid tumours. *Nature* **435**, 677-681, doi:10.1038/nature03579 (2005).

167 Gandhi, L. *et al.* Phase I study of Navitoclax (ABT-263), a novel Bcl-2 family inhibitor, in patients with small-cell lung cancer and other solid tumors. *Journal of clinical oncology : official journal of the American Society of Clinical Oncology* **29**, 909-916, doi:10.1200/JCO.2010.31.6208 (2011).

168 Wilson, W. H. *et al.* Navitoclax, a targeted high-affinity inhibitor of BCL-2, in lymphoid malignancies: a phase 1 dose-escalation study of safety, pharmacokinetics, pharmacodynamics, and antitumour activity. *The lancet oncology* **11**, 1149-1159, doi:10.1016/S1470-2045(10)70261-8 (2010).

169 Roberts, A. W. *et al.* Substantial susceptibility of chronic lymphocytic leukemia to BCL2 inhibition: results of a phase I study of navitoclax in patients with relapsed or refractory disease. *Journal of clinical oncology : official journal of the American Society of Clinical Oncology* **30**, 488-496, doi:10.1200/JCO.2011.34.7898 (2012).

170 Fesik, S. W. Promoting apoptosis as a strategy for cancer drug discovery. *Nat Rev Cancer* **5**, 876-885, doi:10.1038/nrc1736 (2005).

8 Abbreviations

5-FU	5-fluorouracil
ABC	ATP-binding cassette transporters
ABL	V-abl Abelson murine leukemia viral oncogene
ACS	American Cancer Society
AIM2	absent in melanoma 2
AJCC	American Joint Cancer Committee
Akt	Proteinkinase B
ANOVA	Analysis of Variance
ATCC	American Type Culture Collection
BCR	breakpoint cluster region-A
BH3	Bcl-2 homology domain 3
BRAF	Raf murine sarcoma viral oncogene homolog B1
BRCA2	Breast Cancer 2 susceptibility protein
CA19-9	carbohydrate antigen 19-9
CAC	Centroacinar cell
CD133	Prominin-1
CD24	Cluster of Differentiation 24
CD44	Cluster of Differentiation 44
CDKN2A	Cyclin-dependent kinase inhibitor 2A
CEACAM3	Carcinoembryonic antigen-related cell adhesion molecule 5
CEACAM6	Carcinoembryonic antigen-related cell adhesion molecule 6
CEL3A	Elastase-3A
CFTR	Cystic fibrosis transmembrane conductance regulator
CML	Chronic Myloid Leukemia
Cre	Cre Recombinase
DN	Double negative
DNA	Deoxyribonucleic acid
DT	Derived Tumor
EGFR	Epidermal growth factor receptor
eIF4	Eukaryotic initiation factor 4
EMT	Epithelial-to-menenchymal transition
ER	Oestrogen receptor
eSC	Embryonic Stem Cells
FACS	Flourescent activated cell sorting
FCS	Fetal calf serum
FDA	Food and Drug Administration
G1	Gap 1 phase

G2/M	G2-M DNA damage checkpoint
GEM	Genetically engineered mouse model
GSEA	Gene set enrichement analysis
HER2	human epidermal growth factor receptor type 2
HNF1	Hepatocyte nuclear factor 1
IC50	half-maximal inhibitory concentration
IPMN	intraductal papillary mucinous neoplasm
iPS	Induced pluripotent stem cells
Ki67	Antigen KI-67
KRAS2	V-Ki-ras2 Kirsten rat sarcoma viral oncogene homolog
KRT81	Cytokeratin 81
LMD	Laser micro dissection
MCN	mucinous cystic neoplasm
MSig	Molecular Signatures
mTOR	Mammalian target of Rapamycin
NLM	National Library of Medicine
NOD/SCID	Nonobese diabetic with severe combined immunodeficiency
NSC	Neural stem cells
NSG	NOD.Cg-*Prkdc*^{scid} *Il2rg*^{tm1Wjl}
OS	Overall survival
p70S6K	p70S6 kinase
PACO	Pancreatic AdenoCarcinOma
PALB2	Partner and localizer of BRCA2
PanIN	pancreatic intraepithelial neoplasia
PDA	Pancreatic ductal adenocarcinoma
PDAC	Pancreatic Adenocarcinoma
Pdx1	Pancreatic and duodenal homeobox 1
PI3K	Phosphoinositide 3-kinase
PKB	Proteinkinase B
PR	Progesterone receptor
PRSS1	Trypsin-1
PT	Primary Tumor
Ptf1a	Pancreas transcription factor 1 subunit alpha
QM	Quasi-mesenchymal
R^2	Pearson correlation coefficient
RAF-MAPK	Raf murine sarcoma viral oncogene - Mitogen-activated protein (MAP) kinases
RalGDS	Ral guanine nucleotide dissociation stimulator
REG2A	Regenerating islet derived-2
S100A1	S100 calcium-binding protein A1
S100P	S100 calcium-binding protein P
S6RP	S6 ribosomal protein

Ser	Serine
SFK	Src family kinases
SLC2A3	solute carrier 2A3
SLC4A4	solute carrier 4A4
SMAD4	Mothers against decapentaplegic homolog 4
SPINK1	serine protease inhibitor Kazal-type 1
Src	Tyrosinkinase Src
STK11	Serine/threonine kinase 11
TFF3	Terfoil factor 3
TGF-β	Transforming growth factor β
TIC	Tumor initiating cell
TMA	Tissue Microarray
TMN	Tumor Node Metastasis
TP53	tumor protein 53
Tyr	Tyrosine
VEGFR2	vascular endothelial growth factor receptor 2
µg	microgram
µM	micromolar
µm	micrometer